Genomic Analysis and Potential Applications of Pesticide Degrading *Serratia* sp. strain HSTU-BF1R2 Towards Biofertilizer Development for Brinjal Cultivation

A THESIS

BY

SAGAR BARUA

Student ID: 2205036

Session: 2022-2023

Submitted to the Department of Biochemistry and Molecular Biology, Hajee Mohammad Danesh Science and Technology University, Dinajpur in partial fulfilment of the requirements for the degree of

MASTER OF SCIENCE (M.S.)

IN

BIOCHEMISTRY AND MOLECULAR BIOLOGY

DEPARTMENT OF BIOCHEMISTRY AND MOLECULAR BIOLOGY HAJEE MOHAMMAD DANESH SCIENCE AND TECHNOLOGY UNIVERSITY, DINAJPUR-5200

JUNE 2023

Genomic Analysis and Potential Applications of Pesticide Degrading *Serratia* sp. strain HSTU-BF1R2 Towards Biofertilizer Development for Brinjal Cultivation

A THESIS

BY

SAGAR BARUA

Student ID: 2205036

Session: 2022-2023

Approved as to Style and Content By

_____	_____
Supervisor	Co-Supervisor
Dr. Md. Yeasin Prodhan	**Dr. Md. Azizul Haque**
Associate Professor	Associate Professor
Department of Biochemistry and Molecular Biology	Department of Biochemistry & Molecular Biology

_____

Dr. Mst. Nur-E-Nazmun Nahar
Chairman
Examination Committee and Chairman
Department of Biochemistry and Molecular Biology

HAJEE MOHAMMAD DANESH SCIENCE AND TECHNOLOGY UNIVERSITY, DINAJPUR-5200
JUNE 2023

ACKNOWLEDGEMENTS

All the praises and gratitude are due to the omnipotent Almighty Allah, who has kindly enabled the author to complete the research and thesis successfully with knowledge for the degree of Master of Science in Biochemistry and Molecular Biology from Hajee Mohammad Danesh Science and Technology University (HSTU), Dinajpur within the appointed time.

The author wishes to convey his cordial respect and pleasant appreciation to his respected supervisor ***Dr. Md. Yeasin Prodhan*** *Associate professor, Department of Biochemistry and Molecular Biology, Hajee Muhammad Danesh Science and Technology University (HSTU), Dinajpur, Bangladesh, for his scholastic supervision, precious suggestion, and continuous encouragement during the entire period of this research work.*

The author is extremely delightful to express his heartfelt respect, and profound appreciation to his benevolent research co-supervisor ***Dr. Md. Azizul Haque****, Associate professor, Department of Biochemistry and Molecular Biology, Hajee Mohammad Danesh Science and Technology University, Dinajpur.for his valuable assistance and indispensable guidance throughout the period of this research work.*

The author thankful to all the other respected teachers in the Department of Biochemistry and Molecular Biology, Hajee Mohammad Danesh Science and Technology University, Dinajpur for their valuable teaching, sympathetic co-operation and inspiration throughout the period of the study. Also, cordial thanks to all the stuffs of the Dept. of Biochemistry and Molecular Biology of HSTU lab for their cooperation to complete the research work.

The authors are thankful to the world academic sciences (TWAS), Swedish international developed agency (SIDA), and UNESCO for funding advanced collaborative research project (grant award_22-020 RG/BIO-OTH/AH_CG) to Dr.Md.Azizul Haque (co-supervisor).

The author also thankful to his respected brother Al-Amin Shitol &Gautam Debnath for help to strain isolation.

The author expresses his sincere appreciation to his beloved parents, well-wisher's, classmates, senior and junior brothers, and sisters for their inspiration, help and encouragement throughout the study.

The Author
June 2023
HSTU
Dinajpur

ABSTRACT

Pesticides are essential for pest control and enhancing crop productivity in modern agriculture, but they can also have detrimental effects on plants and the environment. Phytotoxicity resulting from improper pesticide application can damage plant tissues and compromise crop yield and quality. To address these challenges and promote sustainable agricultural practices, there is a pressing need to explore biodegradable pesticide alternatives that effectively target pests while minimizing harm to non-target organisms and boosting crop yield. In this context, the current research aims to investigate the entire genomic sequence of a novel pesticide degrading strain isolated from eggplants. The strain characterized by biochemical and genomic analysis showed the strain belongs to the *Serratia* sp. group in *Enterobacteriaceae* family. This strain, named *Serratia* sp. strain HSTU-BF1R2, has not been previously reported, making it a promising candidate for pesticide degradation. This study was aimed at a new endophytic bacterium as well as to observe its effects on brinjal in filed trail. Hence, the recently identified using minimal salt agar (MSM) *Serratia* sp. strain HSTU-BF1R2 degrade chlorpyrifos and cypermethrin. It showed significant result on growth promoting effects compared with control in field experiment significant value was ($p<0.05$). The strain genome was found consisting of genome size is 5,134,224 base pairs with a GC content of 59.6%. It contains 918 protein-coding genes, including genes associated with plant biopolymer degradation, suggesting potential applications and it possesses 22 pesticide-degrading proteins, 131 growth-promoting proteins, and 48 stress proteins, indicating potential applications in bioremediation, agriculture, and stress tolerance. Molecular virtual screening identified pesticide ligands and their interactions with proteins, offering insights into their mode of action. The 3D structure of 11 potential model proteins that can degrade pesticides was validated, and virtual screening using 105 different pesticides revealed that the proteins exhibit strong catalytic interaction with organophosphorus pesticides. Selected docked complexes such as *amp*D-cypermethrin, *pepA*-menazon, *pepB*-EPBP, *pepQ*- Azinphos methyl etc explore their catalytic triads in visualization. Overall, this whole-genome analysis of *Serratia* sp. strain HSTU-BF1R2 provides valuable insights into the genetic basis of pesticide degradation, along with virtual screening and molecular docking analyses. This novel endophytic bacteria strain *Serratia* sp. HSTU-BF1R2 holds promise as an intelligent biofertilizer component, contributing to the sustainable cultivation of brinjal.

LIST OF CONTENTS

LIST OF TABLES

LIST OF FIGURES

LIST OF ABBREVIATIONS

Abbreviations	Full Name
g	Gram
ml	Milliliter
µl	Microliter
g/L	Gram per liter
mg/ml	Milligram per milliliter
ng/µl	Nanogram per microliter
et al	And others
pH	Negative logarithm of Hydrogen ion concentration
rpm	Revolutions per minute
V	Volt
U/ml	Units per milliliter
U/mg	Units per milligram
RNA	Ribonucleic acid
DNA	Deoxyribonucleic acid
bp	Base pair
kb	Kilobase pair
NCBI	National Centre for Biotechnology Information
BLAST	Basic Local Alignment Search Tool
°C	Degree Celsius
(NH4)2SO4	Ammonium sulphate
MgSO4.7H2O	Magnesium sulphate heptahydrate
KH2PO4	Monopotassium phosphate
CaCl2 .2H2O	Calcium chloride dihydrate
NaH2PO4	Monosodium phosphate
Na2HPO4	Disodium phosphate
NaOH	Sodium hydroxide
HCl	Hydrochloric acid
NaCl	Sodium chloride
DNS	3,5- Dinitro-salicylic acid
nm	Nanometer
Alk.CuSO4	Alkaline copper sulphate
Psi	Per square inch
dNTP	Deoxynucleotide triphosphate
M	Molar
mM	Millimolar
N	Normal
EDTA	Ethylenediaminetetraacetic acid

UV	Ultraviolet
RFLP PFGE	Restriction Fragment Length Polymorphism Pulsed Field Gel Electrophoresis
ND	Nano Drop
PCR	Polymerase Chain Reaction
RFP	Restriction Fragment Length Polymorphism
SDSPAGE SP	Sodium Dodecyl Sulphate Polyacrylamide Gel Electrophoresis Species
TAE	Tris Acetate EDTA
TBE	Tris Borate EDTA
KDa	Killo Daltone
cm 1	Per centimeter
a.u.	arbitrary unit
OPs	Organophosphates
PGP	plant growth-promoting
NGS	Next generation sequencing
$HClO_4$	Perchloric acid
ANI	Average nucleotide identity
DDH	DNA-DNA hybridization
RAST	Rapid Annotation using Subsystem Technology

CHAPTER I
INTRODUCTION

INTRODUCTION

The utilization of pesticides has ancient origins, tracing back to the beginning of human civilization when agriculture was established to ensure sustenance. Around 2500 BC, the Sumerians were among the first to intentionally use pesticides. They employed malodorous sulfur compounds by applying them to their bodies to manage insects and mites. Now a days, increase crop/food production, the agricultural sector has employed a number of strategies, including the use of pesticides, chemical fertilizers, and synthetic pesticides, which effectively increase the productivity of food and other agricultural commodities(Popp *et al.,* 2013). Approximately 38% of all pesticides used on crops worldwide are organophosphate (OP) insecticides, which are extremely toxic compounds with strong anti-pest action (Zhang *et al.,* 2009). Agrochemicals including pesticides, herbicides, and fertilizers are used excessively and inappropriately, which has serious negative effects on the environment and human health (Dar *et al.,* 2019).In agricultural industry pesticides are organic or inorganic (chemical pesticides) compounds used to control insects and pests. Pesticides come in a variety of forms, including insecticides, herbicides, rodenticides, bactericides, fungicides,(Randall, 2014) lampricides, molluscicides, and insect growth regulators. Animal repellant, rodenticide, antimicrobial, larvicides, etc. Generally, In Bangladesh, there are two different kinds of pesticides: organic and inorganic. pesticides. Inorganic (chemical) insecticides are widely utilized in Bangladesh. There is a significant long-term impact of inorganic pesticides on people and other animals worldwide. The Inorganic pesticides (chemical pesticides) are mostly used by farmers to manage an insect and agriculture field pest. Any agent intended to eliminate, deter, or regulate specific plant or animal life forms that are regarded as pests is referred to as a pesticide. Herbicides are used to eliminate weeds and other undesirable plants, insecticides to control a broad range of insects, fungicides to stop the growth of mold and mildew, disinfectants to stop the spread of germs, and chemicals to keep mice and rats in check are all examples of pesticides.

The primary goal of using pesticides is to control insects and other pests in agriculture fields (EPA, 2018). Farmers employ pesticides because insects and other pests reduce crop yields to their maximum. Pesticides are used by farmers to avoid agricultural yield loss. The soil is severely harmed by pesticides and pesticides that include heavy metals or metals. The soil's fertility and production are reduced. We should use fewer pesticides

that include heavy metals to manage insects and pests to advance sustainable agriculture. A variety of insecticides, including those with arsenic, zinc, lead, and cadmium, among others, include heavy metals (Damalas & Eleftherohorinos, 2011).The inorganic elements known as heavy metals have a specific gravity that is five times greater than that of water (Fergusson, 1990). The usage of pesticides that contain heavy metals results in the heavy metals entering the food chain and having a detrimental impact on both human and animal health. Pesticide degradation is a process that reduces heavy metal-containing insecticides to simple, tiny particles. Pollutants and heavy metals seriously harm the environment's ecology. The breakdown of pesticides a significant phenomenon that aids in cleaning up toxic soils and water sources. It has been demonstrated that a variety of parameters, including soil moisture content, soil texture, and the mineral composition of the soil. Recently, it has been demonstrated that metals in the soil can impact how quickly pesticides degrade. These metals either come through the long-term application of wastewater and animal manures to agricultural soils or come from the addition of pesticides to the soil. Metals influence the breakdown of pesticides by stimulating their photolysis or hydrolysis or by regulating the activity of microorganisms. Similar to this, complete interactions between metals and pesticides may slow down the rate of pesticide breakdown (Helal *et al.,* 2006).

Bacteria that develop and are detected inside of plants are known as endophytic bacteria. Almost all plants have endophytic bacteria, which infiltrate the interior tissues of their hosts and can create a variety of interactions, including symbiotic, mutualistic, and communalistic ones. Although most endophytes seem to come from the rhizosphere or phyllo sphere, some may spread via the seed. In addition to acting as biocontrol agents, endophytic bacteria can enhance plant growth and productivity. By generating a variety of natural products that may be harvested for possible use in industry, agriculture, or medicine, endophytes can also be advantageous to their host. They may also improve phytoremediation, which can eliminate soil pollutants, and they may contribute to soil fertility through phosphate solubilization and nitrogen fixation. In the present study, one endophytic and pesticide degrading bacterium HSTU-BF1R2 was isolated from eggplant root. Based on the analysis of the complete genome and phylogenetic tree and BLAST from NCBI we confirmed that HSTU-BF1R2 was classified as member of the *Enterobacteriaceae, Serratia* family and named as *Serratia* sp. strain HSTU-BF1R2. It's a gram-negative bacterium. The family *Enterobacteriaceae* contains a large number of

genes that are found in different natural environments and are closely related biochemically and genetically. Here, we present the analysis of biochemical and molecular characterization, plant growth promoting test (PGPT), complete genome sequence, growth promoting activity check by root length, shoot length, leaf length, fresh weight, dry weight. as well as discovering plant growth promoting genes such as nitrogen fixing, phosphate solubilizing, IAA producing etc. With identification of genes responsible for the degradation of pesticides such as chlorpyrifos, cypermethrin etc. from the whole genome sequence of isolated bacterium. And finally, represent pesticide degrading capability investigation of HSTU-BF1R2 genome by Pesticide biodegradation in liquid medium analysis and various types of computational chemistry and biology technique.

Objectives of the research work:

1. To isolate pesticides mineralizing endophytic bacteria from eggplant root.
2. To screen the isolated endophytic bacteria by Biochemical test analysis and Morphological characteristic.
3. To investigate the biodegradation of pesticides in a liquid medium.
4. Molecular identification using whole genome sequencing and analysis.
5. To identify pesticide degrading and growth promoting genes from the complete genome sequence.
6. To investigate catalytic interaction of pesticide degrading protein-ligand complexes by molecular docking.

CHAPTER II
REVIEW OF LITERATURE

REVIEW OF LITERATURE

Pesticides, often seen as poisons, not only harm targeted pests but also pose risks to humans, animals, and the environment. Human exposure to pesticides can lead to various health issues, including respiratory, reproductive, gastrointestinal, and neurological disorders, and even cancer (Nicolopoulou-Stamati, 2016). Living beings can be exposed to pesticides through direct skin contact, inhalation, or ingestion. Once inside the body, pesticides may undergo metabolism, excretion, storage, or bioaccumulation (Nicolopoulou-Stamati *et al.*, 2016) , (Stoytcheva, 2011). The adverse effects of pesticides are not limited to human health and environmental contamination. They can also impact plant germination, physiological processes, and biochemical activities, ultimately affecting crop yields. For instance, the germination rate in Zea mays L. cv NAAC-6002 significantly decreases following pendimethalin treatment (Rajashekar & Murthy, 2012).Those at risk of exposure include sprayers, production workers, mixers, formulators, loaders, and agricultural farm workers. Workers involved in manufacturing and preparing pesticide formulations face greater risks (Aktar *et al.,* 2009). On the other hand, tree planters working with chemical fertilizers did not show increased inhalation or dermal exposure to metal contaminants such as arsenic (As), cadmium (Cd), chromium (Cr), lead (Pb), nickel (Ni). However, there was a weak connection between dermal and respiratory irritation and working with chemical fertilizers (Gorman Ng *et al.,* 2013). Chemical fertilizers typically contain essential nutrients necessary for plant growth, such as nitrogen, phosphorus, and potassium (NPK). They also include micronutrients like copper (Cu), iron (Fe), manganese (Mn), and zinc (Zn). However, these fertilizers may also contain harmful heavy metal contaminants such as arsenic (As), cadmium (Cd), chromium (Cr), and lead (Pb) (Marrone, 2007).These chemical fertilizers can potentially lead to adverse health effects, even at low levels. Studies have documented that such exposure is linked to contact dermatitis and respiratory problems (Hooper *et al.,* 2001). For instance, cases of contact dermatitis were reported in chemical laboratory factory workers due to nickel in fertilizers, in fertilizer factory workers due to phosphates, and in farmers using calcium ammonium nitrate (Witheetrirong *et al.,* 2011). Long-term exposure to chemical fertilizers can result in decreased lung functions, possibly leading to restrictive lung disorders(Hooper *et al.,* 2001). Research indicates that exposure to chemical fertilizers significantly increases the risk of respiratory symptoms (Strobel *et al.,* 2004). High levels of ammonia exposure have been linked to an increased prevalence

of respiratory symptoms and acute reduction of lung functions among urea fertilizer factory workers. Another concern lies in the impact on beneficial soil microorganisms. Pesticides have been shown to exhibit direct lethal effects on these helpful microbes (Staley *et al.,* 2015), disrupting the natural balance in soil ecosystems. To address these challenges, researchers have been exploring various strategies for the degradation of pesticide residues in soil and water. Studies have focused on biodegradation by microorganisms, photodegradation, chemical degradation, and other environmentally friendly approaches (Kaur *et al.,* 2021). The common organophosphate pesticides used in agriculture are chlorpyrifos, diazinon, cypermethrin and Pyrethroids.

Chlorpyrifos

Organophosphorus pesticides constitute a significant group of pesticides, accounting for approximately 38% of global pesticide consumption. These pesticides have replaced organochlorines due to their effectiveness in reducing crop loss caused by pest attacks and improving crop yields. Among the broad-spectrum organophosphates, Chlorpyrifos (O,diethyl O3,5,6-trichloro-2-pyridyl phosphonothioate) is widely used to control various agricultural and household pests. It finds applications in protecting crops such as cotton, rice, sugarcane, peanuts, tobacco, vegetables, fruits, and ornamental plants from sucking, chewing, and boring insects. Chlorpyrifos ranks as the fourth most extensively used organophosphate pesticide, following monocrotophos, acephate, and endosulfan (Ansaruddin & Vijayalakshmi, 2003). CPY adsorbs to surficial sediments in water-bodies, and residues of CPY have been detected in surficial sediments in streams and creeks in areas of use. In a few cases, observed toxicity in sediments collected from agricultural drains, creeks, and rivers in California was linked to the presence of CPY (Phillips *et al.,* 2012) (Weston *et al.,* 2015). However, in most locations CPY contributed less to toxicity of sediments than other pesticides such as pyrethroids (Amweg *et al.,* 2006),(Phillips *et al.,* 2012).CPY is bioconcentrated and/or bioaccumulated into aquatic organisms to a limited extent. Measures of bioconcentration factors (BCFs), bioaccumulation factors (BAFs), and biota-sediment accumulation factors (BSAFs) are relatively small (Mackay *et al.,* 2014). One literature report gave a biomagnification factor (BMF) infish; the value was 0.32 for *Aphaniusiberus* sp.*(Varo et al.,* 2002), which is not indicative of biomagnified cation. The direct effects of CPY will occur at much smaller exposure concentrations than in organisms that lack the target enzyme, such as

plants. Insects and crustaceans are generally more sensitive to CPY than are fish or amphibians (Giesy *et al.,* 1999).

Pyrethroids

Pyrethroids are widely recognized as the most commonly used pesticides(Allinson *et al.,* 2015). Because of their extensive application, pesticides are considered a major contributor to pollution (Hua & Relyea, 2014). Pyrethroid insecticides are synthetic compounds derived from pyrethrins, which are naturally occurring substances found in certain plants like Tanacetum cinerarieafolium or Chrysanthemum cinerariifolium(Vázquez *et al.,* 2008) (Anadón *et al.,* 2009). The chemical structure of pyrethroids is obtained from acids and alcohols present in chrysanthemum acid (ethyl 2,2-dimethyl-3-(1-isobutenyl) cyclopropane-1-carboxylate) (Soderlund, 2012). These insecticides have extensive applications in agriculture for insect control and in managing ectoparasitic infections in both humans and animals (Barbini *et al.,* 2007)..Both pyrethroids and pyrethrins display high toxicity towards the targeted pests, but they quickly degrade in the environment when exposed to appropriate levels of temperature, light, and moisture (Salako *et al.,* 2020). This degradation process generally takes place within one or two days under sunlight and suitable atmospheric conditions. Due to their rapid degradation and low persistence, pyrethroids are considered promising alternatives to conventional pesticides, as they pose minimal risk of groundwater contamination(Bradberry *et al.,* 2005). Pyrethroids are classified into two types based on their chemical structure: (1) Type I, which includes allethrin, tetramethrin, permethrin, resmethrin, and bioresmethrin, and (2) Type II, which comprises cyfluthrin, deltamethrin, cyphenothrin, and Cypermethrin.

Cypermethrin

Cypermethrin is a synthetic pyrethroid insecticide widely used to control various pests in agricultural and domestic settings. It is effective against moth pests in cotton, fruit, and vegetable crops and is also employed for crack, crevice, and spot treatment in various buildings and transportation modes. Additionally, it is used for controlling ectoparasites in cattle, sheep, and poultry. Cypermethrin has four major generations of synthetic pyrethroids, and it degrades relatively quickly in the environment under certain conditions. The pesticide's degradation occurs through photodegradation and microbial

degradation, and it binds tightly to soil particles, minimizing leaching concerns. Although cypermethrin is considered moderately persistent in soils, it is less persistent in sandy soils and under aerobic conditions. The insecticide hydrolyzes more rapidly under alkaline conditions. While cypermethrin has shown toxicity to aquatic species and honeybees, there have been no significant human health issues identified. Some formulations of cypermethrin are classified as Restricted Use Pesticides (RUP) due to their toxicity to fish and may only be used by certified applicators. For any pesticide, caution should be exercised in handling and application to minimize its impact on the environment and human health. Careful usage and adherence to guidelines are essential to prevent adverse effects on the ecosystem and potential health hazards.

Pesticide-Resistant Endophytic Bacterial Diversity

A diverse range of plant-associated bacteria, particularly belonging to the α, β, and γ classes of Proteobacteria, play a crucial role in aiding their host plants in the degradation of toxic organic pesticides (Tétard-Jones & Edwards, 2016). For instance, when Pisum sativum (pea) was inoculated with Pseudomonas putida POPHV6, derived from poplar trees, the bacteria enhanced the removal of 2,4-dichlorophenoxyacetic acid from the soil, and the aerial parts of the pea plant showed no accumulation of the pesticide (Germaine *et al.,* 2006). In a study involving Phragmites communis, Nymphaea tetragona, and Najas marina, eight genera of plant-associated bacteria, including *Bacillus* sp., *Microbacterium* sp., *Paenibacillus* sp., *Aeromonas* sp., *Flavobacterium* sp., *Klebsiella* terrigena, *Pantoea* sp., and *Pseudomonas* sp., were found to possess high rates of pesticide degradation (Chen *et al.,* 2012). Another noteworthy example is *Streptomyces* sp. atz2, isolated from sugarcane leaves, which demonstrated the ability to decrease the concentration of atrazine, a herbicide, and subsequently produced non-toxic metabolites (Mesquini *et al.,* 2015). These findings highlight the beneficial role of plant-associated bacteria in mitigating the harmful effects of pesticides and their potential as environmentally friendly tools for pesticide degradation.

Pesticide Detoxification

Bacterial degradation of pesticides is facilitated by enzymes and influenced by environmental factors like temperature, water potential, pH, and soil nutrient composition (D.K.Singh,2008). Certain bacterial species, including *Pseudomonas,*

Acinetobacter, Flavobacterium, and *Arthrobacter*, harbor catabolic plasmids that encode for pesticide-degrading enzymes (Sayler *et al.,* 1990). Both gram-positive and gram-negative bacteria are known to participate in the biological degradation of various pesticides. For example, Stenotrophomonas maltophilia has demonstrated the ability to detoxify polyaromatic hydrocarbons and xenobiotic compounds (Juhasz *et al.,* 2000); (Lee *et al.,* 2002). The M1 strain of S. maltophilia can degrade methomyl, an extremely toxic pesticide, thanks to the presence of a plasmid (PMb) responsible for this degradation (Nawaz *et al.,* 2011). This plasmid can be transferred to other bacterial strains, potentially enhancing their ability to degrade methomyl.Similarly, the pesticide aldicarb, which is hazardous to human health, can be degraded by bacterial enzymes called esterase and amidase(Burgess *et al.,* 1994); (Lifshitz *et al.,* 1997); *(Saptanmasi et al.,* 2008); (Nawaz *et al.,* 2011). *S. maltophilia* has also been found to contribute to aldicarb degradation by producing esterase enzymes. Additionally, other bacteria like *Alcaligenes denitrificans, Enterobacter gergoviae, Flavimonas oryzihabitans,* and *Bacillus subtilis* have been identified as participants in the degradation of aldicarb (Saptanmasi *et al.,* 2008).These findings underscore the crucial role of bacterial enzymes and plasmids in pesticide degradation and present promising avenues for harnessing bacterial capabilities to counteract the environmental impact of harmful pesticides.

Stress Tolerance in Plants

Drought Stress:

The plant-associated microbiome has been shown to influence plant traits and stress tolerance, including growth and adaptation to biotic and abiotic stresses such as drought (Mendes *et al.,* 2011); (Luo *et al.,* 2012);(Marasco *et al.,* 2012). Drought stress poses a significant threat to agriculture worldwide, and the role of the plant-associated microbiome in aiding plant adaptation to drought is not fully understood. Studies have demonstrated that certain plant growth-promoting bacteria can enhance plant growth under drought conditions in a stress-dependent manner (Rolli *et al.,* 2015). Some bacteria, like *Achromobacter piechaudii ARV8,* enhance drought stress tolerance in plants through the enzyme 1-aminocyclopropane-1-carboxylate (ACC) deaminase, which may inhibit ethylene synthesis and reduce plant stress (Glick *et al.,* 2007) (Arshad *et al.,* 2008) (Duan *et al.,* 2009).

Bacterial priming has shown promising results, significantly increasing plant biomass and photosynthesis under severe drought conditions (Timmusk 10 et al., 2014) (Timmusk et al., 2017). Inoculation with certain bacteria, such as Burkholderia phytofirmans PsJN, has resulted in increased photosynthesis, water use efficiency, chlorophyll content, and grain yield in drought-stressed wheat and maize (Naveed *et al.,* 2014). Microbes isolated from the roots of plants growing in extreme dry conditions have been found to improve the growth of other host species under similar conditions, suggesting a stress-resistance strategy (Marasco *et al.,* 2013). Plant growth-promoting bacteria have demonstrated improved growth in various crops, including sunflower, pea, sorghum, tomato, pepper, rice, common bean, and lettuce, under drought conditions(Alami *et al.,* 2000);(Creus *et al.,* 2004)

Heavy Metal Stress:

Heavy metal contamination resulting from increased industrialization has become a major concern as heavy metals are non-degradable (Kidd *et al.,* 2009);(Rajkumar *et al.,* 2012). Traditional techniques to remove contaminants have proven expensive, environmentally unsafe, and not widely accepted by the public (Boopathy, 2000) (Doble & Kumar, 2005). Phytoremediation, using plants to eliminate soil contaminants, offers a cost-effective and environmentally friendly solution with high public acceptance (Hadi & Bano, 2010) (Beškoski *et al.,* 2011).An alternative approach involves leveraging plant-associated microbiomes to enhance metal uptake by modifying metal mobility and bioavailability in the rhizosphere (Ma *et al.,* 2011). These microbiomes produce plant growth-promoting substances, like hormones, siderophores, and ACC deaminase, which improve plant growth in metal-contaminated soils (Babu & Reddy, 2011). However, high soil contamination can limit phytoremediation due to oxidative stress and reduced microbial density (Gerhardt *et al.,* 2009), Common heavy metals like Mn, Cd, Pb, Cr, Zn, Al, Cu, and metalloids such as Sb and As are known to be toxic (Duruibe *et al.,* 2007). Rhizosphere bacteria are particularly important for phytoremediation, as they can enhance the process by altering soil pH and oxidation/reduction reactions (Khan *et al.,* 2009). Various bacterial species, including Microbacterium sp. G16 and Pseudomonas fluorescens G10, have been shown to increase lead (Pb) solubility in plants through the production of specific substances (Sheng et al. 2008). Mycorrhizal fungi are also significant contributors to phytoremediation, especially for heavy metal-tolerant hyperaccumulators (Zarei *et al.,* 2010).

Whole-genome sequencing:

In recent years, new DNA-sequencing techniques have been developed and made available for easy and cheap sequencing of bacterial genomes. These post-Sanger' sequencing techniques are commonly referred to as 'next generation-sequencing' (NGS). NGS includes sequencing technologies that have high sequence capacity, but produce short sequences (e.g., as developed by Illumina and Ion Torrent), which is compensated for by high sequence coverage. Multiple Next-Generation Sequencing (NGS) platforms with various chemistries are available for high-throughput DNA sequencing, and more technologies are under development (Ansorge, 2009) (Fuller *et al.,* 2016). Illumina is one of the widely used platforms, utilizing reversible fluorescent dideoxy terminators for DNA sequencing on disposable flow cells. Illumina offers different options, such as the iSeq 100 and HiSeq X Ten, capable of producing up to 1.2 billion to 1.8 trillion bases of sequence per run, enabling population-level sequencing of animal and plant genomes. The NovaSeq 5000 and 6000 are recent additions to their platform selection, allowing users to tailor output to their needs. Illumina platforms generate short-read sequences, with a maximum of 2 × 300 bases for paired-end reads available on the MiSeq sequencer. Alternatively, Ion Torrent technology is available, providing short reads with its own advantages, like cost efficiency, but comes with some drawbacks, such as a higher homopolymer error rate (Divoll *et al.*, 2018); (Laehnemann *et al.*, 2016). Ion Torrent utilizes semiconductor technology to detect H+ ions released during DNA strand elongation. In longer reads, the single molecule real-time (SMRT) sequencing of Pacific Biosciences (PacBio) can be employed. SMRT sequencing incorporates fluorescently labeled nucleotides into replicating DNA molecules. PacBio platforms are known for producing relatively long reads, up to around 60 kilobases (kb) with the Sequel system. Although initial concerns about high error rates have been addressed by circularizing DNA molecules, not all reads produced will be high-quality and will be of shorter length (Rhoads & Au, 2015). Oxford Nanopore Technologies offers a different long-read technology through the portable MinION device and benchtop PromethION. These products use nanopores to infer DNA sequence by detecting changes in potential difference across the pore. Though nanopore technology still faces challenges with error rates, new pore chemistries are improving its performance. Notably, nanopore technology has the potential to produce extremely long sequence reads, in the order of megabases. Long-read technologies are valuable for resolving complex genome arrangements and sequencing long PCR amplicons.

Molecular Docking:

Molecular docking has emerged as a crucial tool in drug discovery, facilitating the prediction of ligand-receptor complex structures through computational methods. In this review, we provide an overview of available molecular docking methods, their development, and their applications in drug discovery. We summarize the relevant basic theories, including sampling algorithms and scoring functions, and discuss the performance of existing docking software. One of the challenges in docking is the flexible receptor molecular docking, particularly when considering backbone flexibility in receptors. To address this issue, a promising solution called the Local Move Monte Carlo (LMMC) based approach has been recently introduced (Meng *et al.,* 2011). The process of molecular docking involves two main steps: sampling conformations of the ligand in the active site of the protein, followed by ranking these conformations using a scoring function. Ideally, the sampling algorithms should be able to reproduce the experimental binding mode, and the scoring function should accurately rank the highest affinity poses among all generated conformations. To achieve ligand mapping into the protein's active site based on molecular shape, matching algorithms (MA) are used. The ligand and protein are represented as pharmacophores, and their distances are calculated to find potential matches. This approach accounts for chemical properties such as hydrogen-bond donors and acceptors during the match. Matching algorithms offer speed advantages and are beneficial for enriching active compounds from large libraries. The scoring function's role is crucial in distinguishing correct binding poses from incorrect ones and active compounds (binders) from inactive ones in a computationally efficient manner. However, scoring functions involve estimation rather than direct calculation of the binding affinity between the protein and ligand, incorporating various assumptions and simplifications. These scoring functions can be categorized as force-field-based, empirical, or knowledge-based scoring functions (Sousa *et al.,* 2006).

CHAPTER III
MATERIALS AND METHODS

MATERIALS AND METHODS

3.1. Study of location:

The experiment was carried out in the Hajee Mohammad Danesh Science and Technology University (HSTU), Dinajpur's biochemistry and molecular biology research lab.

1. Isolation of strain HSTU-BF1R2
2. Genomic DNA isolation.

3.2. Glassware and laboratory equipment handling:

All the laboratory apparatus that was used, such as- Conical flasks, glass pipettes, beakers, glass rods, petri plates, micropipette tips, Eppendorf tubes, falcon tubes, PCR tubes, and other laboratory supplies used in this work were all autoclaved at 121°C in 15-unit pressure for 15 minutes before to use to ensure they were sterile.

3.3. Solutions and reagents:

The necessary reagents and solutions for the study were freshly prepared before use. From the lab, all necessary chemicals were obtained. Since all the solutions and reagents were of the reagent grade, they were not further refined. In Appendix A, a list of reagents is provided.

3.4. Media:

In this research, various medium types have been used for specific growth, enrichment culture, and the identification of certain features. According to the procedure and standard recipe in appendix B, media preparation and sterilization were carried out Isolation.

3.5. Instruments:

Electronic Balance, Shaking Incubator, Spectrophotometer, Digital pH meter, Centrifuge, Magnetic stirrer hot plate, Autoclave, Laminar Air Flow Clean Bench, Vortex shaker, Refrigerator (LG) and Microscope etc.

3.6. Pesticide (chlorpyrifos and cypermethrin) collection:

Pesticides (chlorpyrifos and cypermethrin) that are used at the time of experiment collected from the Dinajpur town. During the pesticides collection the quality of different ingredients is checked carefully.

3.7. Isolation of pesticide degrading endophytic bacteria from brinjal plant root:

Washing the samples with running tap water

Surface sterilization using 75% (v/v) ethanol for 2 minutes.

Washing the samples with autoclaved distilled water

Smashing the samples with a mortar and pestle

Addition of distilled water into this paste and then the mixture was poured into test tube

Finally, inoculation of that sterilized sample into PVK agar (Pikovskayas Agar) media

And then the isolates were grown in pesticide containing media.

The eggplant root sample was collected from research field at Hajee Mohammad Danesh Science and Technology University (HSTU), Dinajpur, Bangladesh and transported to the laboratory. The sample was then serially diluted, and the bacteria were then transferred to nutritional agar media using the spread plate technique. The plates with distinct bacterial colonies were those chosen for further performed. The endophytic and pesticide degrading root containing bacteria was isolated in the following ways: Firstly, the roots were cut from the plant sample was washed out by running tap water. Then it was surface sterilized with 70% ethanol for 1 minute then with 0.01% mercuric chloride

for 5 minutes and followed by 0.5% Sodium chloride for 5 minutes. Finally, it was treated with sterile distilled water 5 times and then the roots sample was cut down into small pieces. Then the sample was macerated separately in phosphate buffer of pH 7.2 with a sterile pestle and mortar. After that the sample was spread on Pikovskaya‘s (PKV) agar medium plate. Then the plate was incubated at 37°C for 24 hours. Finally, the bacterial isolate was picked from plates and purified by streaking techniques and incubated at 37°C. Several biochemical tests were conducted for cultural and morphological characterization. The isolate was kept on agar plats at 40^0C for further analysis. Furthermore, the isolate was preserved in 80% (v/v) glycerol at −20°C.

3.8. Phenotypic identification of bacterial strain

The potential lignocellulose degrading strains were observed under microscope to study their properties.

3.9. Morphological & Biochemical characterization

The selected bacterial strains were differentiated based on their metabolic pattern by using different biochemical tests(Bergey, 1994) including catalase, oxidase, MR-VP, TSI, Citrate utilization, Indole, MIU and Individual sugar fermentation tests (dextrose, lactose, maltose and sucrose) (Shahzad *et al.*, 2012). Morphological features were identified by growing the isolated cultures on the minimal nutrient media (composition: $(NH_4)2SO_4$, 0.1%, KH_2PO_4, 0.05%; K_2HPO_4, 0.05%; $CaCl_2$, 0.01%; NaCl, 0.01%; $MgSO_4.7H_2O$, 0.02%; yeast extract, 0.1%, and cellulose, 0.2%) (Bergey, 1994).

3.10. Biochemical characterization:

In biochemical tests were carried out for the bacterial isolate. The following biochemical tests were performed using 24 hours fresh bacterial cultures grown on TSB agar media. The media were autoclaved at 121°C for 15 minutes at 15 psi, whenever required. Methods from Bergey’s Manual of Systematic bacteriology was used for the biochemical identification of the isolates.

3.10.1. Catalase test:

The catalase test was performed by taking a drop of 3% H_2O_2 on a glass slide and mixing it with a small amount of endophytic bacterial culture using an inoculating needle. A positive test result was indicated by the rapid and sustained production of gas bubbles or

effervescence. Conversely, the absence of bubble formation indicated a negative result according to (Aneja, 2007)..

3.10.2. Oxidase test:

The oxidase test was conducted to determine the presence of the oxidase enzyme in different endophytic bacterial isolates. To prepare Kovac's reagent, 1% *N, N, N, N*-tetramethyl-phenylene diamine dihydrochloride was dissolved in warm water and stored in a dark bottle. A strip of filter paper was then immersed in the reagent and allowed to air-dry. Using a sterile wire loop, one-day-old endophytic bacterial colonies from agar plates were transferred onto the filter paper strip. In a positive reaction, the reagent was oxidized, resulting in the development of an intense blue-violet color within 1 minute (Mahmoud *et al*.,) (Shields & Cathcart, 2010).

3.10.3. Citrate utilization test (CIU):

The Citrate utilization test is used to determine the ability of bacteria to utilize sodium citrate as its only carbon source. The endophytic isolates were inoculated into test tubes having Simmons citrate agar medium and incubated for 48 h at 37 °C. Simmons citrate agar contained citrate as its only carbon and energy source. The presence of growth and change of color from green to blue due to pH change indicated positive reaction. No color change shows negative for citrate utilization (Aneja, 2007).

3.10.4. Methyl red (MR) test:

The Methyl red test was done to determine the ability of the bacteria to oxidize glucose with the production and stabilization of high concentration of acid end products. Prepare required amount of Glucose Phosphate Peptone Water (GPPW) broth media and place it into test tube and autoclaved at 121°C for 15 minutes at 15 psi. After sterilization the test GPPW broth was inoculated with pure culture of endophytic bacteria and incubated at 30±2°C for 48 hours. Finally, after incubation, added 5 drops of an alcoholic solution of methyl red reagent directly to the broth in the test tube. The development of stable red color indicated the positive test and yellow or intermediate orange color was negative (Seeley Jr & VanDemark, 1962).

3.10.5. Voges-Proskauer (VP) test:

The Voges-Proskauer (VP) test was done to determine if an organism produces acetyl methyl carbinol from glucose fermentation. Prepare required amount of Glucose Phosphate Peptone Water (GPPW) broth media and place it into test tube and autoclaved at 121°C for 15 minutes at 15 psi. After sterilization the test GPPW broth was inoculated with pure culture of endophytic bacteria and incubated at 30±2°C for 48 hours. After incubation, added 0.6 ml of alpha-naphthol (5 per cent solution in 70 per cent ethyl alcohol) followed by 0.2 ml of KOH (40%). The tube was shaken gently to expose medium to atmospheric oxygen and allowed tube to remain undisturbed for 10-15 minutes. The positive reaction of acetyl methyl carbonyl production 28 was indicated by development of red color. This indicates positive result for the VP test (Harry Jr & VanDemark, 1981).

3.10.6. Urease test:

A loopful of the bacterial culture were aseptically inoculated into sterile Christensen's urea broth containing the pH indicator phenol red using a sterile wire loop and incubated at 30°C for 24 hours. Development of pink color will be considered as positive test (Cappuccino & Sherman, 2005).

3.10.7. Triple sugar iron agar test (TSI):

TSI agar was used to detect late or non-lactose fermenters and dextrose fermenters. The medium also helped to determine the ability of the organisms to produce Hydrogen Sulfide (H_2S). To perform this test, suspend 65 grams of TSI agar in 1000 ml of distilled water, which has containing three sugars (Lactose, Sucrose, and Glucose) and iron and it contains agar as a solidifying agent (TSI is a semi solid media having slant and butt). The ingredients used Triple Sugar Iron Agar (TSI) are Lactose, Sucrose and Glucose in the concentration of 10:10:1 (i.e., 10-part Lactose (1%), 10-part Sucrose (1%) and 1 part Glucose (0.1%)). The organisms under study were heavily seeded with a platinum needle over the surface of the slant and stabbed into the butt of the tubes of TSI agar. After an aerobic incubation period of 24 h at 37°C, aerobically the tubes were examined for all changes in the slant or in the butt. In TSI agar slant, the presence of yellow color and gas bubbles in the media were considered as production of acid and gas respectively in slants or in butt. The red or dark pink coloration of the media in slant or in butt was considered

as alkaline reaction. The black coloration in any part of media was considered as the production of H_2S (Hydrogen Sulfide) (Ako-Nai *et al.,* 1999).

Table 1: TSI result evaluation parameters.

Slant/Butt condition	Slant/Butt colour	Decision taken	Gas formation
Alkaline slant/Alkaline butt	Red/Red	Glucose, lactose and sucrose non-fermentation	Depending on the visibility of bubbles or crack in the test tubes
Alkaline slant/ Acidic butt	Red/Yellow	Glucose fermentation only	Depending on the visibility of bubbles or cracks in the test tubes
Acidic slant/Acidic butt	Yellow/Yellow	Glucose, lactose and sucrose fermentation	Depending on the visibility of bubbles or cracks in the test tubes

3.10.8. Motility indole urease (MIU) test:

MIU test was done for determining the motility of bacteria, indole production and urea degradation by means of the enzyme urease. Casein enzymic hydrolysate provides amino acids and other nitrogenous substances. Sodium chloride maintains osmotic equilibrium. Dextrose is fermentable carbohydrate. Phenol red is the pH indicator which turns pink-red in alkaline conditions. The test cultures are stab inoculated. Motility and urease reactions are read before testing indole production. Motile organisms show either diffused growth or turbidity extending away from stab inoculation line while no motile organisms grow along the stabling. Organisms that utilize urea produce ammonia which makes the medium alkaline, showing pink-red color by changing in the phenol red indicator. Indole is produced from tryptophan present in casein enzymic hydro lysate. The indole produced combines with the aldehyde present in the Kovac's reagent to form a red complex. The ingredients used are Caseinenzymichydrolysate2000, Dextrose 0.200, Sodium chloride 1.000, Phenol red 0.002, and agar 0.400 all in Gm/200L, finally pH (at 37°C) 6.8±0.2 Formula was adjusted, standardized to suit performance parameters. The test tubes were incubated at 37°C for 24 hours after inoculation of bacterial sample in clean bench. Then the colour of the media was examined, and the

results were recorded. Formation of a rose red ring at the top indicates a positive result. A negative result can have a yellow or brown layer(Cappuccino & Sherman, 2005).

Table 2: MIU results evaluation parameter

Condition	Positive	Negative
Urea	A colour change from yellow to orange to pink/red	No colour change
Motility	A cloudy mass of bacteria is seen	Hazy medium without any accumulation
Indole	Pink mauve colour on the bottom of the tube	No pink mauve colour is formed

3.10.9. Fermentation of sugar: lactose, maltose, sucrose, dextrose:

Specific sugar fermentation test was done using phenol red carbohydrate broth to observe if the selected isolates can utilize these sugars. Different sugars (Lactose, Maltose, Dextrose, and Sucrose) media were made according to protocol provided by the manufacturers and 6ml of the media were transferred into each test tube. The final pH of 7.4 ± 0.2 was maintained (Rutter & Collee, 1969). After that the selected isolates were inoculated and incubated at 37°C for 24 hours. The appearance and color of the media was observed after incubation. After incubation the tubes that turned yellow because of acid production by the bacteria were taken as a positive and the ones with no color change were indicated as negative.

3.11. Growth promoting effect of eggplant by *Serratia* sp. strain HSTU-BF1R2

3.11.1. Field experimentation:

Twenty-one (21) days old Eggplants were collected from Raniganj Bazar in Dinajpur, Bangladesh, and then planted in a field adjacent to the Central Mosque of Hajee Mohammad Danesh Science and Technology University, Dinajpur, following a randomized complete block design (RCBD) with three replications. The field experiment involved three types of treatments: T1 with 30% urea and bacterium, Tc with 100% urea as recommended dose but no bacterium, and T0 as the control with no urea and no bacterium. Acinetobacter sp. HSTU- BF3R3 bacterial liquid medium was applied at a rate of 200ml per plot. Each experimental plot covered an area of 1.44 m^2, containing 3

rows measuring 1.20 m in width and 1.20 m in length. The eggplants were sown using the hand drill method, maintaining a row-to-row distance of 40 cm and a spacing of 40 cm, with three plants in each line. The plants were adequately irrigated throughout the experiment. The treatments were applied four times: the first treatment immediately after planting, the second treatment 7 days after planting, the third treatment 14 days after plantation, and the fourth treatment applied 28 days after planting. After 30 days, 45 days, and 60 days of plantation, root length, shoot length, leaf length, number of branch and flower were observed and recorded for analysis.

3.12. Statistical analysis:

Data collected from the present study were assessed with an emphasis on effects of endophytic bacteria on eggplant. Each data was recorded in 3 replicates. Root length, shoot length, germination percentage, seedling length, vigor index, fresh weight and dry weight were analyzed through one way ANOVA method by R version 4.1.2 (2021-11-01) -Bird Hippie. All data were expressed as the mean value and standard deviation of total measurements for 3 replicates where significant differences were performed by using fisher‘s protected LSD test at $\rho \leq 0.05$. Graphical analysis along with standard error was conducted by Microsoft office excel 2013.

3.13. Technical protocol of whole genome sequencing:

3.13.1. DNA extraction, Library preparation, whole genome sequencing:

Genomic DNA Extraction Kit was used to extract genomic DNA of *Serratia* sp. strain HSTU-BF1R2. The library preparation and whole genome sequence was done by using Illumina MiSeq System (Illumina, Inc.). Which was performed in Central Laboratory of HSTU, Dinajpur, Bangladesh by the following ways.

3.13.2. DNA Extraction:

Requirements: Nuclease free water 400 µL, lysis buffer 200 µL, sample: Single colony, Eppendorf tube, Loop/Pipette tip, Maxwell FSC cartridge, Elusion tube, Elusion buffer 60 µL

Procedure:

- First, 400 µL Nuclease-free water was taken in an Eppendorf tube.

- Then, the bacterial colony was collected with a loop/sterile pipette tip and immediately transferred to the Eppendorf tube.
- Next, 200 µL Lysis buffer was added to the same Eppendorf tube and vortexed finely.
- Finally, 400-500 µL sample-containing solution was transferred to reagent cartridge tube 1 (1 no whole positioned just before the magnetic beads whole).
- Then, the sample-containing reagent cartridge was placed inside the machine (N.B. Sample-containing whole of the reagent cartridge was placed inside the machine).
- The plunger was added to 8 no whole, and an elution tube was taken. 60 µL elution buffer was transferred to the elution tube, and the buffer-containing tube was placed just forward of the 8 no whole of the cartridge.
- Finally, the machine was started to extract DNA samples.
- The machine took 40-45 minutes for extraction. After 40-45 minutes, the machine door was opened, and the elution tube (containing DNA) was collected, and the cartridge tube was discarded.

3.13.2.1. DNA concentration measurement:

Requirements: Fluorometer, dsDNA dye-200 µL, standard reagent, extracted DNA sample Procedure

- At first, three (3) fluorometric Eppendorf tubes were collected and labeled as blank, standard, and test, respectively.
- Then, 200 µL of dsDNA dye was added to all three fluorometric Eppendorf tubes, and 2µL of standard reagent was added to the standard tube. Simultaneously, 2 µL of extracted DNA was transferred to the tube labeled as test.
- After that, all three fluorometric Eppendorf tubes were vortexed for mixing.
- Incubation was conducted for 5 minutes in a dark place. After five minutes, measurements were taken of the blank, standard, and test tubes using a fluorometer.

3.13.3. Library Preparation

3.13.3.1. Tagmentation of Genomic DNA:

Requirements: Extracted DNA 5-6 µL, nuclease free water 24-25 µL, Eppendorf tube, bead linked transposomes (BLT)-11 µL, tagmentation buffer 1 (TB1)-11 µL, 96-well PCR plate

Procedure

- Added 2-30 µL extracted DNA to each well of a 96-well PCR plate so that the total input amount was 100-500 ng.
- Transferred 11 µL BLT and 11 µL TB1 reagent to an Eppendorf tube and mixed it gently. From here, 20 µL (11 µL+11 µL) was transferred to the 96-well PCR plate.
- Then, the total amount was 50 µL in the PCR 96 plate, and it was mixed ten times with a pipette and sealed with micro seal 'B' securely.
- The PCR plate was placed on the thermal cycler, and the PCR program was run.
- During PCR, the time and temperature were fixed at 55ºC for 15 min (PCR) and 10ºC for 59:59 (Hold).

3.13.3.2. Post Tagmentation Cleanup:

Requirements: Tagment stop buffer (TSB)-10 µL, tagment wash buffer (TWB)-100 µL, 96-well plate magnet, microseal 'B' adhesive seal

Procedure

- After completing PCR, the PCR 96 plate was removed from the PCR machine. Then, 10 µL Tagment stop buffer (TSB) was added to the removed PCR 96 plate sample containing the whole mixture and was mixed gently with a pipette.
- After that, the plate was sealed with Microseal 'B' and was placed in the PCR machine again.
- The PCR machine ran again, and the time and temperature were 37ºC for 15 min.
- After completing PCR, the stop button was clicked, and the plate was removed from the PCR machine.
- Next, the PCR 96 plate was placed on the bead stand, and it was left for 3 minutes to allow the beads to separate.

- When the beads were separated, and the solution became clear, then 60 µL of suspension was removed very carefully without disturbing the beads.

Wash two times as follows:

a) The sample plate was removed from the magnetic stand, and a deliberately slow pipetting technique was used to add 100 µL TWB directly onto the beads. A deliberately slow pipetting technique minimized the potential of TWB foaming to avoid incorrect volume aspiration and incomplete mixing.
b) Pipetted slowly until beads were fully resuspended.
c) The plate was placed on the magnetic stand where beads were fully resuspended.
d) The pipette was placed on the magnetic stand and was waited until the liquid became clear 3 times.
e) Using a multichannel pipette, the supernatant was removed and discarded.The plate was removed from the magnetic stand and use and deliberately slow pipetting technique to add 100 µL TWB directly onto the beads.

- Each well was pipetted slowly to resuspend the beads.
- The plate was sealed and placed on the magnetic stand until the liquid became clear (3 minutes). It was kept on the magnetic stand until step 4 of the procedure section in amplifying tagmented DNA. The TWB remained in the wells to prevent over drying of the beads.

3.13.3.3. Amplify Tagmented DNA:

Requirements: Nuclease-free water-22 µL, enhance PCR mix (EPM)-22 µL, adapter Index 10 µL (For ready it had to be centrifuged at 280 rcf for 10 sec), 1.7 ml microcentrifuge tubes, microseal ‘B’ adhesive seal Procedure

- 22 µL Nuclease-free water and 22 µL EPM were taken in a separate Eppendorf tube, and they were vortexed and centrifuged.
- Then, 40 µL was transferred to the bead well and was mixed ten times with a pipette.
- 10 µL adapter index was added, and the mixture was mixed ten times with a pipette.
- It was sealed with Microseal ‘B’ and was placed into the PCR machine. During PCR, the temperature and time were fixed at 68ºC for 3 min, 98ºC for 3 min, 98ºC for 45 sec, 62ºC for 30 sec, 68ºC for 2 min, 68ºC for 1 min, 10ºC for 59:59 (Hold)

- After completing PCR, the sample was removed from the PCR machine and was spun/centrifuged, then it was placed on the bead stand for 5 min.

13.3.4. Clean Up Libraries: Requirements:

Nuclease-free water, sample Purification Beads (SPB), freshly prepared 80% ethanol (EtOH), resuspension Buffer (RSB), 96-well PCR plate, microseal 'B', microseal 'f' foil seal, 1.7 ml microcentrifuge tubes Procedure

- At first, a new Maxwell FSC cartridge was taken, and 45 µL of the sample was transferred, which was obtained after PCR, to the new Maxwell FSC cartridge.
- After that, 40 µL nuclease-free water and 45 µL SPB were added to the sample, and it was mixed with a pipette.
- It was sealed with microseal 'B' and was incubated at room temperature for 5 minutes.
- Once again, it was placed on the magnetic bead stand. Then, a new cartridge was taken, and 15 µL SPB solution was transferred.
- 125 µL of the bead-containing solution was added, making a total volume of 140 µL. It was mixed ten times with a pipette and was incubated at room temperature for 5 minutes.
- Again, it was placed on the bead stand and was left for 5 mi. Supernatant (140 µL) was discarded.
- 200 µL of 80% ethanol was added, and it was waited for 30 sec, then supernatant was discarded/removed (2 times). Then, it was incubated at room temperature for 5 min (bead-containing mixture), and 32 µL RSB was added.
- It was mixed with a pipette and was incubated again at room temperature for 2 min.Once more, it was placed on the bead stand for 2 min.
- Then, 30 µL suspension/supernatant was transferred in a new Eppendorf tube and measured the DNA concentration with the help of fluorimeter.

3. 13.3.5. Concentration measure of DNA:

Requirements: Fluorometer, 200 µL dsDNA dye, standard reagent, extracted DNA sample

Procedure

- At first three (3) fluorometric Eppendorf tube were collected and labeled blank, standard and test respectively.

- Then 200 µL dsDNA dye was taken in all the three fluorometric Eppendorf tube and 2µL standard reagent to the std tube. At a time, 2 µL extracted DNA was transferred to the test labeling tube.
- After that all the three fluorometric Eppendorf tube were vortex for mixing
- Incubation for 5 min at dark place. After five minutes measurement was taken of the blank, standard and test tube by Fluorometer.

3. 13.3.6. Check Libraries:

Run 1 µl of undiluted library on an Agilent Technology 2100 Bioanalyzer using a High Sensitivity DNA chip. The following figure shows example traces of libraries successfully sequenced on a MiSeq system. Typical libraries show a broad size distribution of ~250–1000 bp, as shown in the top panel. Various libraries can be sequenced with average fragment sizes as small as 250 bp or as large as 1500 bp.

3. 13.3.7. Normalize Libraries:

Manually normalize libraries when the final library yield is less than 10–15 nM. Bead-based normalization on low yield libraries can result in overly diluted samples and low sequencing yields. For more information, see Best Practices for Standard and Bead-Based Normalization in Nextera XT DNA Library Preparation Kits (Pub.No. 470-2016-007). Requirements LNA1, LNB1, LNW1, LNS1, magnetic stand, PCR plate, centrifuge machine.

Procedure

- Transferred 20 µl of supernatant from the Hard-Shell PCR plate to a new midi plate.
- Added 44 µl of LNA1 per sample to a new 15 ml conical tube. Calculated about 5% extra sample to account for sample loss due to pipetting. For example: for 96 samples, added 4.4 ml of LNA1 to the tube (100 samples × 44 µl = 4.4 ml).
- Thoroughly resuspended LNB1. Pipette to mix.
- Transferred 8 µl LNB1 per sample (including the 5% extra) to the 15 ml conical tube containing LNA1. Invert to mix. For example: for 96 samples, transferred 800 µl LNB1 to the tube of LNA1 (100 samples × 8 µl = 800 µl).
- Poured the bead mixture into a trough.
- Added 45 µl combined LNA1 and LNB1 to each well containing libraries.

- Shook at 1800 rpm for 30 minutes.
- Placed it on a magnetic stand and waited until the liquid was clear (~2 minutes).
- Removed and discard all supernatant from each well.

Wash two times as follows.

a) Add 45 µl LNW1 to each well.
b) Shook at 1800 rpm for 5 minutes.
c) Placed it on a magnetic stand and wait until the liquid was clear (~2 minutes).
d) Removed and discarded all supernatant from each well.

- Add 30 µl 0.1 N NaOH to each well.
- Shook at 1800 rpm for 5 minutes.
- During the 5-minute elution, labeled a new 96-well PCR plate SGP for storage plate.
- Add 30 µl LNS1 to each well of the SGP plate. Set aside.
- After the 5-minute elution, made sure that all samples in the midi plate were resuspended. If they were not, resumed as follows.

a) Pipette to mix or lightly tapped the plate on the bench.
b) Shook at 1800 rpm for 5 minutes.

- Placed it on a magnetic stand and wait until the liquid was clear (~2 minutes).
- Transferred the supernatant from the midi plate to the SGP plate.
- Centrifuged at 1000g for 1 minute.

3. 13.3.8. Pool Libraries:

Preparation

To prepare for the sequencing run, begin thawing reagents according to the instructions for your instrument. If the SGP plate was stored frozen at -25°C to -15°C, thaw at room temperature. Pipette to mix.

Procedure

- Centrifuged at 1000g at 20°C for 1 minute.
- Labeled a new Eppendorf tube PAL.
- Transferred 5 µl of each library from the SGP plate to the PAL tube. Inverted to mix.
- Stored unused pooled libraries in the PAL tube and SGP plate at -25°C to -15°C for up to 7 days.

3.13.3.9. Denaturing and Diluting Libraries and PhiX Control for sequencing

3. 13.3.9.1. Denature and Dilute Libraries Prepare Hybridization Buffer

Prepare Hybridization Buffer:

- Removed the tube of Hybridization Buffer from -25°C to -15°C storage and thawed at room temperature.
- When thawed, store at 2°C to 8°C until ready to dilute denatured libraries.
- Briefly vortexed before use.

3. 13.3.9.2. Dilute Library to Loading Concentration:

- Combined the following volumes of pooled libraries and prechilled Hybridization Buffer in a microcentrifuge tube.

Dilute Library to Loading Concentration

The total volume is 1 ml.

Library Pool	Prechilled Hybridization Buffer
2 µl	998 µl
3 µl	997 µl
4 µl	996 µl
l5 µl	995 µl

- Briefly vortexed and then centrifuged at 280g for 1 minute.
- Transferred 250 µl diluted library to a new microcentrifuge tube.
- Added 250 µl of prechilled Hybridization Buffer.
- Briefly vortexed and then centrifuge at 280 × g for 1 minute.

3. 13.3.9.3. Denature Diluted Library:

- Placed the tube in the preheated incubator for 2 minutes.
- Immediately cooled it on ice.
- Left it on ice for 5 minutes.

3. 13.3.9.4. Denature and Dilute PhiX Control

3. 13.3.9.5. Dilute PhiX to 4 nM:

- Thawed a tube of 10 nM PhiX stock.
- Combined the following volumes in a microcentrifuge tube.
- 10 nM PhiX (10 µl)

- RSB (15 µl)
- The total volume was 25 µl at 4 nM.
- Briefly vortexed and then pulse centrifuged.

3. 13.3.9.6. Denature PhiX:

- Combined the following volumes in a microcentrifuge tube.

a) 4 nM PhiX (5 µl)

b) N NaOH (5 µl)

- Briefly vortexed and then pulse centrifuged.
- Incubated at room temperature for 5 minutes.
- Added 5 µl 200 mM Tris-HCl, pH 7.0.
- Briefly vortexed and then centrifuged at 280g for 1 minute.

3. 13.3.9.7. Dilute Denatured PhiX to Loading Concentration:

- Added 985 µl of prechilled Hybridization Buffer to the tube of denatured PhiX. The total volume was 1 ml at 20 pM.
- Diluted the denatured 20 pM PhiX to 1.8 pM as follows.

a) Denatured PhiX (45 µl)

b) Prechilled Hybridization Buffer (455 µl)

c) The total volume was 500 µl at 1.8 pM.

- Inverted to mix and then centrifuge at 280g for 1 minute.

3. 13.3.9.8. Combine Library and PhiX Control:

- Combined the following volumes.

Combine Library and PhiX Control:

PhiX Control and Library	Volume
Denatured and diluted PhiX control	5 µl
Denatured and diluted library	500 µl

- Set aside on ice until to load it onto the reagent cartridge.

3. 13.4. Preparing Sequencing Consumables

3. 13.4.1. Prepare the Reagent Cartridge:

- Removed the reagent cartridge from -25°C to -15°C storage.

- Thawed reagents using the following water bath options. Did not submerge the cartridged. When thawed, dry the base before proceeding.

If multiple cartridges are thawing in the same water bath, allow additional thawing time. Alternatively, thaw reagents using the following options.

Method	Time to Thaw	Stability Limit
Room temperature air (19°C to 25°C)	5 hours	Up to 24 hours
Chilled at 2°C to 8°C	18 hours	Up to 72 hours

3. 13.4.2. Prepare the Reagent Cartridge:

- Inverted the cartridge 5 times to mix reagents.
- Inspected the large reservoirs from the bottom of the cartridge to ensure that reagents had thawed, and the reservoirs were free of ice crystals.
- Gently tapped on the bench to reduce air bubbles.

3. 13.4.3. Prepare the Flow Cell:

- Removed a new flow cell package from 2°C to 8°C storage.
- Set the unopened flow cell package aside at room temperature for 30 minutes.

3. 13.4.4. Performing a Run on the MiSeq

3. 13.4.5. Load Libraries onto the Reagent Cartridge:

- Cleaned the foil seal covering reservoir #16 labeled Load library here using a low lint tissue.
- Pierced the seal with a clean 1 ml pipette tip.
- Added 500 µl prepared 1.8 pM libraries into reservoir #16. Avoided touching the foil seal as libraries were dispensed.

3.13.5. Set Up a Run:

- From the Home screen, selected Sequence.
- The Sequence command released consumables from a previous run and opened the series of run setup screens.

3. 13.5.1. Log in to Local Run Manager:

- Entered user's name and password.
- Selected Next.

3. 13.5.2. Select Available Run:

- Selected a run name from the list of available runs.
- Used the up and down arrows to scroll through the list or entered a run name in the Search field.
- Selected Next.

3. 13.5.3. Load the Flow Cell:

- Opened the flow cell compartment door.
- Pressed the release button to the right of the flow cell latch.
- If present, removed the used flow cell from the previous run.
- Made sure that the flow cell stage was clean. If debris is present, cleaned the flow cell stage with an alcohol wipe.
- Placed the flow cell on the flow cell stage over the alignment pins.
- Closed the flow cell latch to secure the flow cell.
- Closed the flow cell compartment door.

3. 13.5.4. Load the Reagent Cartridge:

- Opened the reagent compartment door.
- If present, removed the used reagent cartridge.

3. 13.5.5. Confirm Run Parameters:

1. Confirmed run parameters.

The control software confirmed the number of specified cycles using the following criteria:

- Total cycles did not exceed the maximum cycles allowed based on the reagent cartridge loaded for the run.
- Cycles for Read 1 were greater than the 5 cycles required for template generation.
- Index Read cycles did not exceed Read 1 and Read 2 cycles.

2. Select Edit to change run parameters. When finished, selected Save.

- Purged consumables for this run—Change the setting to purge consumables automatically after the current run.
- Run parameters—Changed the read type or number of cycles per read.
- Custom primers—Changed the settings for custom primers.

3. Selected Next.
4. When the automated check was complete, selected Start.

3.13.6. Review Automated Check:

1. Reviewed the automated check results.

- To stop a check in progress, selected Cancel.
- For any items that did not pass, an action was required before proceeding.
- To restart the check, selected Retry. The check resumed at the first incomplete or failed check.

2. To start the run, select from the following options.

- If the system was not configured to start automatically after a successful check, selected Start.
- If the system is configured to start automatically after a successful check, the sequencing run begins automatically. There was no need to be present.

However, if any errors occured during the check, the run did not begin automatically.

3.13.7. Viewing Analysis Results in Local Run Manager:

View Analysis Results

1. From the Local Run Manager dashboard, selected the run name.
2. From the Run Overview tab, reviewed the sequencing run metrics.
3. To change the analysis data file location for future requeues of the selected run, selected and edit the output run folder file path. The file path leading up to the output run folder was editable. The output run folder name could not be changed.
4. Selected the Copy to Clipboard icon to copy the output run folder file path.
5. Selected the Sequencing Information tab to review run parameters and consumables information.
6. Selected the Samples & Results tab to view the analysis report.

- If analysis was requeued, selected the appropriate analysis from the Select Analysis drop-down list.
- From the left navigation bar, selected a sample ID to view the report for another sample.

7. Selected the Copy to Clipboard icon to copy the Analysis Folder file path.

3.13.8. Analysis Report

3. 13.8.1. Analysis Output Files:

The following analysis output files are generated for the Generate FASTQ analysis module.

Analysis Output Files:

File Name	Description
Demultiplexing (*. demux)	Intermediate files containing emultiplexing results.
FASTQ (*.fastq.gz)	Intermediate files containing quality scored base calls. FASTQ files are the primary input for the alignment step.

3.14. Genome assembly, annotation, data deposition and gene prediction:

3. 14.1. FastQC analysis:

Most sequencers will generate a QC report as part of their analysis pipeline, but this is usually only focused on identifying problems which were generated by the sequencer itself. FastQC aims to provide a QC report which can spot problems which originate either in the sequencer or in the starting library material. FastQC can be run in one of two modes. It can either run as a standalone interactive application for the immediate analysis of small numbers of FastQ files, or it can be run in a non-interactive mode where it would be suitable for integrating into a larger analysis pipeline for the systematic processing of large numbers of files. It provides the length of the shortest and longest sequence in the set. If all sequences are the same length only one value is reported %GC: The overall %GC of all bases in all sequences. It seems to be optimum range of %GC (40 to 70)(Rückert *et al.,* 2015).

3. 14.2. ASSEMBLY IN SPAdes:

(1) Stage 1 (assembly graph construction) is addressed by every NGS assembler and is often referred to as de Bruijn graph simplification. We propose a new approach to assembly graph construction that uses the multisized de Bruijn graph, implements new

bulge/tip removal algorithms, detects and removes chimeric reads, aggregates biread information into distance histograms, and allows one to backtrack the performed graph operations(Bankevich *et al.,* 2012). (2) Stage 2 (k-bimer adjustment) derives accurate distance estimates between k-mers in the genome (edges in the assembly graph) using joint analysis of distance histograms and paths in the assembly graph. (3) Stage 3 constructs the paired assembly graph, inspired by the PDBG approach. (4) Stage 4 (contig construction) was well studied in the context of Sanger sequencing. Since NGS projects typically feature high coverage, NGS assemblers generate rather accurate contigs (although the accuracy deteriorates for SCS) (Bankevich *et al.,* 2012). SPAdes construct DNA sequences of contigs and the mapping of reads to contigs by backtracking graph simplifications.

3. 14.3. Prokka Genome Annotation:

The Prokka Genome Annotation BaseSpace App compliments our suite of de novo assembly tools. Prokka expects preassembled genomic DNA sequences in FASTA format (Seemann, 2014). Finished sequences without gaps are the ideal input, but it is expected that the typical input will be a set of scaffold sequences produced by de novo assembly software. This sequence file is the only mandatory parameter to the software. It was used de novo assembly FASTA files as an input that can be generated by the SPAdes Genome Assembler.

3.15. Strain identification and classification

3.15.1. Annotating a Genome Using RAST (Rapid Annotation using Subsystem Technology:

The steps to annotate a genome using RAST are outlined below. To begin, provide the prokaryotic genome in the form of contigs in FASTA format. Typically, RAST will make its own gene calls, but users can also specify their own set of gene calls. The RAST server is freely accessible for annotating prokaryotic genomes, whether they are complete or composed of multiple contigs (although the quality of annotations may be affected in the latter case). To use the service, new users must register by providing their contact information and creating a password. This registration process ensures that users only have access to the genomes they have submitted and allows us to notify them when the automatic annotation is complete or if user intervention is needed. Once logged in,

users can track their submitted job(s) on the Job Overview page. After the annotation is finished, users have the option to download the annotated genome in various export formats (such as GenBank, FASTA, GFF3, or Excel) or explore the genome in the SEED Viewer, without installing the data in the SEED. These options are available for 120 days or until the user delete the data. If desired, users can also request to have the annotated genome added to the SEED. The SEED-Viewer environment provides users with several analysis options for the annotated genome. The Organism Overview page displays basic information about the genome, including taxonomy, size, the number of contigs, the number of coding sequences and RNAs, as well as counts of non-hypothetical and hypothetical gene annotations. It also shows the number of subsystems automatically identified in the genome (Aziz *et al.,* 2008).

3.15.2. Average nucleotide identity (ANI):

Archaea and bacterial species boundaries can be identified using the computational analysis category of average nucleotide identity (ANI). Genome sequence fragmentation, nucleotide sequence search, alignment, and identity computation are typically the steps involved in ANI calculations. The BLAST program served as the search engine for the initial method used to construct ANI. To consider the idea of orthology, a better ANI algorithm was created. Here, we compared the performance of four ANI computation algorithms: OrthoANIb (OrthoANI utilizing 37 BLAST), ANIm (ANI using MUMmer), and ANIb (ANI using BLAST). OrthoANIb and OrthoANIu showed high correlation over the whole range of ANI values when values were compared to the ANIb, which is regarded as a benchmark. The correlation between ANI and ANIm was just about 90%. The self-written parser used by the original JSpecies stand-alone implementation is replaced with the dandruff script of the MUMmer tool version 3.0 for average nucleotide identity based on MUMmer (ANIm) computation.

3.15.3. DNA-DNA hybridization (DDH):

In taxonomical analysis of prokaryotic species at genomic level DNA-DNA hybridization is used to decided relatedness among bacterial strain and defined as the main rule in the outline of bacterial species. 70% DDH value for species deception compared to 95% ANI and 69% moderated DNA (Goris *et al.,* 2007).

3.15.4. Pangenome analysis using by CG View Server:

Sequence features, base composition plots, analysis results, and sequence similarity plots are displayed on graphical maps of circular genomes created by the CG view Server. Raw, FASTA, GenBank, or EMBL formats are available for sequences. GFF (General Feature Format) files can be used to submit additional analysis or feature data. The server utilizes Impact to contrast the essential arrangement with up to three correlation genomes or grouping sets. A graphical map representing the entire sequence or an expanded and more in-depth view of a particular region of interest is generated from the BLAST results and feature information. A few choices are incorporated to control which types of highlights are shown and the way that they are drawn. Any bacterial, plasmid, chloroplast, or mitochondrial genome can be viewed using the CG View Server, which can also help identify conserved genome segments, horizontal gene transfer instances, and gene copy number variations. Maps can also be used to visualize regions of a known genome covered by newly obtained sequence reads because a collection of sequences can be used in place of a comparison genome. The CG view was defined as the normalized excess of C over G in a given sequence, (CG)/(C + G), which is calculated using sliding windows along the genome.When the amount of C equals the amount of G, the GC skew is zero. Cumulative skew can be calculated as the sum of the walker graph scores at each nucleotide position along the genome, with scores A = 0, T = 0, G = 1, and C = 1. This eliminates the need for window slides. To normalize the strength of the cumulative skew without taking into account the genome's length, this study, on the other hand, used the cumulative sum of the GC skew in each window to calculate the cumulative GC skew.

3.15.5. Progressive mauve analysis:

Mauve is a Java-based tool that allows for the alignment of whole genomes. It comes with a built-in viewer and offers the ability to export comparative genomic information in different formats (Darling *et al.*, 2010). The method visualized the results in different colour boxes, representing the genome comparisons (Edwards & Holt, 2013). In addition to its alignment functions, Mauve can also be used to arrange and orient contigs against an existing assembly. By providing a set of genome assemblies as input, Mauve generates multiple whole-genome alignments. It detects blocks of sequence homology and assigns each block a unique color. This enables the visualization of genomes as a sequence of colored blocks, making it easier to compare and identify conserved regions

among all input genomes. It also helps in identifying regions that are unique to specific subsets of genomes, often referred to as "islands". Moreover, Mauve's ability to generate genome sequence alignments allows for the identification of single nucleotide polymorphisms (SNPs) or point mutations, which can be utilized for downstream phylogenetic or evolutionary analyzes (for more details, refer to the mauve user guide).

3.15.6. Phylogenic tree analysis:

Whole genome phylogeny Sequences were obtained from NCBI. The sequences were manually aligned using MUSCLE. Phylogenetic distances were calculated with the Kimura 2-parameter model (Anwar *et al.,* 2014) and the tree reconstruction was done using the neighbor-joining method , with bootstrap analysis (1,000 replication) using the software realphy and MEGA version 11.

3.15.7. Venn diagram analysis:

Venn Diagram is a diagram used in set theory, showing the distribution of the number of elements between 3 sets (4 or more sets can be drawn) It is elements belonging to each set are shown in the circle, and overlapping parts are shown as common elements. It is used for biological applications to illustrate the number of orthologous or unique genes between closely related genomes. In Venn diagram analysis usually used Genebank, fasta file format for genomic comparison. This analysis was done by (http://bioinformatics.psb.ugent.be/webtools/Venn/) web base software.

3.16. Insecticide degradation demonstrated by Enzyme catalytic reaction.

3. 16.1. Homology modeling, protein preparation and validation:

The protein sequences were gathered from the PGAP annotation file of *Serratia* sp. HSTU-BF1R2. To construct the homology model, we utilized the Iterative Threading Assembly Refinement (I-TASSER) Server, as described by (Yang *et al.,* 2015). Subsequently, the model underwent energy minimization to resolve unfavorable interactions among protein atoms. The steepest descent and conjugate gradient techniques were employed for this purpose. The computations were performed in vacuo, using the GROMOS 96 43B1 parameters set, with the Swiss-PDB Viewer serving as the implementation tool. The final 3D structures of the protein were saved in .pdb format. To

ensure the validity and assess the quality of the minimized protein, we employed the SAVES v6.0 online server, accessible at https://saves.mbi.ucla.edu/.

3. 16.2. Small molecule/Ligand collection and optimization:

105 Various types of insecticides, weed killer and nerve agent ‘s small molecules were collected from the Pubchem database (https://pubchem.ncbi.nlm.nih.gov/). After collecting, the ligands were optimized and minimized by using the mmff94 force field and the steepest 31 descent algorithm in the PyRx software environment. The small molecules 3D structures were stored in a file with sdf format.

3. 16.3. Virtual screening, molecular docking and visualization:

Virtual screening, molecular docking, and visualization techniques were employed to investigate a set of 105 small molecules with respect to 11 protein structures. The virtual screening involved individual screening of all proteins against the 105 ligands using PyRx software (Dallakyan & Olson, 2015). Protein-ligand complexes were generated using Chimera software (Pettersen *et al.*, 2004), and the Discovery Studio 2020 Client (Dassault Systèmes BIOVIA, 2021) was utilized for both 2D and 3D structure visualization. Virtual screening results were presented using boxplot analysis, which was performed with Origin Pro 8.0 software (OriginLab Corporation, 2021). Additionally, the Discovery Studio 2020 Client was used to analyze protein-ligand non-bonded interactions. The binding affinity of the protein-ligand interactions was quantified in kcal/mole as a unit for a negative score (Trott & Olson, 2010).

CHAPTER IV
RESULTS

RESULTS

4.1. Biochemical characterization:

4.1.1. Oxidase Test results

The oxidase test determines the presence of cytochrome c oxidases in bacteria. Isolated bacterial strains BF1R2 showed oxidase activity as observed by a dark blue color on filter paper soaked with *N, N, N′,N′*-tetramethyl-p-phenylenediamine dihydrochloride substrate. Oxidase-positive bacteria produce cytochrome oxidase or indophenol oxidase, aiding in electron transfer. The cytochrome system is found in aerobic organisms using oxygen as the terminal electron acceptor, leading to water or hydrogen peroxide as end-products (catalase breaks it down).

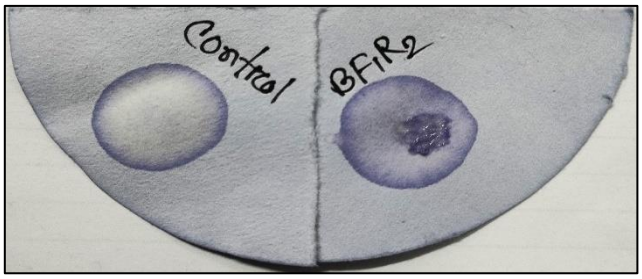

Figure 1: Oxidase Test

4. 1.2 Catalase test:

The catalase test detects catalase enzymes in bacteria that neutralize harmful oxygen metabolites like H_2O_2. Bacterial strains BF1R2 showed positive results with significant bubble formation on slides after adding 30% H_2O_2. This enzyme is vital for protecting cells from oxidative damage by reactive oxygen species in oxygenated environments.

Figure 2: Catalase Test

4. 1.3. Citrate Utilization Test:

The breakdown of citrate releases bicarbonate (HCO_3-) into the media when bacteria can use citrate as a carbon source. The medium's PH is increased by the bicarbonate ions, and as a result, the bromothymol blue indicator turns a dark blue color. The isolate has demonstrated in this test Positive results.

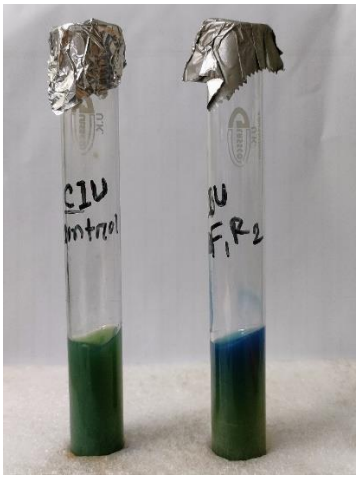

Figure 3: Citrate Utilization Test

4. 1.5. Methyl Red (MR) Test results:

The endophytic isolate showed positive result compared to positive and negative control. MR-VP Test was performed for identifying an organism's metabolic pathway. Methyl Red (MR) test determines whether the microbe performs mixed acids fermentation when supplied glucose.

Figure 4: Methyl Red (MR) Test

4. 1.6. Voges-Proskauer (VP):

After the addition of prepared reagent, *Serratia* sp. strain HSTU-BF1R2 isolate has displayed negative result.

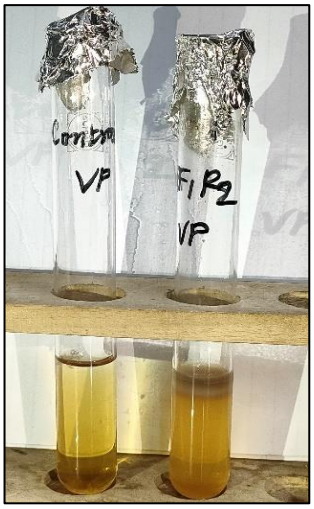

Figure 5: Voges-Proskauer (VP)Test

4. 1.7. Carbohydrate fermentation test (lactose, sucrose, dextrose, and maltose):

The carbohydrate fermentation test serves the purpose of determining a bacterium's ability to ferment a particular carbohydrate. This test is valuable in distinguishing between different bacterial groups or species. It examines the production of acid and gas resulting from carbohydrate fermentation. The test involves four different sugars: lactose, sucrose, dextrose, and maltose. To study the utilization of these four sugars, fermentation broth was employed in test tubes. Demonstrated the capability to ferment all four types of sugar. The results of this fermentation test are presented in the table below.

Sample name	Lactose	Dextrose	Maltose	Sucrose
BF1R2	+	+	+	+

Figure 6: carbohydrate fermentation test

4. 1.8. Triple Sugar Iron Agar Test (TSI):

This test is used to identify the capability of bacteria to ferment 3 sugars including lactose, sucrose, glucose and iron. The isolated bacterium has shown positive results. According to the principle, *Serratia* sp. strain HSTU-BF1R2 isolate bacteria can ferment glucose and produce gas.

Figure 7: Triple Sugar Iron Agar Test

4. 1.9. Urease Test:

The urease test was done by using urea agar base. Urea provides a source of nitrogen for those microorganisms producing urease enzymes. Organisms containing urease hydrolyses urea into ammonia and CO_2. The isolate was observed for urease activity and has shown positive result that means *Serratia* sp. strain HSTU-BF1R2 can degrade urea rapidly.

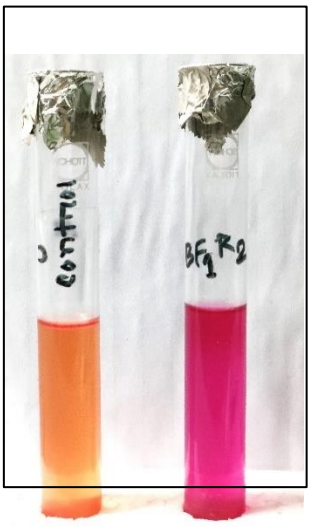

Figure 8: Urease Test

4. 1.10. Mortality Indole Urease (MIU) test:

The MIU (Motility, Indole, and Urease) medium base serves as a specialized medium designed to identify motility, urease activity, and indole production in bacteria. Positive results for indole and urease are indicated by the presence of a red ring, while motility is detected by a white turbid appearance. The indole test helps identify organisms with the ability to break down tryptophan. In the case of *Serratia* sp. strain HSTU-BF1R2, it exhibited motility activity on the MIU medium base.

Figure 9: Mortality Indole Urease (MIU)

4.2. Field experimentation:

The results obtained from the study on brinjal plant growth and anther development after 30, 45, and 60 days of plantation were presented in Table 1. The observations showed that the T1 treatment group, which utilized 30% urea, exhibited the highest root length, shoot length, leaf length, number of flowers and number fruits at all three time points. After 30 days of plantation, the T1 treatment group showed significantly superior growth compared to both the Tc and To groups, which used 100% urea and no urea, respectively highest root length, shoot length, leaf length, number of flowers and number fruits were recorded as 16.5cm, 50.0 cm, 21.8 cm, 8.33 and 3.66 respectively, for T1, while the T0 treatment group had the lowest measurements with 6.60 cm, 17.6 cm, 7.50 cm, 1.33 and 0.0 for root length, shoot length, leaf length, and anther size, respectively. At the 45-day mark, the T1 treatment group continued to display remarkable growth, with root length, shoot length, leaf length, number of flowers and number fruits reaching 18.3 cm, 77.7 cm, 25.8 cm,13.6 and 7.00 respectively. Again, these measurements were significantly higher than those of the Tc and To groups, which showed root length, shoot length, leaf length, and anther size of 7.06 cm, 35.7 cm, 9.13 cm, 4.0 and 0.66 respectively. The trend

persisted even after 60 days of plantation. The T1 treatment group recorded the highest root length, shoot length, leaf length, number of flowers and number fruits at 21.5cm, 93.1 cm, 28.0 cm, 18.3 and 12.0 respectively, while the T0 treatment group showed the lowest values with 11.5 cm, 52.9 cm, 12.2 cm, 8.33 and 2.00 respectively. Comparing the To and Tc groups with T1 group, a statistically significant result was observed (p-value > 0.05). These results indicate that the T1 treatment group, with 30% urea concentration, outperformed both the Tc and To groups in terms of growth and anther development. This finding highlights the importance of bacteria concentration in influencing the growth and reproductive characteristics of the brinjal plant. Additionally, the comparison within the T1 treatment group also revealed statistically significant differences, further emphasizing the impact of using different urea percentages on plant growth. It is worth noting that the T1 treatment group achieved these impressive results with only 30% urea, while the Tc treatment group, which used 100% urea, did not show the same level of growth and anther development. This suggests that factors other than urea concentration might also play a role in determining the growth patterns of the brinjal plant.

Data collection time	**Strain with urea fertilizer treatment**	**Root length (cm)**	**Shoot length (cm)**	**Leaf length (cm)**	**Number Of flowers**	**Number of fruits**
30 days after plantation	30% Urea with Bacteria (T1)	16.5 ± 1.13^{bc}	50.0 ± 2.50^{d}	21.8 ± 2.15^{b}	8.33 ± 0.57^{c}	3.66 ± 0.57^{c}
	100% Urea & No Bacteria (Tc)	8.96 ± 0.87^{ef}	25.7 ± 0.70^{ef}	14.3 ± 0.65^{cd}	4.66 ± 0.57^{d}	1.00 ± 1.00^{de}
	No Urea & No Bacteria (To)	6.60 ± 0.17^{f}	17.6 ± 0.35^{f}	7.50 ± 0.70^{e}	1.33 ± 0.57^{e}	0.0 ± 0.0^{e}
45 days after plantation	30% Urea with Bacteria (T1)	18.3 ± 1.52^{b}	77.2 ± 5.30^{b}	25.8 ± 1.93^{a}	13.6 ± 2.08^{b}	7.00 ± 1.00^{b}
	100% Urea & No Bacteria (Tc)	12.0 ± 1.00^{d}	50.2 ± 1.86^{d}	16.4 ± 1.36^{c}	8.00 ± 1.00^{c}	3.33 ± 0.57^{c}
	No Urea & No Bacteria (To)	7.06 ± 0.20^{f}	35.7 ± 1.44^{e}	9.13 ± 0.40^{e}	4.00 ± 1.00^{d}	0.66 ± 0.57^{de}

60 days after plantation	30% Urea with Bacteria (T1)	21.5±1.32^{a}	93.1±5.77^{a}	28.0±2.00^{a}	18.3±1.52^{a}	12.0±1.00^{a}
	100% Urea & No Bacteria (Tc)	14.6±0.35^{c}	65.1±2.00^{c}	20.2±1.36^{b}	12.3±1.52^{b}	7.33±0.57^{b}
	No Urea & No Bacteria (To)	11.5±0.50^{de}	52.9±1.15^{d}	12.2±0.55^{d}	8.33±0.57^{c}	2.00±1.00^{de}

Table 3: Effect of bacteria and fertilizer in different time of period, among different treatment group

Figure 10: Growth of 60 days eggplant in response to different treatments (To=no bacteria and urea, Tc= only 100% urea, T1(BF1R2) = bacteria+30% urea

4.3. Pesticide biodegradation in liquid medium:

Chlorpyrifos and cypermethrin, a chemically intricate organophosphate pesticide, exhibits resistance to complete degradation due to its structural complexity. Microbial degradation can result in either full breakdown or partial conversion into intermediary metabolites. Various bacterial species, including *Pseudomonas aeruginosa, P. putida, Bacillus pumilus, Bacillus cereus, Serratia marcescens, Klebsiella* sp., *Alcaligenes* sp.,

Alcaligenes faecalis, *Flavobacterium* sp., and *Enterobacter* strain B-14, have been documented as capable of chlorpyrifos degradation, utilizing it as their sole carbon source. This degradation process correlates with an inverse pesticide concentration trend as bacterial populations expand. We cultured the strain *Serratia* sp. strain HSTU-BF1R2 within a medium of Mineral Salts Medium (MSM) containing chlorpyrifos and cypermethrin, both in liquid broth and on agar. Measurement of our strain's absorbance, carried out at a wavelength of 600 nm in chlorpyrifos-containing MSM broth, yielded a reading of 0.828 nm. This was contrasted with a control sample lacking bacteria, which exhibited an absorbance reading of 1.369 nm. Furthermore, we observed the formation of distinct bacterial colonies on the agar plate.

Fig 11: Chlorpyrifos and cypermethrin control (without bacteria) and chlorpyrifos with bacteria in MSM

Table 4: Spectrophotometric analysis of chlorpyrifos biodegradation:

Sample name	Absorbance of chlorpyrifos bacterial solution (600nm) Absorbance after centrifugation
Chlorpyrifos control (Tc)	1.369
Serratia sp. HSTU-BF1R2	0.828

4.4. Genomic features and annotations of *Serratia* sp. strain HSTU-BF1R2

4.4.1. Annotation a genome using RAST:

The basic steps were used to annotate a genome using RAST are described in the subsections below. Input to the process is a prokaryotic genome in the form of a set of contigs in FASTA format. After annotating the contig fasta file showed in seed viewer result below table and showed genomic features in subsystem about 29% genome coverage. In subsystem –a total of 1420 proteins are involved where the strain *Serratia* sp. strain HSTU-BF1R2 is predicted to encode for about 333 proteins involved in carbohydrate metabolism and 339 proteins involved in amino acid metabolism and non- in subsystem total proteins are 3498. In addition to isolating pesticide-degrading protein sequence from RAST seed viewer server, isolated protein is shown below table.

Features Annotation statistics	Features Annotation statistics
Genome	*Serratia* sp. HSTU-BF1R2
Domain	Bacteria
Taxonomy	Bacteria; *Serratia* sp. HSTU-BF1R2
Size	5,134,224
GC content	59.6
N50	317020
L50	5
Number of contigs (with PEGs)	42
Number of subsystems	369
Number of coding‘s sequences	918
Number of RNAs	83

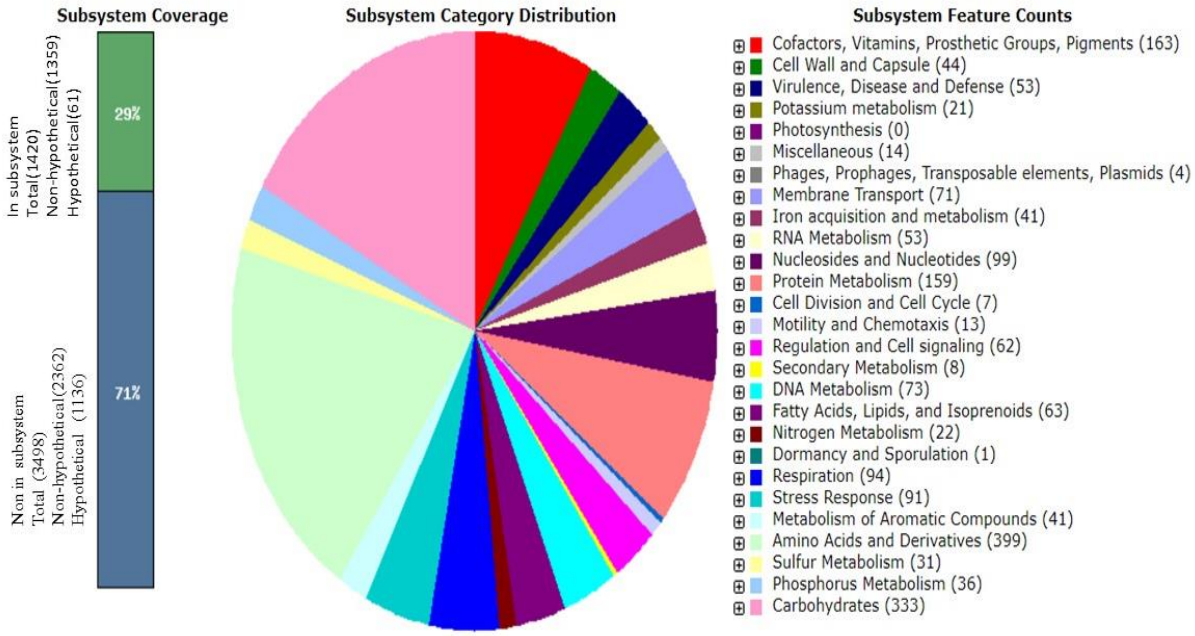

Figure 12: Subsystem of the RAST annotation

4. 4.2. The genomic map of the strain *Serratia* sp. strain HSTU-BF1R2:

As seen in figure 13, the CG view analysis shows all the proteins of a bacterium in a proper genomic map. We hereby transcribed the *Serratia* sp. strain HSTU-BF1R2 bacterial protein into a genomic map where 4,766 protein coding sequence (CDS), 74 tRNAs were shown in 5.1 mbp length sequences. In figure 13, the GC-skew positive indicates that the CDS is present in downstream and GC-skew negative indicates that the CDS is present in upstream. The GC skew is observed in local genomic regions primarily introduced by RNA synthesis, but the analysis of GC skew was first utilized for the computational prediction of ori and ter positions by examining available genome sequences.

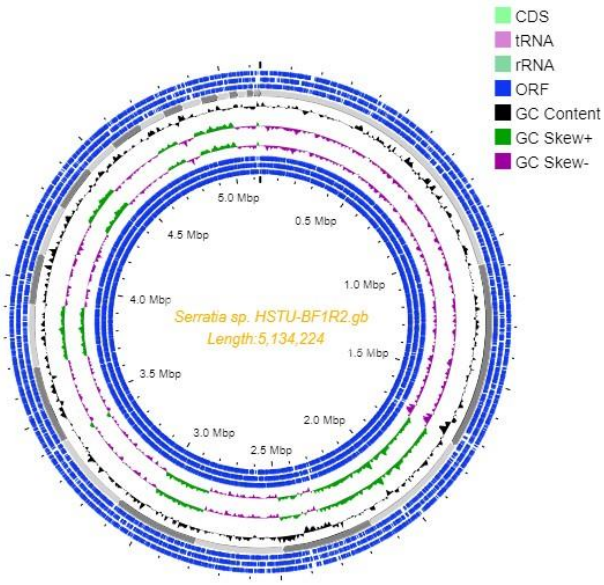

Figure 13: The genomic map of the strain *Serratia* sp. HSTU-BF1R2

4. 4.3. Venn diagram analysis:

Venn diagram showed the *Serratia* sp.strain HSTU-BF1R2 predicted essential amino acid sequence in different studies. *Serratia* sp.strain HSTU-BF1R2 strain was showed total 142572 numbers of amino acid sequence present in this genome in which 111426 amino acid sequences were shown unique and 16003 numbers of amino acid sequence were common among each other (Fig 14). In addition to maximum 31146 amino acid sequence were matched.

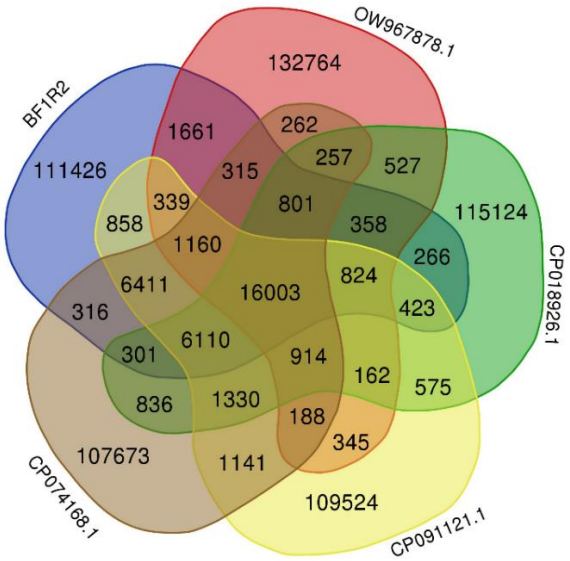

Figure 14: Venn diagram of *Serratia* sp.strain HSTU-BF1R2 predicted essential amino acid sequence

4. 4.4.Average nucleotide identity (ANI):

Average Nucleotide Identity (ANI) measurement is a powerful tool for assessing the genetic relatedness and evolutionary connections among bacterial species. In this study, we compared the genetic similarity of *Serratia* sp. strain HSTU-BF1R2 with 14 bacterial species retrieved from the NCBI database using two distinct ANI programs: ANI b (ANI blast) and ANI m (ANI mammber). Analysis, presented in Table 14, demonstrated that *Serratia* sp. strain HSTU-BF1R2 exhibited a significantly higher ANI value of 98.98% with the CP033504.1 *Serratia* sp. LS-1 chromosome. This result suggests that *Serratia* sp. HSTU-BF1R2 can be identified as the closest relative species, meeting the investigation cutoff score for belonging to the same species. Additionally, other *Serratia* strains, namely *Serratia* sp. JKS000199 (LT 907843.1), *Serratia* ureilytica strain KML.E1 (CP 117886.1), *Serratia* ureilytica strain S24 (CP 076651.1), *Serratia* ureilytica strain MGH225 (CP 060483.1), and *Serratia* marcescens isolate 0 genome assembly (OW 967878.1), displayed ANI values of 98.93%, 98.93%, 98.92%, 98.86%, and 98.86%, respectively. Furthermore, the remaining eight different *Serratia* species/strains exhibited ANI values ranging from 98.98% to 98.84%, indicating a close genetic likeness with *Serratia* sp. HSTU-BF1R2. Using BLAST for the analysis of average nucleotide identity, we found that *Serratia* sp. HSTU-BF1R2 showed a remarkable correspondence with the CP033504.1 *Serratia* sp. LS-1 chromosome, displaying a nucleotide sequence identity value of 98.98%. This value represents the highest similarity among all 14 bacterial sequences analyzed in terms of average nucleotide identity, as presented in Table 5

	Serratia sp. HSTU-BF1R2.	*Serratia* marcescens isolate 0 genome	*Serratia* marcescens strain 4201	*Serratia* marcescens strain AR 0130	*Serratia* marcescens strain C110	*Serratia* marcescens strain SJC1005	*Serratia* marcescens strain UMH6	*Serratia* marcescens strain WVU-006	*Serratia*sp.JKS000199	*Serratia* sp. LS-1 chromosome	*Serratia* ureilytica strain CM2016 324	*Serratia* ureilytica strain FDAARGOS 1089	*Serratia* ureilytica strain KML.E1	*Serratia* ureilytica strain MGH225	*Serratia* ureilytica strain S24
***Serratia* sp. HSTU-BF1R2**	*	**98.9**	**98.8**	**98.4**	94.0	**98.8**	**98.5**	**98.8**	**98.9**	**98.9**	**98.4**	**98.9**	**98.9**	**98.8**	**98.9**
***Serratia* marcescens isolate 0**	**98.8**	*	**98.8**	**98.1**	94.0	**99.1**	**98.2**	**98.9**	**98.9**	**98.9**	**98.3**	**99.0**	**98.8**	**98.8**	**98.9**
***Serratia* marcescens strain 4201**	**98.8**	**98.8**	*	**98.2**	94.1	**98.8**	**98.2**	**98.7**	**98.9**	**98.7**	**98.2**	**98.8**	**99.0**	**98.9**	**98.7**
***Serratia* marcescens strain AR 0130**	**98.4**	**98.2**	**98.3**	*	93.8	**98.3**	**98.8**	**98.3**	**98.2**	**98.3**	**99.0**	**98.3**	**98.2**	**98.3**	**98.3**
***Serratia* marcescens strain C110**	93.9	94.0	94.0	93.7	*	94.0	93.7	93.9	94.1	94.0	93.8	94.0	94.1	94.0	94.0
***Serratia* marcescens strain SJC1005**	**98.7**	**99.1**	**98.7**	**98.2**	94.0	*	**98.2**	**98.8**	**98.8**	**98.7**	**98.2**	**98.8**	**98.7**	**98.7**	**98.7**
***Serratia* marcescens strain UMH6**	**98.5**	**98.3**	**98.3**	**98.8**	93.8	**98.3**	*	**98.4**	**98.4**	**98.4**	**98.9**	**98.3**	**98.4**	**98.4**	**98.4**
***Serratia* marcescens strain WVU-006**	**98.7**	**98.8**	**98.7**	**98.2**	94.0	**98.9**	**98.2**	*	**98.9**	**98.8**	**98.2**	**98.9**	**98.8**	**98.7**	**98.9**
***Serratia* sp. JKS000199**	**98.9**	**98.9**	**98.**	**98.2**	94.2	**99.0**	**98.3**	**99.0**	*	**98.9**	**98.3**	**99.0**	**98.9**	**98.9**	**99.0**
***Serratia* sp. LS-1 chromosome**	**98.9**	**99.0**	**98.8**	**98.3**	94.2	**98.9**	**98.4**	**98.9**	**99.0**	*	**98.4**	**98.9**	**98.9**	**98.9**	**99.0**
***Serratia* ureilytica strain CM2016 324**	**98.4**	**98.3**	**98.3**	**99.0**	93.8	**98.3**	**98.9**	**98.2**	**98.3**	**98.4**	*	**98.3**	**98.2**	**98.2**	**98.4**
***Serratia* ureilytica strain FDAARGOS 1089**	**98.8**	**98.9**	**98.7**	**98.2**	94.1	**98.9**	**98.2**	**98.9**	**99.0**	**98.8**	**98.3**	*	**98.8**	**98.8**	**98.9**
***Serratia* ureilytica strain KML.E1**	**98.9**	**98.9**	**99.1**	**98.3**	94.2	**98.9**	**98.3**	**98.9**	**98.9**	**98.9**	**98.3**	**98.9**	*	**99.0**	**98.9**
***Serratia* ureilytica strain MGH225**	**98.8**	**98.9**	**99.0**	**98.2**	94.1	**98.8**	**98.3**	**98.8**	**98.9**	**98.8**	**98.1**	**98.8**	**99.0**	*	**98.8**
***Serratia* ureilytica strain S24**	**98.9**	**98.8**	**98.7**	**98.2**	94.1	**98.9**	**98.4**	**98.9**	**99.0**	**98.9**	**98.4**	**98.9**	**98.8**	**98.8**	*

Table 5: Average Nucleotide Identity (ANI) (%) based on whole genome alignments

4. 4.5. DNA-DNA hybridization (DDH):

In the depiction of relatedness among prokaryotic organism could determine by the DNA-DNA hybridization method. .70% value or above is referred as the highest similarity value for species among others. Here in table below the dDDH % value proved that, examined species *Serratia*_sp. We analysed the quantitative connection between DDH values and genome arrangement determined boundaries of *Serratia*_sp._HSTU-BF1R2 with fourteen different bacterial strains, in table no. 06 all results are manifested.

We found *Serratia*-sp HSTU-BF1R2 and CP 117886.1 *Serratia*_ureilytica_strain _KML.E1 bacterial strain showed highest similarity DNA hybridization value in three formula of this programmed chronologically 97, 91.8 and 97.7 %. Also, this group displayed a higher relatedness probability percentage as followed 99.05% in formula 1, 96.38% in formula 2 and 99.93% in formula 3. On other hand, LT 907843 *Serratia*_sp._JKS000199 showed second highest value in three formulae were – 96.2, 92, 97.2% and probability 98.9, 96.42, 99.92%. And CP033504.1 *Serratia*_sp._LS-1 and OW967878.1 *Serratia*_marcescens_isolate_0_genome_assembly had showed third and fourth highest DDH and probability value of likeness among others input strains. Interestingly, all 14 referred to strain of bacillus sp. had crossed the connection cut-off score.

		Formula 1		**Formula 2**		**Formula 3**		G+C difference
Query genome	Reference genome	DDH	Prob. DDH >= 70%	DDH	Prob. DDH >= 70%	DDH	Prob. DDH >= 70%	
*Serratia*_sp._HSTU-BF1R2	*Serratia*_marcescens_isolate_0_genome_assembly	95	98.67	92	96.42	96.4	99.89	0.07
*Serratia*_sp._HSTU-BF1R2	*Serratia*_marcescens_strain_4201chromosome	94.6	98.57	91.4	96.25	96	99.88	0.22
*Serratia*_sp._HSTU-BF1R2	*Serratia*_marcescens_strain_AR_0130	90.2	97.37	89.7	95.7	92.7	99.69	0.16
*Serratia*_sp._HSTU-BF1R2	*Serratia*_marcescens_strain_C110	79	89.94	58.4	46.82	77.3	92.5	0.07
*Serratia*_sp._HSTU-BF1R2	*Serratia*_marcescens_strain_SJC1005_	92.5	98.08	92.4	96.53	94.7	99.82	0.3
*Serratia*_sp._HSTU-BF1R2	*Serratia*_marcescens_strain_UMH6_	90.1	97.33	89.6	95.68	92.6	99.69	0.12
*Serratia*_sp._HSTU-BF1R2	*Serratia*_marcescens_strain_WVU-006	95	98.66	91.6	96.31	96.3	99.89	0.11
*Serratia*_sp._HSTU-BF1R2	*Serratia*_sp._JKS000199	96.2	98.9	92	96.42	97.2	99.92	0.04
*Serratia*_sp._HSTU-BF1R2	*Serratia*_sp._LS-1	96	98.87	92.4	96.52	97.1	99.92	0.05
*Serratia*_sp._HSTU-BF1R2	*Serratia*_ureilytica_strain_CM2016_324	90.8	97.54	89.4	95.61	93	99.72	0.14
*Serratia*_sp._HSTU-BF1R2	*Serratia*_ureilytica_strain_FDAARGOS_1089	94.8	98.62	92.4	96.52	96.3	99.89	0.08
*Serratia*_sp._HSTU-BF1R2	*Serratia*_ureilytica_strain_KML.E1	97	99.05	91.8	96.38	97.7	99.93	0.04
*Serratia*_sp._HSTU-BF1R2	*Serratia*_ureilytica_strain_MGH225_	95.9	98.84	91.7	96.34	97	99.91	0.05
*Serratia*_sp._HSTU-BF1R2	*Serratia*_ureilytica_strain_S24	95.8	98.83	92.5	96.57	97	99.91	0.03

Table 6: Digital DNA-DNA hybridization (dDDH) for species determination depends on whole genome sequences.

4. 4.6. Phylogenetic tree:

The phylogenetic tree analysis was based on whole genome sequence selected *Serratia* sp. strain HSTU-BF1R2 isolate from eggplant root with the comparison strains sequence collected from public database Gene Bank (NCBI). Here tree construction engaged 15 nucleotides sequences were shown. The optimal tree with the sum of branch length (SBL) = 0.09592704 is shown. The percentage of replicate trees in which the associated taxa clustered together in the bootstrap test (1000 replicates) are shown next to the branches. *Serratia* sp. strain HSTU-BF1R2 is closely related to two groups. Group one includes Serratia Subtilis strainCP041129 (WVU006chromosome), CP06651.1(S24chromosome), LT9078433.1 (SPJK000199 genome assembly), CP068214.1(FDAARGOS 1089 chromosome), OW967878.1(isolate 0 genome assembly), OX291765.1(SJC1005 genome assembly) and groups two includes Serratia Subtilis strain CP033504.1(LS-1 chromosome) are sister taxa with the more intimately related to each other because they share are more common ancestor than any other groups.In group one individually we get two sister taxa group CP041129(WVU-006 chromosome), CP06651.1 (S24 chromosome) and OW967878.1(isolate0genome assembly), OX291765.1(SJC1005 genome assembly). Interestingly OW967878.1 and OX291765.1 sister taxa group also create a monophyletic clade with CP033504.1(LS-1 chromosome). The tree is drawn to scale, with branch lengths in the same units as those of the evolutionary distances used to infer the phylogenetic tree. This analysis involved 15 nucleotide sequences. Evolutionary analyses were conducted in MEGA 11.

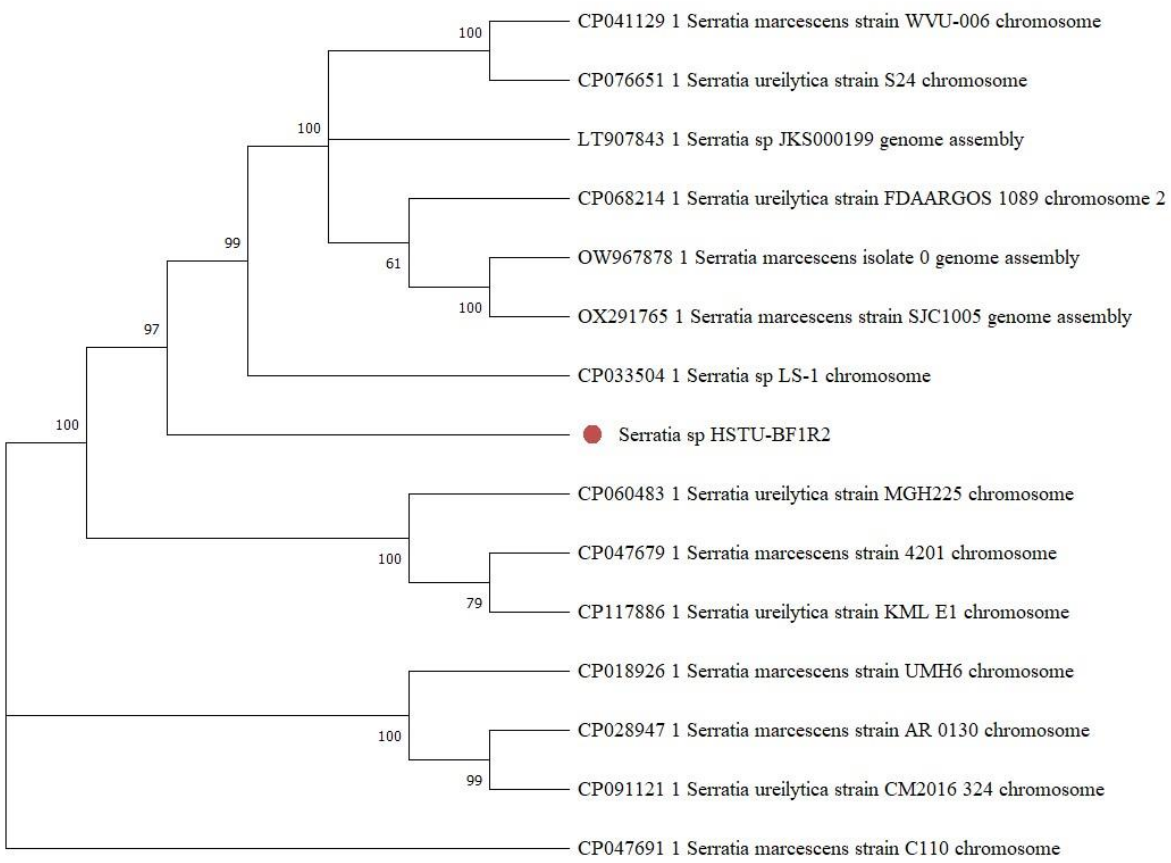

Figure 15: The phylogenetic tree based on whole genome of *Serratia* sp. HSTU-BF1R2 strain with closely related whole genome strains.

4. 4.7. Multiple genome alignment:

In the genomic characteristics of *Serratia* sp. strain HSTU-BF1R2, we conducted a comprehensive multiple genome alignment study by comparing it with four bacterial strains, including *Serratia* marcescens isolate 0 genome assembly (OW967878.1), *Serratia* sp. JKS000199 genome assembly (LT907843.1), *Serratia* sp. LS-1 chromosome (CP033504.1), and *Serratia* ureilytica strain KML.E1 chromosome (CP117886). In this analysis, each genome was represented as a series of coordinated colored square shapes, indicating homologous fragments across the genomes. Conserved segments of genome rearrangement were visualized with the same color code, as illustrated in Figure 16. From the progressive mauve alignment output, we gained insights into the evolutionary coordination and functional equivalence among the different strains. My findings reveal that the highest level of evolutionary coordination and functional equivalence was observed among three strains: *Serratia* marcescens isolate 0 genome assembly (OW967878.1), *Serratia* sp. JKS000199 genome assembly (LT907843.1), and *Serratia* ureilytica strain KML.E1 chromosome (CP117886). These strains displayed substantial

conservation of genomic segments and rearrangements, suggesting potential shared evolutionary histories and functional genomic elements.

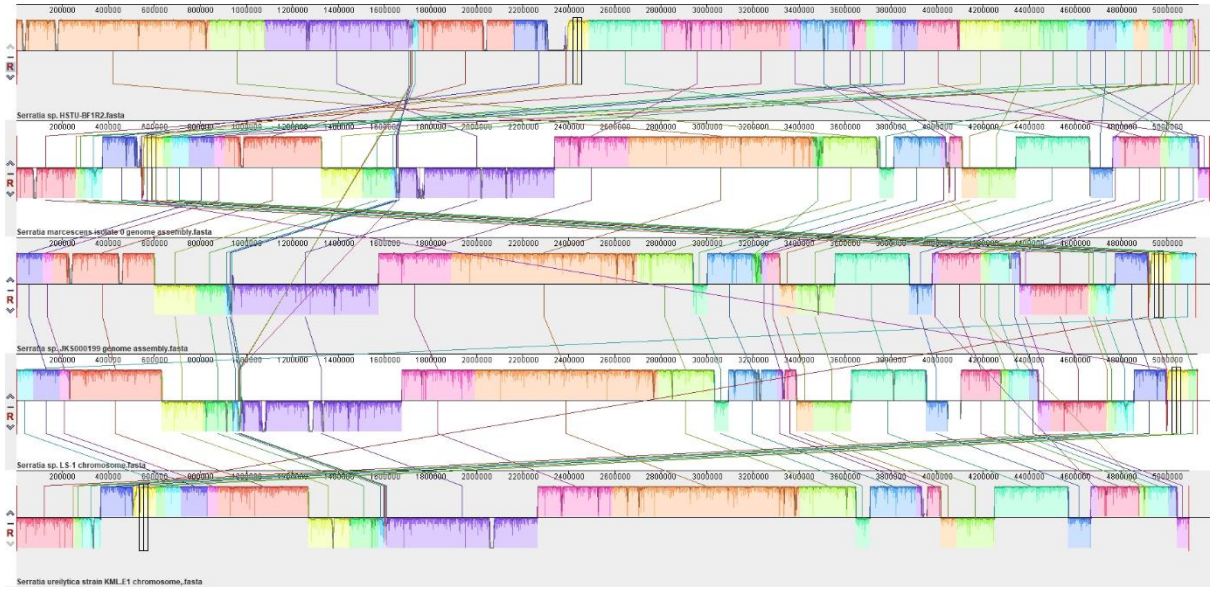

Figure 16: Multiple genome analysis of *Serratia* sp. HSTU BF1R1 with other closely related strains.

4. 4.8. Pan-genomic analysis:

Pangenome refer to the entire gene contents of a bacterial species or set of strains. In pan-genomic analysis of *Serratia* sp. strain HSTU BF1R1 for homologous genes within the set of analyzed genomes as shown in figure no17. These homologous genes are divided into orthologous and paralogous genes.23 Orthologous genes diverged via evolutionary speciation. Paralogous genes diverged via gene duplication. We found 0 kbps to 700 kbps all reference genomes are showed paralogous relation among each other and then after 700 kbps the studied genome becoming too evolutionary unique. GC content showed the quality of genome and GC skew confirm here is no contaminant in the studied genome.

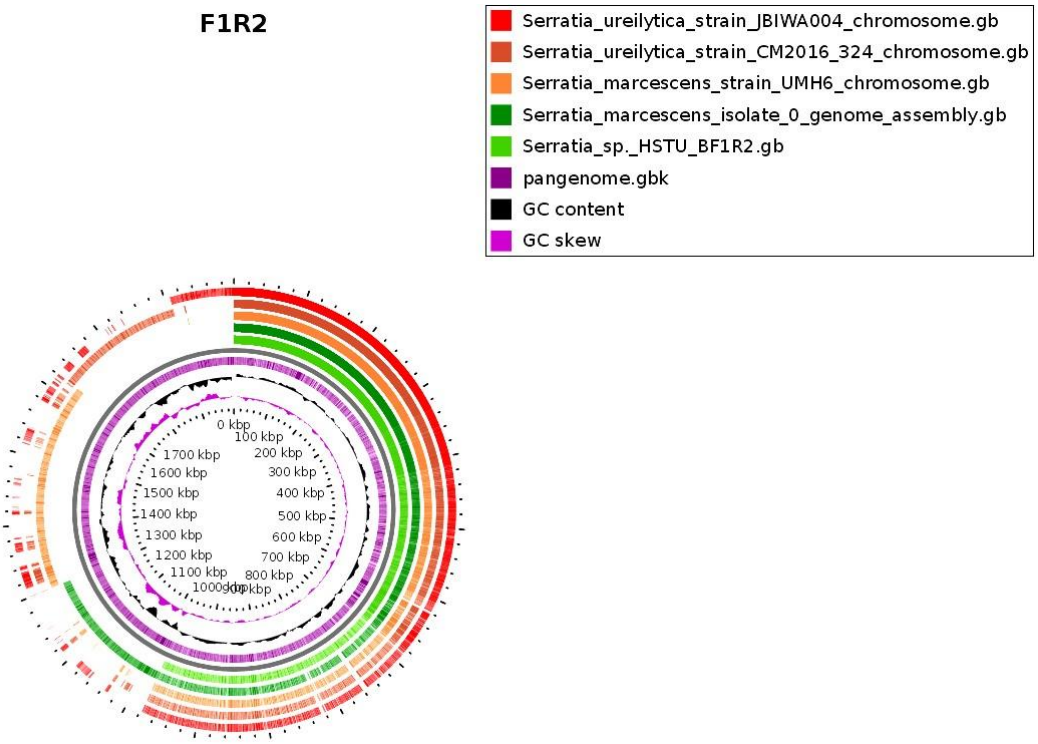

Figure 17: Pangenome analysis of *Serratia* sp. HSTU BF1R1 strain with nearest homologs strain for genomic comparison

4.5. Gene harboring by *Serratia* sp. HSTU BF1R2 genome

4. 5.1. Genes associated with pesticide degradation:

The pesticide-degrading bacterial isolates obtained from plant root. It can degrade the ecotoxic strong chlorpyrifos, diazinon, cypermethrin and profenofos. These bacteria can bioremediate soil with high chlorpyrifos, diazinon, cypermethrin and profenofos concentration and finally the people will feel safe during up taking that crop with no health hazardous. These microbes possess not only pesticide degrading capacities but lower the toxic effects of these pesticides on plants. But various other traits that help in plant growth promotion and involved in cell wall degradation by producing enzymes with dye degrading capability.

Gene Name	Locus Tag	CDS	Product	E.C. number
*amp*D	NW222_18130	149065..149661	1,6-anhydro-N-acetylmuramyl-L-alanine amidase AmpD	3.5.1.28
*glp*A	NW222_15100	65165..66814	anaerobicglycerol-3-phosphate ehydrogenase subunit A	1.1.5.3
*glp*B	NW222_15095	63907..65175	glycerol-3-phosphate dehydrogenase subunit GlpB	1.1.5.3
*glp*Q	NW222_15110	68617..69696	glycerophosphodiester phosphodiesterase	3.1.4.46
*pde*H	NW222_23710	14097..14888	cyclic-guanylate-specific phosphodiesterase	3.1.4.52
*pde*R	NW222_23680	5206..7200	cyclicdi-GMP phosphodiesterase	3.1.4.52
*pep*A	NW222_11045	132194..133705	leucyl aminopeptidase	3.4.11.1
*pep*B	NW222_16840	156504..157799	aminopeptidase PepB	3.4.11.23
*pep*D	NW222_08625	55068..56528	beta-Ala-His dipeptidase	3.4.13.20
*pep*Q	NW222_14805	4643..5974	Xaa-Pro dipeptidase	3.4.13.9
*phn*F	NW222_10915	99558..100286	Phosphonate etabolism transcriptional egulator PhnF	-
*phn*D	NW222_19470	33834..34766	phosphonateABC transportersubstrate-binding protein	7.3.2.2
*phn*G	NW222_10910	99114..99557	phosphonate C-P lyase system protein PhnG	-
*phn*H	NW222_10905	98529..99110	phosphonate C-P lyase system protein PhnH	-
*phn*J			alpha-D-ribose1-methylphosphonate5-phosphateC-P-lyase PhnJ	-
*phn*K	NW222_10890	95803..96591	phosphonate C-P lyase system protein PhnK	-
*phn*L	NW222_10880	94886..95590	phosphonate C-P lyase system protein PhnL	-
*phn*M	NW222_10875	93750..94886	alpha-D-ribose1-methylphosphonate 5-triphosphate diphosphatase	3.6.1.63
*phn*O			aminoalkylphosphonate N-acetyltransferase	2.3.1.-
*phn*P	NW222_10860	91787..92569	phosphonate metabolism	3.1.4.55

			protein PhnP	
-			Phosphodiesterase	3.1.4.-
*paa*C	NW222_02870	599672..600430	phenylacetate-CoA oxygenase subunit PaaC	1.14.13.149
*hpx*K	NW222_08445	21711..22955	Allantoate amidohydrolase	-
-	NW222_11930	320253..321116	Amidohydrolase family protein	-
-	NW222_14375	205817..206545	alpha/beta old hydrolase	-

4. 5.2. stress tolerance:

Interestingly, we found stress tolerance gene such as cspA, cspD, cspE (which are mainly responsible for cold shock), heat shock proteins- smpB, *ibp*A, *hsp*Q, *lep*A, (In here we found two class of chaperone protein one group of heat shock chaperone- ibpA, ibpB, hspQ and another group of molecular chaperone–dnaJ, dnaK, *rpo*H), Interestingly, the gene associated with drought stress tolerance includes proA, proB, proQ ,proX found within the genome of *Serratia* sp. HSTU BF1R1 .And Heavy metal resistance Arsenic tolerance arsA, arsB, arsC, acrA, trkA. and some Copper homeostasis copA, copC, cutC etc were found in the genome of *Serratia* sp. strain HSTU BF1R1

	Gene Name	**Locus Tag**	**CDS**	**Product name**	**E.C. number**
Cold Shock protein	*csp*A	NW222_05960	178430..178642	RNA chaperone/antiterminator CspA	-
	*csp*E	NW222_09895	312546..312755	transcription antiterminator/RNA stability regulator CspE	-
	*csp*D	NW222_07680	520531..520752	cold shock-like protein CspD	-
Heat Shock protein	*smp*B	NW222_17165	225632..226114	SsrA-binding protein SmpB	-
	*ibp*A	NW222_15825	229782..230195	heat shock chaperone IbpA	-
	*ibp*B	NW222_15820	229247..229675	heat shock chaperone IbpB	-
	*hsp*Q	NW222_07290	422795..423112	heat shock protein HspQ	-
	*dna*J	NW222_17720	51526..52650	molecular chaperone DnaJ	-
	*dna*K	NW222_17715	49506..51419	molecular chaperone DnaK	-
	*rpo*H	NW222_15005	48143..49000	RNA polymerase sigma	-

				factor RpoH	
	*lep*A	NW222_17070	207411..209210	translation elongation factor 4	3.6.5.n1
	*grp*E	NW222_17135	220725..221309	nucleotide exchange factor GrpE	-
Drought resistance	*nha*A	NW222_17725	52886..54052	Na+/H+ antiporter NhaA	-
	*cha*A	NW222_02055	435244..436347	sodium-potassium/proton antiporter ChaA	-
	*cha*B	NW222_02045	433775..434002	putative cation transport regulator ChaB	-
	*pro*A	NW222_08650	60567..61820	glutamate-5-semialdehyde dehydrogenase	1.2.1.41
	*pro*B	NW222_08645	59454..60557	glutamate 5-kinase	2.7.2.11
	*pro*Q	NW222_05710	128020..128730	RNA chaperone ProQ	-
	*pro*V	NW222_17390	263489..264691	glycine betaine/L-proline ABC transporter ATP-binding protein ProV	-
	*pro*W	NW222_17395	264684..265790	glycine betaine/L-proline ABC transporter permease ProW	-
	*pro*X	NW222_17400	265860..266861	glycine betaine/L-proline ABC transporter substrate-binding protein ProX	-
	*pro*P	NW222_06965	365444..366946	glycine betaine/L-proline transporter ProP	
	*pro*S	NW222_23095	62333..64051	proline--tRNA ligase	6.1.1.15
	*bet*A	NW222_21175	44946..46613	choline dehydrogenase	1.1.99.1
	*bet*B	NW222_21180	46838..48310	betaine-aldehyde dehydrogenase	1.2.1.8
	*bet*T	NW222_20555	71046..73043	choline BCCT transporter BetT	
	*trk*A	NW222_23975	7492..8868	Trk system potassium transporter TrkA	
	*trk*H	NW222_14795	2543..3994	Trk system potassium transporter TrkH	-
	*kdp*A	NW222_10210	375668..377356	potassium-transporting ATPase subunit KdpA	7.2.2.6
	*kdp*B	NW222_10205	373572..375641	potassium-transporting ATPase subunit KdpB	7.2.2.6
	*kdp*C	NW222_10200	372984..373553	potassium-transporting ATPase subunit KdpC	7.2.2.6

Heavy metal resistance Arsenic tolerance	**Gene Name**	**Locus Tag**	**CDS**	**Product name**	**E.C. number**
	arsC	NW222_02705	566316..566747	glutaredoxin-dependent arsenate reductase	1.20.4.1
	acrR	NW222_09460	218229..218888	multidrug efflux transporter anscriptional repressor AcrR	
	acrD	NW222_16155	4113..7247	multidrug efflux RND transporter permease AcrD	
	trkA	NW222_23975	7492..8868	Trk system potassium transporter TrkA	
Magnesium transport	corA	NW222_15150	76497..77447	magnesium/cobalt transporter CorA	
	corC	NW222_10035	338922..339800	CNNM family agnesium/cobalt transport protein CorC	
Copper homeostasis	copA	NW222_09615	257194..259905	copper-exporting P-typeATPase CopA	7.2.2.8
	copD	NW222_06485	273840..274721	copper homeostasis membrane protein CopD	
	cutC	NW222_01475	318305..319063	copper homeostasis protein CutC	
Zinc homeostasis	znuA	NW222_01390	303361..304305	zinc ABC transporter substrate-binding protein ZnuA	7.2.2.-
	znuB	NW222_01400	305139..305924	zinc ABC transporter permease subunit ZnuB	7.2.2.-
	znuC	NW222_01395	304384..305142	zinc ABC transporter ATP-binding protein ZnuC	7.2.2.-
Zinc, cadmium, lead and mercury homeostasis					
Manganese homeostasis	adhP	NW222_14115	141011..142027	alcohol dehydrogenase AdhP	1.1.1.1
	htpX	NW222_05670	118794..119672	protease HtpX	3.4.24.-
	zntB	NW222_00375	84216..85199	zinc transporter ZntB	
	mntR	NW222_06660	306326..306808	manganese-binding transcriptional regulator MntR	

	mntP	NW222_01630	349962..350531	manganese efflux pump MntP	

4. 5.3. Plant growth promoting genes:

The genome of *Serratia* sp. strain HSTU-BF1R2 contains several genes related to various aspects of plant growth promotion (PGP). Notably, it possesses nitrogen fixation genes (nif JSUL, iscUAR) which contribute to nitrogen metabolism. Additionally, genes associated with nitrogen metabolism regulation (glnD, glnB), phosphate metabolism (pstN), siderophore production (fes, entFS, fepA), sulfur metabolism, and biofilm formation were identified. These genes collectively contribute to the development of plant growth.

PGP activities description	**Gene Name**	**Locus Tag**	**CDS**	**Product**	**E.C. number**
Nitrogen fixation	*isc*U	NW222_16870	161439..161825	Fe-S cluster assembly scaffold *IscU*	-
	*nif*J	NW222_00360	78751..82284	pyruvate:ferredoxin (flavodoxin) oxidoreductase	-
	*isc*A	NW222_16865	161061..161384	iron-sulfur cluster assembly protein IscA	-
	*isc*R	NW222_16880	163119..163613	Fe-S cluster assembly transcriptional regulator IscR	-
	*isc*S	NW222_16875	161850..163064	cysteine desulfurase	2.8.1.7
	*suf*A	NW222_05320	45032..45403	Fe-S cluster assembly scaffold SufA	-
	*suf*B	NW222_05315	43521..45017	Fe-S cluster assembly protein SufB	-
	*suf*C	NW222_05310	42731..43477	Fe-S cluster assembly ATPase SufC	-
	*suf*D	NW222_05305	41470..42756	Fe-S cluster assembly protein SufD	-
	*suf*S	NW222_05300	40247..41473	cysteine desulfurase SufS	2.8.1.7
	*suf*E	NW222_05295	39795..40211	cysteine desulfuration protein SufE	-
	fdx	NW222_16850	158256..158591	ISC system 2Fe-2S type ferredoxin	-
	*isc*X	NW222_16845	158023..158223	Fe-S cluster assembly protein IscX	-
	*hsc*A	NW222_16855	158594..160444	Fe-S protein assembly	3.6.4.-

				chaperone HscA	
	*hsc*B	NW222_16860	160477..160998	co-chaperone HscB	-
	*nsr*R	NW222_10460	14192..14617	nitric oxide-sensing transcriptional repressor NsrR	-
	*gln*K	NW222_09290	189152..189490	P-II family nitrogen regulator	-
Nitrogen metabolism regulatory protein	*gln*D	NW222_22935	24720..27383	bifunctional uridylyltransferase/uridylyl-removing protein GlnD	2.7.7.59
	*gln*B	NW222_16970	184355..184693	nitrogen regulatory protein P-II	-
	*pts*N	NW222_13140	254065..254526	PTS IIA-like nitrogen regulatory protein PtsN	-
Ammonia assimilation	*glt*B	NW222_13010	228923..233383	glutamate synthase large subunit	1.4.1.13
ACC deaminase					
	*rim*M	NW222_23480	8042..8590	ribosome maturation factor RimM	-
Siderophore enterobactin					
	*ent*S	NW222_14480	225882..227165	enterobactin transporter EntS	-
	*ent*D			enterobactin synthase subunit *EntD*	6.3.2.14
	*fhu*A	NW222_12105	25777..27975	ferrichrome porin FhuA	-
	*fhu*B	NW222_12090	22039..24027	Fe(3+)-hydroxamate ABC transporter permease FhuB	-
	*fhu*C	NW222_12100	24932..25729	Fe3+-hydroxamate ABC transporter ATP-binding protein FhuC	7.2.2.-
	*fhu*D	NW222_12095	24024..24932	Fe(3+)-hydroxamate ABC transporter substrate-binding protein FhuD	7.2.2.-
	*ton*B	NW222_00910	205633..206376	TonB system transport protein TonB	-
	*fep*B	NW222_23420	60307..61314	Fe2+-enterobactin ABC transporter substrate-binding protein	7.2.2.-
	*fep*G	NW222_23410	57999..59036	iron-enterobactin ABC transporter permease	7.2.2.-

	*exb*B	NW222_12515	121840..122817	tol-pal system-associated acyl-CoA thioesterase	3.1.2.-
IAA production					
	*trp*S	NW222_18675	40648..41655	tryptophan--tRNA ligase	6.1.1.2
	*trp*B	NW222_00865	197806..199011	tryptophan synthase subunit beta	4.2.1.20
	*trp*D	NW222_00855	194818..196414	bifunctional anthranilate synthase glutamate amidotransferase component TrpG/anthranilate phosphoribosyltransferase TrpD	2.4.2.18 /4.1.3.27
Phosphate metabolism	*pit*A	NW222_19180	155727..157229	inorganic phosphate transporter PitA	-
	*pst*S	NW222_15990	261026..262066	phosphate ABC transporter substrate-binding protein PstS	7.3.2.1
	*pst*C	NW222_15985	259978..260934	phosphate ABC transporter permease PstC	7.3.2.1
	*pst*A	NW222_16435	60469..62118	phosphate ABC transporter permease PstA	-
	*pst*B	NW222_15975	258261..259037	phosphate ABC transporter ATP-binding protein PstB	7.3.2.1
	*pho*U	NW222_15970	257515..258249	phosphate signaling complex protein PhoU	3.5.2.6
	*ugp*A	NW222_14950	35396..36283	sn-glycerol-3-phosphate ABC transporter permease UgpA	7.6.2.-
	*ugp*B	NW222_14955	36362..37681	sn-glycerol-3-phosphate ABC transporter substrate-binding protein UgpB	7.6.2.-
	*ugp*E	NW222_14945	34554..35399	sn-glycerol-3-phosphate ABC transporter permease UgpE	7.6.2.-

	*pho*A	NW222_21125	32004..33431	alkaline phosphatase	3.1.3.1
	*pho*B	NW222_09015	128099..128788	phosphate response regulator transcription factor PhoB	-
	*pho*R	NW222_09020	128813..130129	phosphate regulon sensor histidine kinase PhoR	2.7.13.3
	*pho*H	NW222_02065	437522..438310	phosphate starvation-inducible protein PhoH	-
	*pnt*A	NW222_00245	53866..55395	Re/Si-specific NAD(P)(+) transhydrogenase subunit alpha	1.6.1.2
	*pnt*B	NW222_00240	52461..53855	Re/Si-specific NAD(P)(+) transhydrogenase subunit beta	-
	*pho*Q	NW222_06145	209009..210466	two-component system sensor histidine kinase PhoQ	2.7.13.3
Biofilm formation	*tom*B	NW222_09415	209276..209644	Hha toxicity modulator TomB	-
	*lux*S	NW222_23455	3325..3840	S-ribosylhomocysteine lyase	4.4.1.21
	efp	NW222_22605	12731..13297	elongation factor P	-
	*flg*A	NW222_02295	483529..484182	flagellar basal body P-ring formation chaperone FlgA	-
	*flg*B	NW222_02290	482955..483368	flagellar basal body rod protein FlgB	-
	*flg*C	NW222_02285	482545..482949	flagellar basal body rod protein FlgC	-
	*flg*D	NW222_02280	481855..482532	flagellar hook assembly protein FlgD	-
	*flg*G	NW222_02265	479008..479790	flagellar basal-body rod protein FlgG	-
	*flg*H	NW222_02260	478223..478924	flagellar basal body L-ring protein FlgH	-
	*flg*J	NW222_02250	476168..477112	flagellar assembly peptidoglycan hydrolase FlgJ	3.2.1.-
	*flg*K	NW222_02245	474312..475961	flagellar hook-associated protein FlgK	-

	*flg*L	NW222_02240	473293..474252	flagellar hook-associated protein FlgL	-
	*flg*N	NW222_02305	484664..485098	flagellar export chaperone FlgN	-
	*flg*M	NW222_02300	484312..484623	flagellar biosynthesis anti-sigma factor FlgM	-
	*mot*A	NW222_02380	500068..500958	flagellar motor stator protein MotA	-
	*mot*B	NW222_02375	499007..500071	flagellar motor protein MotB	-
	hfq	NW222_10430	8283..8591	RNA chaperone Hfq	-
Sulfur assimilation	*cys*Z	NW222_23335	41822..42580	sulfate transporter CysZ	-
	*cys*K	NW222_23330	40668..41636	cysteine synthase A	2.5.1.47
	*cys*M	NW222_23300	34457..35338	cysteine synthase CysM	2.5.1.47
	*cys*A	NW222_23295	33288..34376	sulfate/thiosulfate ABC transporter ATP-binding protein CysA	7.3.2.-
	*cys*W	NW222_23290	32423..33298	sulfate/thiosulfate ABC transporter permease CysW	7.3.2.-
	*cys*C	NW222_18300	191900..192589	adenylyl-sulfate kinase	2.7.1.25
	*cys*N	NW222_18295	190534..191961	sulfate adenylyltransferase subunit CysN	2.7.7.4
	*cys*D	NW222_18290	189614..190522	sulfate adenylyltransferase subunit CysD	2.7.7.4
	*cys*H			phosphoadenosinephosphosulfate reductase	1.8.4.8
	*cys*I	NW222_18270	184262..185977	assimilatory sulfite reductase (NADPH) hemoprotein subunit	1.8.1.2
	*cys*J	NW222_18265	182463..184262	NADPH-dependent assimilatory sulfite reductase flavoprotein subunit	1.8.1.2
	*cys*T	NW222_23285	31584..32423	sulfate/thiosulfate ABC transporter permease CysT	7.3.2.-
Sulfur metabolism	*cys*C	NW222_18300	191900..192589	adenylyl-sulfate kinase	2.7.1.25
	*cys*N	NW222_18295	190534..191961	sulfate adenylyltransferase subunit CysN	2.7.7.4
	*cys*D	NW222_18290	189614..190522	sulfate adenylyltransferase	2.7.7.4

				subunit CysD	
	*cys*I	NW222_18270	184262..185977	assimilatory sulfite reductase (NADPH) hemoprotein subunit	1.8.1.2
	*cys*J	NW222_18265	182463..184262	NADPH-dependent assimilatory sulfite reductase flavoprotein subunit	1.8.1.2
	*cys*E	NW222_21810	51243..52064	serine O-acetyltransferase	2.3.1.30
	*cys*Q	NW222_10550	28846..29586	3'(2'),5'-bisphosphate nucleotidase CysQ	3.1.3.7
	*cys*K	NW222_23330	40668..41636	cysteine synthase A	2.5.1.47
	*cys*S	NW222_09690	273927..275312	cysteine--tRNA ligase	6.1.1.16
	*cys*Z	NW222_23335	41822..42580	sulfate transporter CysZ	-
	*cys*M	NW222_23300	34457..35338	cysteine synthase CysM	2.5.1.47
	*cys*A	NW222_23295	33288..34376	sulfate/thiosulfate ABC transporter ATP-binding protein CysA	7.3.2.-
	*cys*W	NW222_23290	32423..33298	sulfate/thiosulfate ABC transporter permease CysW	7.3.2.-
	*fdx*H	NW222_15640	186684..187586	formate dehydrogenase subunit beta	1.17.1.9
Antimicrobial peptide	*pag*P	NW222_08790	86503..87093	lipid IV(A) palmitoyltransferase PagP	2.3.1.251
	*sap*B	NW222_00495	109094..110059	putrescine ABC transporter permease SapB	7.6.2.-
Chemotaxis	*che*Z	NW222_02335	489792..490436	protein phosphatase CheZ	3.6.1.-
	*che*Y	NW222_02340	490447..490836	chemotaxis response regulator CheY	-
	*che*R	NW222_02350	491988..492860	protein-glutamate O-methyltransferase CheR	2.1.1.80
	*che*W	NW222_02365	496456..496956	chemotaxis protein CheW	-
	*che*A	NW222_02370	496989..499010	chemotaxis protein CheA	-
	*mal*E	NW222_22295	41936..43129	maltose/maltodextrin ABC transporter substrate-binding	7.5.2.1

				protein MalE	
	*rbs*B	NW222_16105	286984..287871	ribose ABC transporter substrate-binding protein RbsB	-
Motility	*fli*Z	NW222_02115	452378..452887	flagella biosynthesis regulatory protein FliZ	-
	*Fli*D	NW222_02130	455198..456598	flagellar filament capping protein FliD	-
	*fli*S	NW222_02135	456625..457035	flagellar export chaperone FliS	-
	*fli*T	NW222_02140	457035..457403	flagella biosynthesis regulatory protein FliT	-
	*fli*F	NW222_02170	461786..463480	flagellar basal-body MS-ring/collar protein FliF	-
	*fli*E	NW222_02165	461156..461470	flagellar hook-basal body complex protein FliE	-
	*fli*G	NW222_02175	463477..464469	flagellar motor switch protein FliG	-
	*fli*H	NW222_02180	464462..465166	flagellar assembly protein FliH	-
	*fli*I	NW222_02185	465166..466527	flagellar protein export ATPase FliI	-
	*Fli*J	NW222_02190	466548..466994	flagellar export protein FliJ	-
	*fli*M	NW222_02205	468880..469884	flagellar motor switch protein FliM	-
	*fli*P	NW222_02220	470694..471455	flagellar type III secretion system pore protein FliP	-
	*fli*Q	NW222_02225	471477..471746	flagellar biosynthesis protein FliQ	-
	*fli*R	NW222_02230	471749..472531	flagellar biosynthetic protein FliR	-
Adhesive structure	*hof*C	NW222_18110	144819..146018	protein transport protein HofC	-
Flageller protein	*fli*P	NW222_02220	470694..471455	flagellar type III secretion system pore protein FliP	-
	*mot*A	NW222_02380	500068..500958	flagellar motor stator protein MotA	-
	*mot*B	NW222_02375	499007..500071	flagellar motor protein MotB	-
	*mur*J	NW222_01500	323508..325043	murein biosynthesis integral membrane protein	-

				MurJ	
Superoxide dismutase	*sod*A	NW222_15650	191063..191683	superoxide dismutase [Mn]	1.15.1.1
	*sod*B	NW222_05215	26569..27147	superoxide dismutase [Fe]	1.15.1.1
	*sod*C	NW222_05150	13892..14413	superoxide dismutase [Cu-Zn] SodC	1.15.1.1
Trehalose metabolism	*tre*B	NW222_10960	110399..111814	PTS trehalose transporter subunit IIBC	2.7.1.201
	*tre*C	NW222_10955	108667..110331	alpha,alpha-phosphotrehalase	3.2.1.93
	*tre*R	NW222_10965	111944..112891	trehalose operon repressor TreR	-

4.6. Virtual screening and molecular docking:

4. 6.1. Protein model quality

The pesticide-degrading protein models of *Serratia* sp. strain HSTU BF1R1 underwent a comprehensive evaluation based on various parameters, as detailed in Table 7. A total of 22 model proteins were generated using the template-based method in "I-TASSER." The quality assessment included the following criteria: TM score, RMSD (Root Mean Square Deviation), Identity (Iden.), Coverage (cov.), orientation of secondary structures (α-helix, β-strand, η-coil, and disordered regions), "ERRAT" score (which evaluates the quality of non-bonded interactions between different types of atoms), "VERIFY 3D" (a verification method comparing 3D representations with refined structures from the PDB), and Ramachandran plot analysis to assess core, allowed, generously allowed, and disallowed percentages. From this analysis, it was found that among the 22 model proteins, 11 models were validated based on the "VERIFY 3D" criteria. Additionally, the "ERRAT" scores for the 11 validated models ranged from 94.739 to 98.3871 as shown in Table7. These results provide valuable insights into the reliability and accuracy of the generated protein models for *Serratia* sp. strain HSTU BF1R1.

Model protein	Best PDB hit	TMscore,RMSD, Iden, cov	α -helix, β -strand η - coil, disordered	ERRAT (quality score)	VERIFY (3D-ID score) %	Ramachandran plot(core,allow, gener,disallow) %
AmpD	1j2sA	0.935,0.54, 0.706, 0.944	25, 19, 56	90	98.48	91.5, 8.5 0.0, 0.0
*glp*A	2rgoA	0.860,2.62, 0.220, 0.925	38, 19, 42	94.139	71.04	90.4, 9.0 0.4, 0.2
*glp*B	1jehA	0.745,2.13, 0.152,0.791	39, 14, 47	93.1373	79.81	94.3, 5.7 0.0, 0.0
*glp*Q	1ydyA	0.909, 0.49 0.802, 0.914	35, 16, 50	93.049	93.31	89.8, 9.3 0.9, 0.0
*pde*H	4rnfA	0.914, 1.62 0.181, 0.962	53, 21, 26	98.3871	68.70	93.2, 6.0 0.9, 0.0
*pde*R	5xgbA	0.810, 0.74 0.277,0.815	48, 21, 31	97.7671	73.49	95.6, 4.0 0.2 ,0.2
*pep*A	1gytL	0.996, 0.49 0.911, 1.000	40, 20, 39	95.9191	83.43	91.9, 7.5 0.3, 0.3
*pep*B	6cxdA	0.966, 0.32 0.839, 0.968	35, 24, 41	94.739	85.28	92.9, 6.8 0.3, 0.0
*pep*D	3mruA	0.999, 0.27 0.621,1.000	31, 28, 41	91.5433	80.45	93.5, 6.5 0.0, 0.0
*pep*Q	4qr8A	0.995,0.20 0.728,0.996	38, 17, 45	91.8981	87.07	92.8, 6.8 0.4, 0.0
*phn*F	2wv0D	0.975, 0.54 0.227,0.984	40, 27, 33	94.7137	76.86	92.6, 6.9 0.0, 0.5
*phn*D	5o2jA	0.804, 1.36 0.255,0.836	42, 19, 39	95.122	84.19	86.9,12.0 0.7, 0.4
*phn*G	4xb6A	0.953, 0.69 0.524, 0.973	67, 10, 23	97.5	65.31	96.1, 3.1 0.0, 0.8
*phn*H	2fsuA	0.851, 0.67, 0.524, 0.860	25, 24, 50	97.2678	60.10	89.7, 9.7 0.0, 0.6
*phn*K	7z17I	0.914, 1.18 0.855, 0.947	41, 24, 35	96.0474	86.26	95.5, 4.0 0.4, 0.0
*phn*L	7z15K	0.941, 0.77 0.737, 0.957	40, 27, 33	97.2973	67.38	92.7, 7.3 0.0, 0.0

*phn*M	5e5cA	0.913, 1.71 0.157, 0.958	37, 24, 40	98.6264	75.93	93.1, 6.0 0.3, 0.6
*phn*P	3g1pB	0.952, 0.45 0.542,0.958	18, 29, 52	86.5672	85.71	89.5, 7.5 2.4, 0.5
*paa*C	1otkA	0.966, 0.31 0.643,0.968	73, 0, 27	99.177	80.16	95.9, 4.1 0.0, 0.0
*hpx*K	4pxbA	0.952, 1.74, 0.336,1.000	34, 22, 44	95.4315	73.19	96.9, 2.8 0.3, 0.0
Alpha-beta fold hydrolase	6ba8A	0.917, 1.36 0.210, 0.963	37, 18, 45	98.6842	71.90	93.3, 5.7 0.0 ,1.0
amidohydrolase family protein	4dlfA	0.956,0.50 0.518, 0.962	40, 18, 41	96.7626	94.08	93.9, 5.7 0.4, 0.0

Table 7: pesticide degrading model protein quality assessment of *serratia* sp. strain HSTU-BF1R2

4. 6.2. Virtual Screening:

The virtual screening results revealed that several pesticide ligands exhibited significant binding affinity with the organophosphate degrading potential protein from *Serratia* sp. strain HSTU BF1R1 strains, with a crossing threshold of -7.00 Kcal/mol. Among these ligands, pepB demonstrated the highest binding score of -8.7 Kcal/mol with cypermethrin, and a total of 11 protein docking scores surpassed the 1.5 box length. Additionally, pepB showed favorable docking scores of -8.2 and -7.9 with carbendazim and Pyridaphenthion, respectively. PepA also displayed promising binding affinities of -8.6 and -7.4 with cypermethrin and Isoxathion, while PepQ exhibited good binding results of -7.4 to -7.5 with Menazon and EPBP. These findings are encouraging, especially considering the potential for synergistic interactions. Moreover, the analysis of limiting energies provided valuable insights into *Serratia* sp. HSTU BF1R1 (Fig -18).

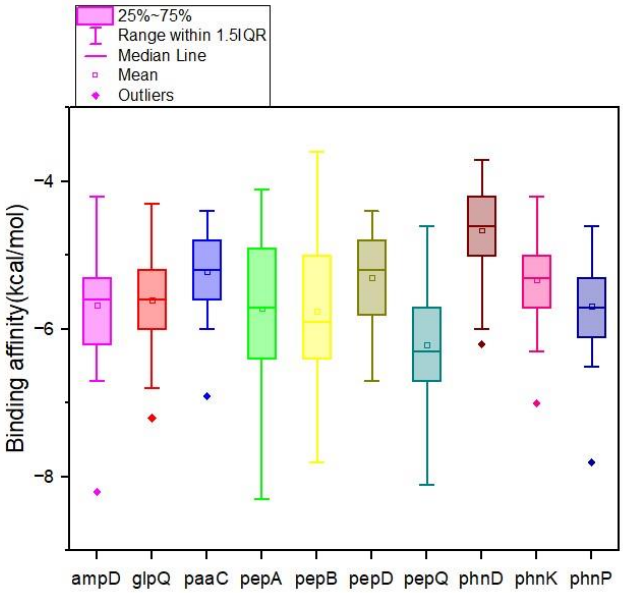

Figure 18: Virtual screening graphical result representation by origin 8.0 pro

4.7. Molecular docking and visualization:

ampD binding domain protein:

ampD protein- cypermethrin docked complex demonstrated the interaction with multiple residues. Conventional H-bonds were made by the LYS 162, SER 37 to the O-atom and N-atom of cypermethrin compound. Besides, a great number of residues were interacted with the ligand molecule by alkyl, pi-alkyl, and pi-Anion bonds namely, VAL 72, PRO40 and GLU 116 sequentially. These multiple interactions account for the good binding affinity of ampD cypermethrin as showed -8.2 docking value (Figure 19)

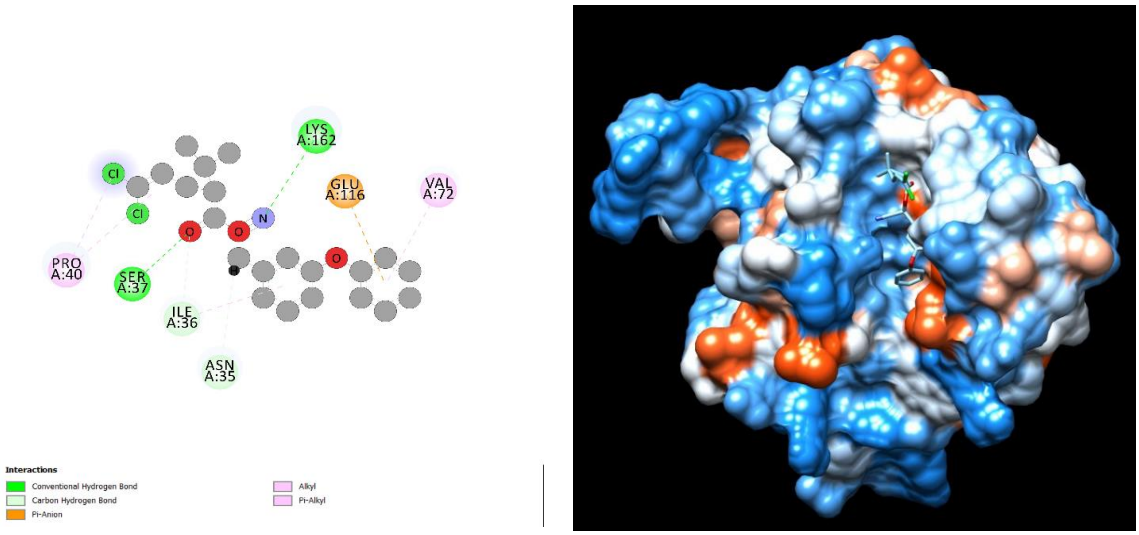

Figure 19: Molecular docking and catalytic interaction of ampD binding domain protein with cypermethrin.

pepB binding domain protein: and the attractive

charge interaction is made via Asp152 with the +P-atom of Crotoxyphos

The conventional hydrogen bond interaction was observed for GLY 374, THR337, ARG282 with the side chain of the benzene ring attached, the O-atom, of EPBP compound, while VAL 366 formed Pi-alkyl bonds.Only one amino acid made attractive charge and was interconnected ASP278 with sulfur atom. These sulfur atom bind with +P atom of EPBP compound. The pepB protein and EPBP ligand interactions affinity was -8.8 were observed by the different residues (Figure 20).

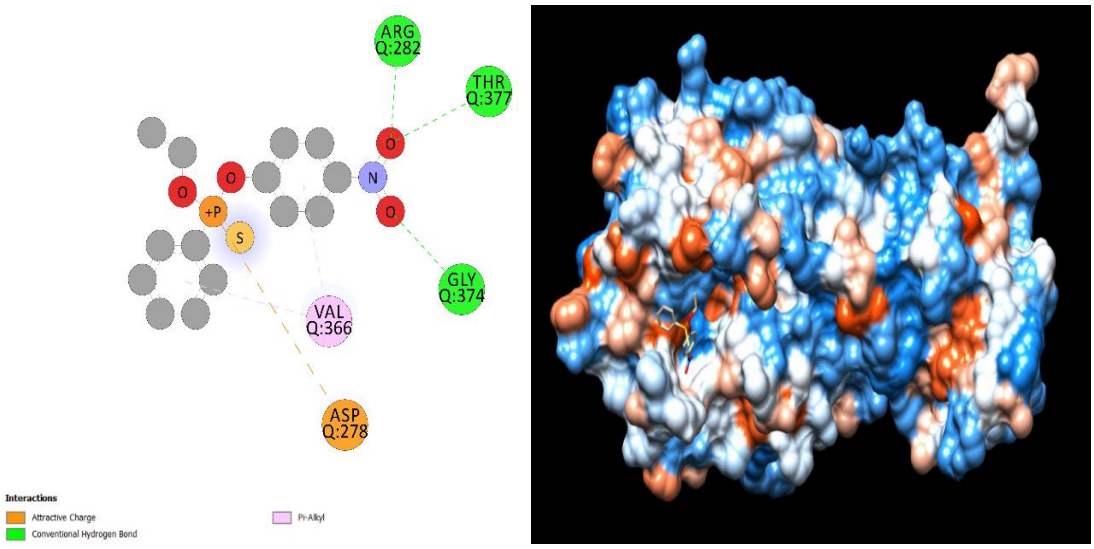

Figure 20: Molecular docking and catalytic interaction of pepB binding domain protein with EPBP.

pepB protein- carbendazim docked complex demonstrated the interaction with multiple residues. Conventional H-bonds were made by the ARG 420 interaction to the O-atom and GLN340 interact with N-H -atom of carbendazim compound. Besides, a great number of residues interacted with the ligand molecule by alkyl, pi-alkyl, and carbon hydrogen bond bonds namely, TRP 73, LEU 42and GLU 70 sequentially. These multiple interactions account for the good binding affinity of pepB carbendazim as showed -8.2 docking value (Figure 21)

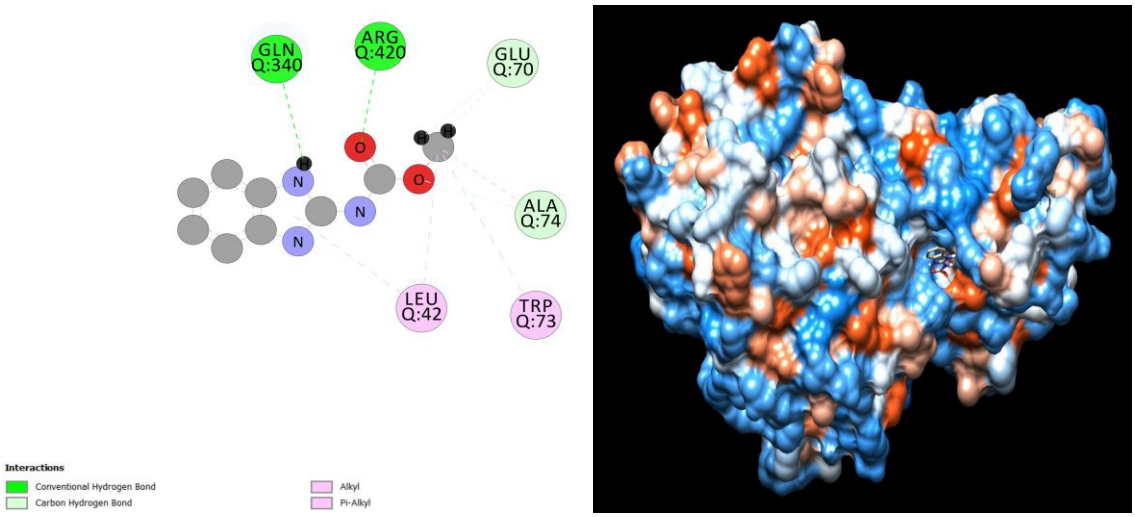

Figure 21: Molecular docking and catalytic interaction of pepB binding domain protein with carbendazim.

pepA binding domain protein:

In (Figure 22) pepA protein conventional hydrogen bond GLY382and ALA383 interaction with the O-atom, and the ASP293,TYR292 bind with N-H atom of menazon compound, and also the carbon hydrogen bond Thr381 bind with O-atom. while ASP 352 formed PI-cation bonds with the +P and N atom of menazon. The pepA protein and menazon insecticide docked complex ligand interactions were observed by the different residues.the binding affinity showed -8.9

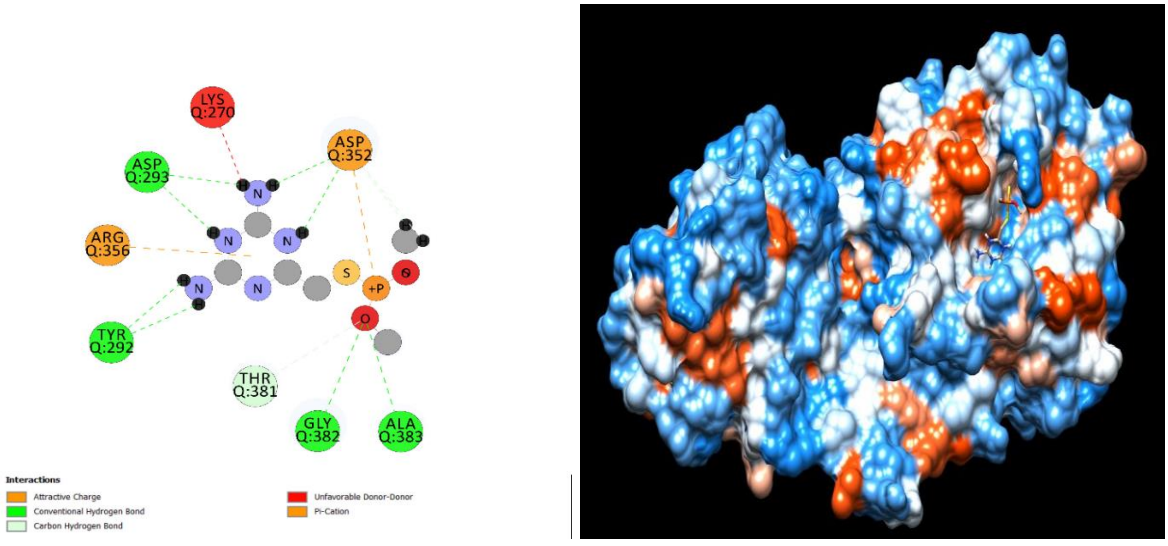

Figure 22: Molecular docking and catalytic interaction of pepA binding domain protein with menazon.

pepQ binding domain protein:

pepQ protein- azinphos methyl docked complex demonstrated the interaction with multiple residues. In particular, conventional H-bonds were made by the ARG 370 to the O-atom of cypermethrin compound. Besides, a great number of residues were interacted with the ligand molecule by pi-alkyl, pi-pi T shaped bonds namely, TYR 214,and LEU 227 sequentially . Only one amino acid made an attractive charge and was interconnected ASP 246 with O atom. These O atoms bind with +P atom with and Pi-sulfer interect with S atom. These multiple interactions account for the good binding affinity of pepQ, Azinphos methyl as showed -7.2 docking value (Figure 23)

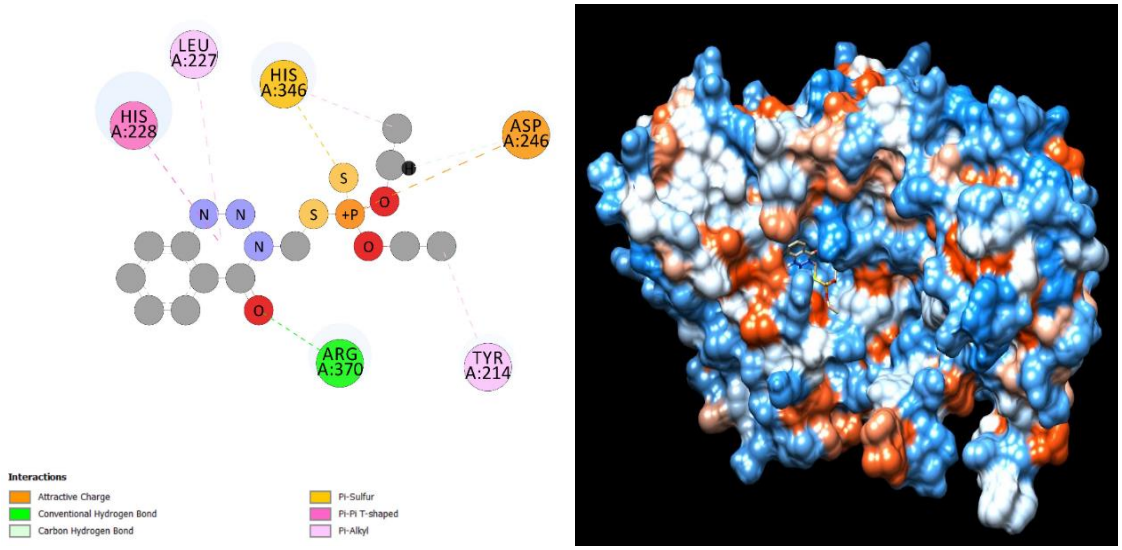

Figure 23: Molecular docking and catalytic interaction of pepQ binding domain protein with Azinphos methyl.

In particular, HIS 335 conventional hydrogen bond provided an attractive charge interaction with the phosphate atom. In addition, Pi alkyl and Pi-pi T shaped are ARG 370 interactions were observed with H residues. .This interactions is responsible for pepQ high affinity with Triazophos (Figure 24).

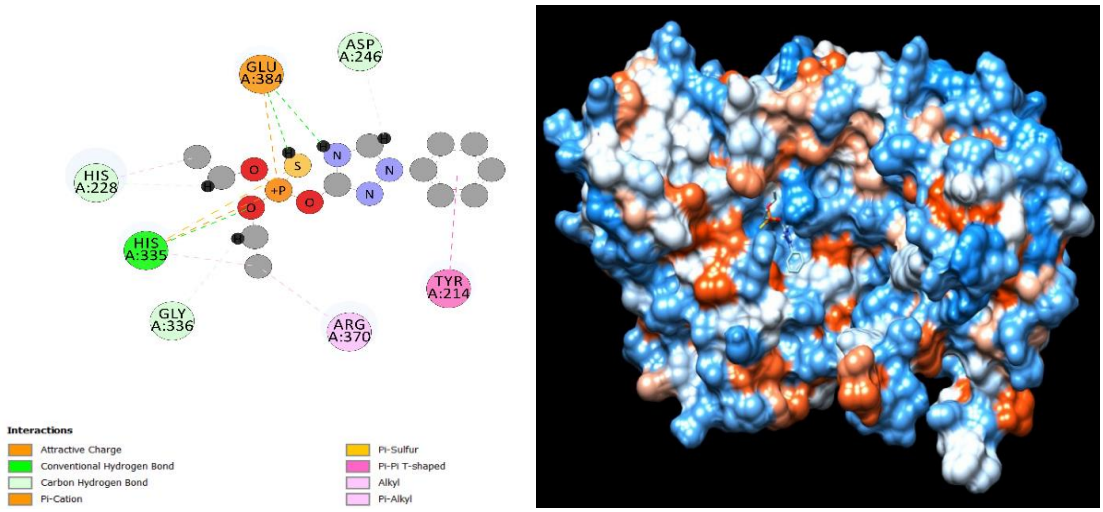

Figure no 24: Molecular docking and catalytic interaction of pepQ binding domain protein with Triazophos.

Moreover, pepQ protein- carbofuran docked complex demonstrated the interaction with multiple residues (figure 25). In particular, orthodox conventional hydrogen bond was made by GLN 39 to the O-atom of carbofuran compound. Besides, the carbon hydrogen bond and pi-alkyl GLU37, PRO49, PHE 50, TYR131 engage by H atom and the pi-pi T shaped are attached to benzene ring. The binding affinity of pepQ and carbofuran is 7.1

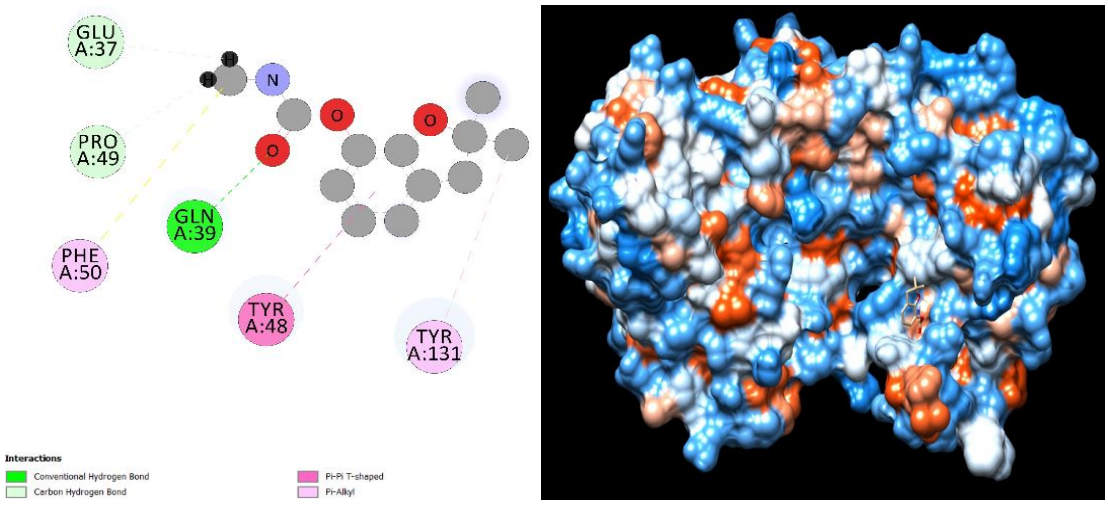

Figure 25: Molecular docking and catalytic interaction of pepQ binding domain protein with Carbofuran.

CHAPTER V
DISCUSSON AND CONCLUSION

Discussion

Endophytes play a fundamental role in agriculture, as they contribute to improved crop production, pathogen resistance, and aid in pesticide detoxification. These distinct endophytic bacteria offer potential as biofertilizers, promoting sustainable agricultural practices. In this study, we conducted an extensive investigation of a recently isolated eggplant root endophyte strain with the ability to mineralize chlorpyrifos as its carbon source. Additionally, we demonstrated the strain's positive effects on tomato plant growth promotion at various stages -germination, vegetative, and reproductive. Notably, our strain classification analysis revealed its novel evolutionary origin in Bangladesh, significantly diverging from its closest homologs (Haque *et al.,* 2022). In biochemical test we can see in MR-VP test MR show positive result its indicated by the development of a red color after adding Methyl Red indicator to the broth, signifies that the microorganism being tested is capable of performing mixed acid fermentation. On the other hand, the Voges-proskauer (VP) test showed negative result that indicates the bacterium being tested does not produce significant amounts of acetoin during glucose fermentation. Instead, it likely utilizes other pathways, such as the butanediol fermentation pathway, to metabolize glucose. The absence of acetoin production is reflected in the lack of a color change in the medium after the addition of the reagents. A positive catalase test result is observed when bubbles of oxygen gas are rapidly formed when hydrogen peroxide is added to the bacterial colony or culture. The bubbles signify that the catalase enzyme is present and actively catalyzing the decomposition of hydrogen peroxide into water and oxygen gas. Similar result was observed by (Son *et al.,* 2006), who had conducted experiment on isolation, identification and screening of endophytic bacteria .This enzymatic reaction is helps bacterial cells to protect themselves from the toxic effects of hydrogen peroxide, a byproduct of metabolism and an oxidative stress-inducing compound. In oxidase test indicate positive result the oxidase reagent reacts with the oxidase enzyme in the bacterial sample, resulting in the appearance of a blue or purple color on the filter paper. The rapid development of color indicates the presence of the oxidase enzyme in the bacterial cells. The oxidase enzyme, also known as cytochrome c oxidase or simply oxidase, plays a critical role in the final step of the electron transport chain during aerobic respiration. This enzyme is found in the inner mitochondrial membrane of eukaryotic cells and in the cell membrane of many aerobic bacteria .The triple Sugar Iron (TSI) test positive indicated that various color changes

and gas production within the medium.The TSI test is a differential media used in microbiology to differentiate bacteria based on their ability to ferment sugars (glucose, lactose, and/or sucrose) and produce hydrogen sulfide gas. The TSI test and the MIU test both include the detection of hydrogen sulfide production. Because of produce gas and showed motility properties it was confirmed that the isolate was Motility Indole Urease (MIU) Test positive. The strain was urease positive, the result in an endophytic bacterium suggests that it has the enzymatic capability to hydrolyze urea and produce ammonia. The ability of an endophytic bacterium to produce urease and potentially fix nitrogen can contribute to plant growth promotion. By increasing nutrient availability and enhancing nitrogen uptake, the bacterium can positively influence the host plant's growth and development. In agricultural research, they hold potential as biofertilizers and bioenhancers, which can reduce the need for synthetic fertilizers and promote sustainable agriculture. The result was similar with the results obtained by (Kumaresan & Suryanarayanan, 2001), who investigated on occurrence and distribution of endophytic bacteria. A positive result in the Citrate Utilization Test is indicated by the change of the medium's color from green to blue, along with an increase in pH due to the utilization of citrate. The Test result in an endophytic bacterium signifies that it has the enzymatic capability to utilize citrate as a carbon source for growth. That means the bacterium can use citrate as an alternative carbon source when other carbon compounds may be limited in the plant's internal environment. After field experimentation, the statistical analysis showed the significant results in case of root, shoot, leaf length, fresh weight, and anther of T1treatments group compared to To and Tc treatment and the p value was >0.05. Although. Comparing within T1 treatment group statistically significant result were also observed, indicating the impact of using different urea percentage. In this study represents the pioneering report of successfully cultivating a bacterium in a minimal salt agar medium containing pesticide as the sole carbon source. The experimental results have unequivocally verified that the present study's strain displayed robust growth in the pesticide-containing minimal salt agar medium. (MSM). In the present study strain *Serratia* sp. HSTU-BF1R2 completely degraded 250 mg l-1 of chlorpyrifos+ cypermethrin within 15 days of incubation in the minimal salt medium. Recent published article reported Enterobacter sp. B-14 was degrade parent chlorpyrifos compound rapidly in the MSM medium and this strain used chlorpyrifos as only the carbon and phosphorus sources(B.K.Singh *et al.*,2004). Forty isolates obtained from the roots, shoots, and leaves of Kalijeera (indigenous variety) and BRRI-28 rice plants were

screened based on their capabilities of utilizing chlorpyrifos as their sole carbon source—a characteristic of pesticide-degrading bacteria (Prodhan *et al.,* 2023). The *Serratia* sp. HSTU-BF1R2 strain degraded the chlorpyrifos from aqueous medium and chlorpyrifos was used as sole carbon sources. (Das *et al.,* 2022). We found that the absorbance of our strain was 0.827nm compared to control with no bacteria was showed 1.371 nm from spectrophotometer in 600 nm wavelength. The biodegradation of organophosphates by bacteria were reported by several researchers as follows: *Pseudomonas aeruginosa*, *putida, Bacillus pumilus, Bacillus cereus, Serratia* marcescens, *klebsilla* sp, *Alcaligenes* sp., *Alcaligenes faecalis*, *flavobacterium* sp, and *Enterobacter* strain B-14 (Vidya Lakshmi *et al.,* 2009) (B.K. Singh *et al.,* 2003). These pesticide degradation by bacterial strains was exhibited as a decrease in pesticide concentration that was proportional to increase in bacterial growth Depending on the field experiment and chlorpyrifos detoxification results analysis we decided to performed complete genome sequence of the strain *Enterobacter* sp. HSTU-ASh6. The quality of the genome sequence was predicted according to GC% of strains DNA (Rodríguez-Medina *et al.,* 2020). The good sequence quality ensured by its GC%, and at least 40-70% GC% is accepted in research (Abdullah-Al-Mamun *et al.,* 2022). The study strain showed 55.1% GC percent after fastQC analysis, and it was confirmed that the sequence quality was excellent. In analysis part we collect most related bacterial genome species from NCBI with compared my bacteria *Serratia* sp. HSTU-BF1R2 to identified the intimate relations of ingenus match among those genome sequence .Distance measures determined by Average Nucleotide Identity (ANI) analysis can be effectively employed to reconstruct prokaryotic phylogenies, capturing the shared ancestry among different species. This approach naturally facilitates the grouping of species into genera and families, contributing to the taxonomic classification (Ekici *et al.,* 2008). The concept of using ANI for identification purposes was initially introduced by Kim et al. in 2016, building upon the method's proposal in 2005 (Kim *et al.,* 2009). From ANI table (14) it is reasoning that the *Serratia* sp. HSTU-BF1R2 genome has been compared with 14 similar genes where maximum results show 98.43-98.93% nucleotide sequence identity. Among all of them the highest identity 98.98% is showing with CP033504.1 *Serratia* sp. LS-1 chromosome nucleotide sequence. The ANI calculation is performed by the jspecies was server In Table 15, the DDH (DNA-DNA Hybridization) values are presented, reflecting the hybridization relationship between the examined strain Bacillus species HSTU bmn18 and other whole genome sequenced strains. To assess DNA-DNA hybridization,

we performed comparisons between our sequenced genome strain and fourteen similar bacterial genome sequenced strains obtained from the public databank NCBI.The hybridization values of the referenced and examined genome strains were determined using three specific formulae (Abdullah-Al-Mamun *et al.,* 2022). These formulae allowed us to quantify the genomic relatedness and establish the hybridization relationships among the strains.We found from the reported table, *Serratia* sp. HSTU-BF1R2 and CP 117886.1 *Serratia*_ureilytica_strain_KML.E1 had showed highest DNA hybridization value. To view genomic rearrangement among our examined *Serratia* sp. HSTU-BF1R2 strain with other five similar bacterial strain which were matched ancestor qualified from prior identification method like – ANI, DDH. which is a method of representing arrangement of nucleotide bases in color blocks (Darling *et al.,* 2010). The evolutionary phylogenetic tree was inferred using the neighbor-joining method. The percentages of replicate trees in which the associated taxa clustered together in the bootstrap test are shown next to the branches. (Kumar *et al.,* 2016). From the figure of phylogenetic tree (Figure 16), *Serratia* sp. HSTU-BF1R2 is closely related to two groups. Group one includes *Serratia* sp strain closely related to two groups. Group one includes serrati asp strain P041129, CP06651, LT9078433.1, CP068214.1, OW967878.1 and OX291765.1 and groups two includes *Serratia* sp strain CP033504.1are sister taxa with the more intimately related to each other because they share are more common ancestor than any other group. The tree is drawn to scale, with branch lengths in the same units as those of the evolutionary distances used to infer the phylogenetic tree.This analysis involved 15 nucleotide sequences.The tree are drawn by REALPHY online server and editing from MEGA X software.We conducted a pan-genomic analysis of *Serratia* sp. strain HSTU BF1R1 along with its four nearest homologs to gain insights into the genomic variations within this bacterial species. Pangenome refer to the entire gene contents of a bacterial species or set of strains (Tettelin *et al.,* 2005). The circular plot in Figure 17 revealed interesting patterns. From 0 kbp to 700 kbp, all strains exhibited similarities, indicating a conserved genomic segment with shared genetic ancestry and essential core genes. Beyond 700 kbp up to 1000 kbp, the circular plot displayed a fractionated pattern with gaps, suggesting substantial genomic variance. These differences may arise from genetic rearrangements, insertions, deletions, or horizontal gene transfer events, potentially contributing to strain-specific traits or adaptations and 1000 kbp to 1900 kbp, a large missing region was observed in *Serratia* sp. strain HSTU BF1R1 compared to the other strains. This implies a genomic deletion

or large-scale rearrangement specific to this strain, potentially influencing its phenotypic characteristics, ecological niche, or pathogenicity. Overall, the circular plot provides a visual representation of the genomic variations among *Serratia* sp. strain HSTU BF1R1 and its four nearest homologs. The observed differences in specific genomic regions emphasize the importance of pan-genomic analyses in understanding the genetic diversity and evolutionary dynamics within bacterial species. The number of sequenced bacteriophage genomes is growing at an exponential rate. The majority of sequenced bacteriophage genomes are annotated by one or more of several freely available gene identification programs (Glimmer, GeneMark, RAST, Prodigal, etc.) (Lazeroff *et al.,* 2021). RAST are described in the subsections in the (Figure no. 11). Input to the process is a prokaryotic genome in the form of a set of contigs in gene bank (GB) format. After annotating it showed genomic features in subsystem 29% genome and the total protein is 1420 and the non-in subsystem is 71% genome with 3498 proteins. In *Serratia* sp. HSTU-BF1R2 we found 22 pesticide degrading protein where 11 protein are valid 3D score from savevs6 server and generated using template-based method in "I-TASSER.Within this analysis the valid protein are docking with 105 ligand A molecular docking and visualization study were performed for the checking of binding affinity and position of binding of pesticide degrading ligands in protein's binding region whether it is in the position or not and also review about distance of joining residues. First, toperformed docking we was collected protein sequence from PGAP annotation site of two bacterial strains than to confirmed 3D structure and quality of protein we uploaded in I-TASSER. Result table showed higher 3D structure verify value for ampD – 98.48 glpQ -93.31, pepA – 83.43, pepB – 85.28, pepD – 80.45, pepQ – 87.07, phnD-84.19, phnK-86.26, phnP-85.71, paaC-80.16 and amidohydrolase family protein-94.08. After that the validated protein was docked with 105 different ligands using Pyrx software (Abdullah-Al-Mamun et al.;2022) 5 protein docking score showed binding affinity up above -7. and all the collected protein were in high concentration. in this context, all these proteins catalytically important residues according to docking analyses of molecular targets to improve aspects related to ligand binding which is a core approach in molecular modelling (Honarparvar *et al.,* 2014)

Conclusion

Endophytic bacteria have significant potential in various biotechnological sectors, particularly agriculture, owing to their close association with plants and protected environment. *Serratia* sp. strain HSTU-BF1R2 shows promise in addressing challenges related to plant growth promotion and pesticide detoxification, offering environment friendly and efficient agricultural practices. This research focused on the novel *Serratia* sp. HSTU-BF1R2 strain, identified through sophisticated genomic analysis. The impact of this strain on plant development and pesticide detoxification is noteworthy. Whole genome sequencing confirmed essential genes for plant growth, stress tolerance, and pesticide breakdown, making it valuable for agriculture. The degradation of pesticides was definitively validated through testing in a minimal salt medium (MSM), where in *Serratia* sp. strain HSTU-BF1R2 effectively broke down chlorpyrifos and cypermethrin. *Serratia* sp. strain HSTU-BF1R2, is a versatile Plant Growth-Promoting Bacterium (PGPB), offers an eco-friendly solution for enhancing crop development and aiding pesticide detoxification. By harnessing its capabilities, agriculture can become more sustainable in crop production by biofertilizer, pesticide management and effective in plant growth while safeguarding the environment.

REFERENCES:

Abdullah-Al-Mamun, M., Hossain, M. S., Debnath, G. C., Sultana, S., Rahman, A., Hasan, Z., Das, S. R., Ashik, M. A., Prodhan, M. Y., & Aktar, S. (2022). Unveiling lignocellulolytic trait of a goat omasum inhabitant Klebsiella *variicola* strain HSTU-AAM51 in light of biochemical and genome analyses. *Brazilian Journal of Microbiology*, *53*(1), 99–130.

Ako-Nai, K., Adejuyigbe, J., Ajayi, V., & Onipede, M. (1999). The bacteriology of neonatal septicaemia in Ile-Ife, Nigeria. *Journal of Tropical Pediatrics*, *45*(3), 146–151.

Aktar, M. W., Sengupta, D., & Chowdhury, A. (2009). Impact of pesticides use in agriculture: Their benefits and hazards. *Interdisciplinary Toxicology*, *2*(1), 1.

Alami, Y., Achouak, W., Marol, C., & Heulin, T. (2000). Rhizosphere Soil Aggregation and Plant Growth Promotion of Sunflowers by an Exopolysaccharide-Producing *Rhizobiumsp*. Strain Isolated from Sunflower Roots. *Applied and Environmental Microbiology*, *66*(8), 3393–3398. https://doi.org/10.1128/AEM.66.8.3393-3398.2000

Allinson, G., Zhang, P., Bui, A., Allinson, M., Rose, G., Marshall, S., & Pettigrove, V. (2015). Pesticide and trace metal occurrence and aquatic benchmark exceedances in surface waters and sediments of urban wetlands and retention ponds in Melbourne, Australia. *Environmental Science and Pollution Research*, *22*, 10214–10226.

Amweg, E. L., Weston, D. P., You, J., & Lydy, M. J. (2006). Pyrethroid insecticides and sediment toxicity in urban creeks from California and Tennessee. *Environmental Science & Technology*, *40*(5), 1700–1706.

Anadón, A., Martínez-Larrañaga, M. R., & Martínez, M. A. (2009). Use and abuse of pyrethrins and synthetic pyrethroids in veterinary medicine. *The Veterinary Journal*, *182*(1), 7–20.

Aneja, K. R. (2007). *Experiments in microbiology, plant pathology and biotechnology*. New Age International.

Ansaruddin, P. A., & Vijayalakshmi, K. (2003). The womb is not safe anymore. *Indegenous Agriculture News*, *2*(3).

Ansorge, W. J. (2009). Next-generation DNA sequencing techniques. *New Biotechnology*, *25*(4), 195–203.

Anwar, Z., Gulfraz, M., & Irshad, M. (2014). Agro-industrial lignocellulosic biomass a key to unlock the future bio-energy: A brief review. *Journal of Radiation Research and Applied Sciences*, *7*(2), 163–173.

Arshad, M., Shaharoona, B., & Mahmood, T. (2008). Inoculation with Pseudomonas spp. Containing ACC-Deaminase Partially Eliminates the Effects of Drought Stress on Growth, Yield, and Ripening of Pea (Pisum sativum L.) *1 *1Project supported by the Higher Education Commission, Islamabad, Pakistan (No. PIN 041 211534 A-031). *Pedosphere*, *18*(5), 611–620. https://doi.org/10.1016/S1002-0160(08)60055-7

Aziz, R. K., Bartels, D., Best, A. A., DeJongh, M., Disz, T., Edwards, R. A., Formsma, K., Gerdes, S., Glass, E. M., & Kubal, M. (2008). The RAST Server: Rapid annotations using subsystems technology. *BMC Genomics*, *9*(1), 1–15.

Babu, A. G., & Reddy, M. S. (2011). Dual inoculation of arbuscular mycorrhizal and phosphate solubilizing fungi contributes in sustainable maintenance of plant health in fly ash ponds. *Water, Air, & Soil Pollution*, *219*, 3–10.

Bankevich, A., Nurk, S., Antipov, D., Gurevich, A. A., Dvorkin, M., Kulikov, A. S., Lesin, V. M., Nikolenko, S. I., Pham, S., & Prjibelski, A. D. (2012). SPAdes: A new genome assembly algorithm and its applications to single-cell sequencing. *Journal of Computational Biology*, *19*(5), 455–477.

Barbini, D. A., Vanni, F., Girolimetti, S., & Dommarco, R. (2007). Development of an analytical method for the determination of the residues of four pyrethroids in meat by GC–ECD and confirmation by GC–MS. *Analytical and Bioanalytical Chemistry*, *389*, 1791–1798.

Bergey, D. H. (1994). *Bergey's manual of determinative bacteriology*. Lippincott Williams & Wilkins.

Beškoski, V. P., Gojgić-Cvijović, G., Milić, J., Ilić, M., Miletić, S., Šolević, T., & Vrvić, M. M. (2011). Ex situ bioremediation of a soil contaminated by mazut (heavy residual fuel oil)–A field experiment. *Chemosphere*, *83*(1), 34–40.

Boopathy, R. (2000). Factors limiting bioremediation technologies. *Bioresource Technology*, *74*(1), 63–67. https://doi.org/10.1016/S0960-8524(99)00144-3

Bradberry, S. M., Cage, S. A., Proudfoot, A. T., & Vale, J. A. (2005). Poisoning due to pyrethroids. *Toxicological Reviews*, *24*, 93–106.

Burgess, J. L., Bernstein, J. N., & Hurlbut, K. (1994). Aldicarb poisoning: A case report with prolonged cholinesterase inhibition and improvement after pralidoxime therapy. *Archives of Internal Medicine*, *154*(2), 221–224.

Cappuccino, J. G., & Sherman, N. (2005). Microbiology: A laboratory manual (p. 507). *San Francisco: Pearson/Benjamin Cummings. Sultenfuss, JH, & Doyle, WJ (1999). Functions of Phosphorus in Plants. Better Crops*, *83*(1), 6–7.

Chen, W.-M., Tang, Y.-Q., Mori, K., & Wu, X.-L. (2012). Distribution of culturable endophytic bacteria in aquatic plants and their potential for bioremediation in polluted waters. *Aquatic Biology*, *15*(2), 99–110.

Creus, C. M., Sueldo, R. J., & Barassi, C. A. (2004). Water relations and yield in *Azospirillum*- inoculated wheat exposed to drought in the field. *Canadian Journal of Botany*, *82*(2), 273–281. https://doi.org/10.1139/b03-119

Dallakyan, S., & Olson, A. J. (2015). Small-molecule library screening by docking with PyRx. *Chemical Biology: Methods and Protocols*, 243–250.

Damalas, C. A., & Eleftherohorinos, I. G. (2011). Pesticide exposure, safety issues, and risk assessment indicators. *International Journal of Environmental Research and Public Health*, *8*(5), 1402–1419.

Dar, M. A., Kaushik, G., & Villarreal-Chiu, J. F. (2019). Pollution status and bioremediation of chlorpyrifos in environmental matrices by the application of bacterial communities: A review. *Journal of Environmental Management*, *239*, 124–136.

Darling, A. E., Mau, B., & Perna, N. T. (2010). progressiveMauve: Multiple genome alignment with gene gain, loss and rearrangement. *PloS One*, *5*(6), e11147.

Das, S. R., Haque, M. A., Akbor, M. A., Abdullah-Al-Mamun, M., Debnath, G. C., Hossain, M. S., Hasan, Z., Rahman, A., Islam, M. A., & Hossain, M. A.-A. (2022). Organophosphorus insecticides mineralizing endophytic and rhizospheric soil bacterial consortium influence eggplant growth-promotion. *Archives of Microbiology*, *204*(3), 199.

Divoll, T. J., Brown, V. A., Kinne, J., McCracken, G. F., & O'Keefe, J. M. (2018). Disparities in second-generation DNA metabarcoding results exposed with

accessible and repeatable workflows. *Molecular Ecology Resources*, *18*(3), 590–601.

Doble, M., & Kumar, A. (2005). *Biotreatment of Industrial Effluents*. Elsevier.

Duan, J., Müller, K. M., Charles, T. C., Vesely, S., & Glick, B. R. (2009). 1-Aminocyclopropane-1-Carboxylate (ACC) Deaminase Genes in Rhizobia from Southern Saskatchewan. *Microbial Ecology*, *57*(3), 423–436. https://doi.org/10.1007/s00248-008-9407-6

Duruibe, Ogwuegbu, & Egwurugwu. (2007). Heavy metal pollution and human biotoxic effects. *International Journal of Physical Sciences*, *2*(5), 112–118.

Edwards, D. J., & Holt, K. E. (2013). Beginner's guide to comparative bacterial genome analysis using next-generation sequence data. *Microbial Informatics and Experimentation*, *3*, 1–9.

Ekici, Ö. D., Paetzel, M., & Dalbey, R. E. (2008). Unconventional serine proteases: Variations on the catalytic Ser/His/Asp triad configuration. *Protein Science*, *17*(12), 2023–2037.

EPA, U. (2018). Basic information about pesticide ingredients. *US Environmental Protection Agency*.

Fergusson, J. E. (1990). The heavy elements: Chemistry, environmental impact and health effects. *(No Title)*.

Fuller, C. W., Kumar, S., Porel, M., Chien, M., Bibillo, A., Stranges, P. B., Dorwart, M., Tao, C., Li, Z., & Guo, W. (2016). Real-time single-molecule electronic DNA sequencing by synthesis using polymer-tagged nucleotides on a nanopore array. *Proceedings of the National Academy of Sciences*, *113*(19), 5233–5238.

Gerhardt, K. E., Huang, X.-D., Glick, B. R., & Greenberg, B. M. (2009). Phytoremediation and rhizoremediation of organic soil contaminants: Potential and challenges. *Plant Science*, *176*(1), 20–30.

Germaine, K. J., Liu, X., Cabellos, G. G., Hogan, J. P., Ryan, D., & Dowling, D. N. (2006). Bacterial endophyte-enhanced phytoremediation of the organochlorine herbicide 2, 4-dichlorophenoxyacetic acid. *FEMS Microbiology Ecology*, *57*(2), 302–310.

Giesy, J. P., Solomon, K. R., Coats, J. R., Dixon, K. R., Giddings, J. M., & Kenaga, E. E. (1999). *Chlorpyrifos: Ecological risk assessment in North American aquatic environments*. Springer.

Glick, B. R., Cheng, Z., Czarny, J., & Duan, J. (2007). Promotion of plant growth by ACC deaminase-producing soil bacteria. In P. A. H. M. Bakker, J. M. Raaijmakers, G. Bloemberg, M. Höfte, P. Lemanceau, & B. M. Cooke (Eds.), *New Perspectives and Approaches in Plant Growth-Promoting Rhizobacteria Research* (pp. 329–339). Springer Netherlands. https://doi.org/10.1007/978-1-4020-6776-1_8

Goris, J., Konstantinidis, K. T., Klappenbach, J. A., Coenye, T., Vandamme, P., & Tiedje, J. M. (2007). DNA–DNA hybridization values and their relationship to whole-genome sequence similarities. *International Journal of Systematic and Evolutionary Microbiology*, *57*(1), 81–91.

Gorman Ng, M., Stjernberg, E., Koehoorn, M., Demers, P. A., Winters, M., & Davies, H. W. (2013). Fertilizer use and self-reported respiratory and dermal symptoms among tree planters. *Journal of Occupational and Environmental Hygiene*, *10*(1), 36–45.

Hadi, F., & Bano, A. (2010). Effect of diazotrophs (Rhizobium and Azatebactor) on growth of maize (Zea mays L.) and accumulation of lead (Pb) in different plant parts. *Pak J Bot*, *42*(6), 4363–4370.

Haque, M. A., Hossain, M. S., Ahmad, I., Akbor, M. A., Rahman, A., Manir, M. S., Patel, H. M., & Cho, K. M. (2022). Unveiling chlorpyrifos mineralizing and tomato plant-growth activities of Enterobacter sp. Strain HSTU-ASh6 using biochemical tests, field experiments, genomics, and in silico analyses. *Frontiers in Microbiology*, *13*, 1060554.

Harry Jr, W., & VanDemark, P. J. (1981). *Selected Exercises from Microbes in Action: A Laboratory Manual of Microbiology 3rd Ed*. WH Freeman.

Helal, A. A., Imam, D. M., Khalifa, S. M., & Aly, H. F. (2006). Interaction of pesticides with humic compounds and their metal complexes. *Radiochemistry*, *48*, 419–425.

Honarparvar, B., Govender, T., Maguire, G. E., Soliman, M. E., & Kruger, H. G. (2014). Integrated approach to structure-based enzymatic drug design: Molecular modeling, spectroscopy, and experimental bioactivity. *Chemical Reviews*, *114*(1), 493–537.

Hooper, L. V., Wong, M. H., Thelin, A., Hansson, L., Falk, P. G., & Gordon, J. I. (2001). Molecular analysis of commensal host-microbial relationships in the intestine. *Science*, *291*(5505), 881–884.

Hua, J., & Relyea, R. (2014). Chemical cocktails in aquatic systems: Pesticide effects on the response and recovery of> 20 animal taxa. *Environmental Pollution*, *189*, 18–26.

Juhasz, A. L., Stanley, G. A., & Britz, M. L. (2000). Microbial degradation and detoxification of high molecular weight polycyclic aromatic hydrocarbons by

Stenotrophomonas maltophilia strain VUN 10,003. *Letters in Applied Microbiology*, *30*(5), 396–401.

Kaur, R., Singh, D., Kumari, A., Sharma, G., Rajput, S., Arora, S., & Kaur, R. (2021). Pesticide residues degradation strategies in soil and water: A review. *International Journal of Environmental Science and Technology*, 1–24.

Khan, A. A., Jilani, G., Akhtar, M. S., Naqvi, S. S., & Rasheed, M. (2009). Phosphorus solubilizing bacteria: Occurrence, mechanisms and their role in crop production. *J. Agric. Biol. Sci*, *1*(1), 48–58.

Kidd, P., Barceló, J., Bernal, M. P., Navari-Izzo, F., Poschenrieder, C., Shilev, S., Clemente, R., & Monterroso, C. (2009). Trace element behaviour at the root–soil interface: Implications in phytoremediation. *Environmental and Experimental Botany*, *67*(1), 243–259. https://doi.org/10.1016/j.envexpbot.2009.06.013

Kim, E. S., Lee, H. J., Bang, W.-G., Choi, I.-G., & Kim, K. H. (2009). Functional characterization of a bacterial expansin from Bacillus subtilis for enhanced enzymatic hydrolysis of cellulose. *Biotechnology and Bioengineering*, *102*(5), 1342–1353.

Kumar, S., Stecher, G., & Tamura, K. (2016). MEGA7: Molecular evolutionary genetics analysis version 7.0 for bigger datasets. *Molecular Biology and Evolution*, *33*(7), 1870–1874.

Kumaresan, V., & Suryanarayanan, T. S. (2001). Occurrence and distribution of endophytic fungi in a mangrove community. *Mycological Research*, *105*(11), 1388–1391.

Laehnemann, D., Borkhardt, A., & McHardy, A. C. (2016). Denoising DNA deep sequencing data—High-throughput sequencing errors and their correction. *Briefings in Bioinformatics*, *17*(1), 154–179.

Lazeroff, M., Ryder, G., Harris, S. L., & Tsourkas, P. K. (2021). Phage commander, an application for rapid gene identification in bacteriophage genomes using multiple programs. *Phage*, *2*(4), 204–213.

Lee, E. Y., Jun, Y. S., Cho, K.-S., & Ryu, H. W. (2002). Degradation characteristics of toluene, benzene, ethylbenzene, and xylene by Stenotrophomonas maltophilia T3-c. *Journal of the Air & Waste Management Association*, *52*(4), 400–406.

Lifshitz, M., Shahak, E., Bolotin, A., & Sofer, S. (1997). Carbamate poisoning in early childhood and in adults. *Journal of Toxicology: Clinical Toxicology*, *35*(1), 25–27.

Luo, S., Xu, T., Chen, L., Chen, J., Rao, C., Xiao, X., Wan, Y., Zeng, G., Long, F., Liu, C., & Liu, Y. (2012). Endophyte-assisted promotion of biomass production and metal-uptake of energy crop sweet sorghum by plant-growth-promoting endophyte Bacillus sp. SLS18. *Applied Microbiology and Biotechnology*, *93*(4), 1745–1753. https://doi.org/10.1007/s00253-011-3483-0

Ma, Y., Prasad, M. N. V., Rajkumar, M., & Freitas, H. (2011). Plant growth promoting rhizobacteria and endophytes accelerate phytoremediation of metalliferous soils. *Biotechnology Advances*, *29*(2), 248–258.

Mackay, D., Giesy, J. P., & Solomon, K. R. (2014). Fate in the environment and long-range atmospheric transport of the organophosphorus insecticide, chlorpyrifos and its oxon. *Ecological Risk Assessment for Chlorpyrifos in Terrestrial and Aquatic Systems in the United States*, 35–76.

Mahmoud, M. A., Nassif, F. A., Twab, A., Ata, E. A. H., & Soltan, H. A. (n.d.). *Molecular and physiological identification of endophytic bacterial isolates of tomato (lycoperiscon esculentum) and their in vitro antagonistic activity*.

Marasco, R., Rolli, E., Ettoumi, B., Vigani, G., Mapelli, F., Borin, S., Abou-Hadid, A. F., El-Behairy, U. A., Sorlini, C., Cherif, A., Zocchi, G., & Daffonchio, D. (2012). A Drought Resistance-Promoting Microbiome Is Selected by Root System under Desert Farming. *PLOS ONE*, *7*(10), e48479. https://doi.org/10.1371/journal.pone.0048479

Marasco, R., Rolli, E., Vigani, G., Borin, S., Sorlini, C., Ouzari, H., Zocchi, G., & Daffonchio, D. (2013). Are drought-resistance promoting bacteria cross-compatible with different plant models? *Plant Signaling & Behavior*, *8*(10), e26741. https://doi.org/10.4161/psb.26741

Marrone, P. G. (2007). Barriers to adoption of biological control agents and biological pesticides. *CABI Reviews*, *2007*, 12-pp.

Mendes, R., Kruijt, M., De Bruijn, I., Dekkers, E., Van Der Voort, M., Schneider, J. H., Piceno, Y. M., DeSantis, T. Z., Andersen, G. L., & Bakker, P. A. (2011). Deciphering the rhizosphere microbiome for disease-suppressive bacteria. *Science*, *332*(6033), 1097–1100.

Meng, X.-Y., Zhang, H.-X., Mezei, M., & Cui, M. (2011). Molecular docking: A powerful approach for structure-based drug discovery. *Current Computer-Aided Drug Design*, *7*(2), 146–157.

Mesquini, J. A., Sawaya, A. C., López, B. G., Oliveira, V. M., & Miyasaka, N. R. (2015). Detoxification of atrazine by endophytic Streptomyces sp. Isolated from sugarcane and detection of nontoxic metabolite. *Bulletin of Environmental Contamination and Toxicology*, *95*, 803–809.

Naveed, M., Hussain, M. B., Zahir, Z. A., Mitter, B., & Sessitsch, A. (2014). Drought stress amelioration in wheat through inoculation with Burkholderia phytofirmans

strain PsJN. *Plant Growth Regulation*, *73*(2), 121–131. https://doi.org/10.1007/s10725-013-9874-8

Nawaz, K., Hussain, K., Choudary, N., Majeed, A., Ilyas, U., Ghani, A., Lin, F., Ali, K., Afghan, S., & Raza, G. (2011). Eco-friendly role of biodegradation against agricultural pesticides hazards. *Afr J Microbiol Res*, *5*(3), 177–183.

Nicolopoulou-Stamati, P., Maipas, S., Kotampasi, C., Stamatis, P., & Hens, L. (2016). Chemical pesticides and human health: The urgent need for a new concept in agriculture. *Frontiers in Public Health*, *4*, 148.

Phillips, B. M., Anderson, B. S., Hunt, J. W., Siegler, K., Voorhees, J. P., Tjeerdema, R. S., & McNeill, K. (2012). Pyrethroid and organophosphate pesticide-associated toxicity in two coastal watersheds (California, USA). *Environmental Toxicology and Chemistry*, *31*(7), 1595–1603.

Popp, J., Pet\Ho, K., & Nagy, J. (2013). Pesticide productivity and food security. A review. *Agronomy for Sustainable Development*, *33*, 243–255.

Prodhan, M. Y., Rahman, M. B., Rahman, A., Akbor, M. A., Ghosh, S., Nahar, M. N.-E.-N., Simo, Shamsuzzoha, M., Cho, K. M., & Haque, M. A. (2023). Characterization of Growth-Promoting Activities of Consortia of Chlorpyrifos Mineralizing Endophytic Bacteria Naturally Harboring in Rice Plants—A Potential Bio-Stimulant to Develop a Safe and Sustainable Agriculture. *Microorganisms*, *11*(7), Article 7. https://doi.org/10.3390/microorganisms11071821

Rajashekar, N., & Murthy, T. S. (2012). Seed germination and physiological behavior of maize (cv. NAC-6002) seedlings under abiotic stress (pendimethalin) condition. *Asian Journal of Crop Science*, *4*(2), 80–85.

Rajkumar, M., Sandhya, S., Prasad, M. N. V., & Freitas, H. (2012). Perspectives of plant-associated microbes in heavy metal phytoremediation. *Biotechnology Advances*, *30*(6), 1562–1574. https://doi.org/10.1016/j.biotechadv.2012.04.011

Randall, C. (2014). *Pest Management National Pesticide Applicator Certification Core Manual*. Washington: National Association of State Department of Agriculture.

Rhoads, A., & Au, K. F. (2015). PacBio sequencing and its applications. *Genomics, Proteomics & Bioinformatics*, *13*(5), 278–289.

Rodríguez-Medina, N., Martínez-Romero, E., De la Cruz, M. A., Ares, M. A., Valdovinos-Torres, H., Silva-Sánchez, J., Lozano-Aguirre, L., Martínez-Barnetche, J., Andrade, V., & Garza-Ramos, U. (2020). A Klebsiella variicola plasmid confers hypermucoviscosity-like phenotype and alters capsule production and virulence. *Frontiers in Microbiology*, *11*, 579612.

Rolli, E., Marasco, R., Vigani, G., Ettoumi, B., Mapelli, F., Deangelis, M. L., Gandolfi, C., Casati, E., Previtali, F., Gerbino, R., Pierotti Cei, F., Borin, S., Sorlini, C., Zocchi, G., & Daffonchio, D. (2015). Improved plant resistance to drought is promoted by the root-associated microbiome as a water stress-dependent trait. *Environmental Microbiology*, *17*(2), 316–331. https://doi.org/10.1111/1462-2920.12439

Rückert, C., Albersmeier, A., Winkler, A., & Tauch, A. (2015). Complete genome sequence of Corynebacterium kutscheri DSM 20755, a corynebacterial type strain with remarkably low G+ C content of chromosomal DNA. *Genome Announcements*, *3*(3), 10–1128.

Rutter, J. M., & Collee, J. G. (1969). Studies on the soluble antigens of Clostridium oedematiens (Cl. Novyi). *Journal of Medical Microbiology*, *2*(4), 395–417.

Salako, A. F., Amaeze, N. H., Shobajo, H. M., & Osuala, F. I. (2020). Comparative acute toxicity of three pyrethroids (Deltamethrin, cypermethrin and lambda-cyhalothrin) on guppy fish (Poecilia reticulata peters, 1859). *Scientific African*, *9*, e00504.

Saptanmasi, B., Karayilanoglu, T., Kenar, L., Serdar, M., Kose, S., & Aydin, A. (2008). Bacterial biodegradation of aldicarb and determination of bacterium which has the most biodegradative effect. *Turk. J. Biochem*, *33*, 209–214.

Sayler, G. S., Hooper, S. W., Layton, A. C., & King, J. H. (1990). Catabolic plasmids of environmental and ecological significance. *Microbial Ecology*, *19*, 1–20.

Seeley Jr, H. W., & VanDemark, P. J. (1962). Microbes in action. A laboratory manual of microbiology. *Microbes in Action. A Laboratory Manual of Microbiology.*

Seemann, T. (2014). Prokka: Rapid prokaryotic genome annotation. *Bioinformatics*, *30*(14), 2068–2069.

Shahzad, F., Shafee, M., Abbas, F., Babar, S., Tariq, M. M., & Ahmad, Z. (2012). Isolation and biochemical characterization of Rhizobium meliloti from root nodules of Alfalfa (Medico sativa). *The Journal of Animal and Plant Sciences*, *22*(2), 522–524.

Shields, P., & Cathcart, L. (2010). Oxidase test protocol. *American Society for Microbiology*, 1–9.

Singh, B. K., Walker, A., Morgan, J. A. W., & Wright, D. J. (2003). Effects of soil pH on the biodegradation of chlorpyrifos and isolation of a chlorpyrifos-degrading bacterium. *Applied and Environmental Microbiology*, *69*(9), 5198–5206.

Singh, B. K., Walker, A., Morgan, J. A. W., & Wright, D. J. (2004). Biodegradation of chlorpyrifos by Enterobacter strain B-14 and its use in bioremediation of contaminated soils. *Applied and Environmental Microbiology*, *70*(8), 4855–4863.

Singh, D. K. (2008). Biodegradation and bioremediation of pesticide in soil: Concept, method and recent developments. *Indian Journal of Microbiology*, *48*, 35–40.

Soderlund, D. M. (2012). Molecular mechanisms of pyrethroid insecticide neurotoxicity: Recent advances. *Archives of Toxicology*, *86*, 165–181.

Son, H.-J., Park, G.-T., Cha, M.-S., & Heo, M.-S. (2006). Solubilization of insoluble inorganic phosphates by a novel salt-and pH-tolerant Pantoea agglomerans R-42 isolated from soybean rhizosphere. *Bioresource Technology*, *97*(2), 204–210.

Sousa, S. F., Fernandes, P. A., & Ramos, M. J. (2006). Protein–ligand docking: Current status and future challenges. *Proteins: Structure, Function, and Bioinformatics*, *65*(1), 15–26.

Staley, Z. R., Harwood, V. J., & Rohr, J. R. (2015). A synthesis of the effects of pesticides on microbial persistence in aquatic ecosystems. *Critical Reviews in Toxicology*, *45*(10), 813–836.

Stoytcheva, M. (2011). *Pesticides in the modern world: Effects of pesticides exposure*. BoD–Books on Demand.

Strobel, G., Daisy, B., Castillo, U., & Harper, J. (2004). Natural products from endophytic microorganisms. *Journal of Natural Products*, *67*(2), 257–268.

Tétard-Jones, C., & Edwards, R. (2016). Potential roles for microbial endophytes in herbicide tolerance in plants. *Pest Management Science*, *72*(2), 203–209.

Tettelin, H., Masignani, V., Cieslewicz, M. J., Donati, C., Medini, D., Ward, N. L., Angiuoli, S. V., Crabtree, J., Jones, A. L., & Durkin, A. S. (2005). Genome analysis of multiple pathogenic isolates of Streptococcus agalactiae: Implications for the microbial "pan-genome." *Proceedings of the National Academy of Sciences*, *102*(39), 13950–13955.

Timmusk, S., Behers, L., Muthoni, J., Muraya, A., & Aronsson, A.-C. (2017). Perspectives and Challenges of Microbial Application for Crop Improvement. *Frontiers in Plant Science*, *8*. https://doi.org/10.3389/fpls.2017.00049

Timmusk, S., El-Daim, I. A. A., Copolovici, L., Tanilas, T., Kännaste, A., Behers, L., Nevo, E., Seisenbaeva, G., Stenström, E., & Niinemets, Ü. (2014). Drought-Tolerance of Wheat Improved by Rhizosphere Bacteria from Harsh Environments: Enhanced Biomass Production and Reduced Emissions of Stress Volatiles. *PLOS ONE, 9*(5), e96086. https://doi.org/10.1371/journal.pone.0096086

Trott, O., & Olson, A. J. (2010). AutoDock Vina: Improving the speed and accuracy of docking with a new scoring function, efficient optimization, and multithreading. *Journal of Computational Chemistry*, *31*(2), 455–461.

Varo, I., Serrano, R., Pitarch, E., Amat, F., Lopez, F. J., & Navarro, J. C. (2002). Bioaccumulation of chlorpyrifos through an experimental food chain: Study of protein HSP70 as biomarker of sublethal stress in fish. *Archives of Environmental Contamination and Toxicology*, *42*, 229–235.

Vázquez, P. P., Mughari, A. R., & Galera, M. M. (2008). Solid-phase microextraction (SPME) for the determination of pyrethroids in cucumber and watermelon using liquid chromatography combined with post-column photochemically induced fluorimetry derivatization and fluorescence detection. *Analytica Chimica Acta*, *607*(1), 74–82.

Vidya Lakshmi, C., Kumar, M., & Khanna, S. (2009). Biodegradation of chlorpyrifos in soil by enriched cultures. *Current Microbiology*, *58*, 35–38.

Weston, D. P., Chen, D., & Lydy, M. J. (2015). Stormwater-related transport of the insecticides bifenthrin, fipronil, imidacloprid, and chlorpyrifos into a tidal

wetland, San Francisco Bay, California. *Science of The Total Environment*, *527*, 18–25.

Witheetrirong, Y., Tripathi, N. K., Tipdecho, T., & Parkpian, P. (2011). Estimation of the effect of soil texture on nitrate-nitrogen content in groundwater using optical remote sensing. *International Journal of Environmental Research and Public Health*, *8*(8), 3416–3436.

Yang, J., Yan, R., Roy, A., Xu, D., Poisson, J., & Zhang, Y. (2015). The I-TASSER Suite: Protein structure and function prediction. *Nature Methods*, *12*(1), 7–8.

Zarei, M., Hempel, S., Wubet, T., Schäfer, T., Savaghebi, G., Jouzani, G. S., Nekouei, M. K., & Buscot, F. (2010). Molecular diversity of arbuscular mycorrhizal fungi in relation to soil chemical properties and heavy metal contamination. *Environmental Pollution*, *158*(8), 2757–2765.

Zhang, H., Yang, C., Zhao, Q., & Qiao, C. (2009). Development of an autofluorescent organophosphates-degrading Stenotrophomonas sp. With dehalogenase activity for the biodegradation of hexachlorocyclohexane (HCH). *Bioresource Technology*, *100*(13), 3199–3204.

APPENDICES

APPENDIX A

CHEMICALS

Table A.1. Chemicals Used in Experiments

Sr.	Chemical Name	Code
1	Agar-Agar Merck	Merck 1.01613
2	D-Glucose	AppliChem A3666
3	Yeast Extract	Merck 1.03753
4	Glycerol	AppliChem A2926
5	NaCl	Biochem/ and NIB
6	K_2HPO_4	AppliChem A2942
7	$MgSO_4.7H_2O$	Merck 1.05886
8	Polygalacturonic acid	Fluka 81325
9	H_2SO_4	Merck 1.0735
10	Carboxymethyl cellulose sodium salt	Fluka Biochemical 21902 14 Soluble Starch Merck 1.01252.0250
11	Ammonium sulfate	AppliChem A3485
12	Potassium Di-hydrogen Phosphate	Merck 1.04871
13	Immersion oil	AppliChem A0699
14	Calcium chloride	AppliChem A3652
15	Crystal violet	Sigma C3886
16	Safranin	Merck 1.15948
17	Nutrient broth	Merck1.05443
18	Congo Red	Sigma C6767
19	Potassium Iodide	Sigma P8256
20	DNA isolation kit	AppliChem A3421
21	N, N, N`, N`-Tetra methyl-p-phenyl	enedione Sigma T3134
22	Tris Base	Sigma T6066
23	EDTA	AppliChem A2937
24	Isopropanol	AppliChem A3928
25	Proteinase	AppliChem A3830
26	Ethidium bromide	AppliChem A1151
27	Ethanol	AppliChem A3678
28	Taq DNA polymerase MBI,	Ferments EP0401
29	dNTP set MBI,	Fermatas R0181
30	Taq I	Fermatas ER0671
31	Primers	Ege 1, Ege 2, L1 Promega
32	Chloroform	AppliChem A3633
33	Standard agarose	AppliChem A2114

APPENDIX B

MEDIA

Media Used for Isolation (Bacillus subtilis Medium) (Broth)

Solution A

Yeast extract	1 g
$(NH_4)_2SO_4$	0.2 g
$MgSO_4 \times 7H_2O$	0.5 g
$CaCl_2 \times 2H_2O$	0.25 g
KH_2PO_4	0.6 g
Distilled water	500 ml
Adjust pH to	3.7 with 1 M H_2SO_4

Media Used for Extracellular Enzyme Screening

Media used for cellulase Screening.

Medium I	g/l
Ammonium sulfate	1
Na_2HPO_4	6
KH_2PO_4	3
Agar	20

Ingredients (except agar) were dissolved in distilled water. The pH of the medium was adjusted to 4.0 with 1M H2SO4. Agar was added. Medium was sterilized by autoclaving at 121 ºC for 15 min.

Medium II	g/l
Yeast extract	1
Ammonium sulfate	2
Na_2HPO_4	6
KH_2PO_4	3
Commercial grade cellulose	5
Agar	20

Ingredients (except agar) were dissolved in distilled water. The pH was adjusted to 4.0with 1M H2SO4. Agar was added and the medium was sterilized by autoclaving at 121º C for 15 min.

Medium III	g/l
Nutrient Broth	13
$CaCl_2 \times 2H_2O$	0.1

Ingredients were dissolved in deionized water. The pH of the medium was adjusted to 4.0 with 1 M H2SO4. Agar was added and the Medium was sterilized by autoclaving at 121º C for 15 min. Tween 20 was autoclaved separately and added to the medium.